WATER RESOURCES research center

PUBLICATION NO. 93

DEVELOPMENT OF A NUMERICAL MODEL OF INJECTION

INTO A THREE-DIMENSIONAL DENSITY STRATIFIED AQUIFER

by

STEVEN J. LAUX

UNIVERSITY OF FLORIDA

PUBLICATION NO. 93

FLORIDA WATER RESOURCES RESEARCH CENTER

DEVELOPMENT OF A NUMERICAL MODEL OF INJECTION INTO A THREE-DIMENSIONAL DENSITY STRATIFIED AQUIFER

BY

STEVEN J. LAUX

A THESIS PRESENTED TO THE GRADUATE SCHOOL
OF THE UNIVERSITY OF FLORIDA IN
PARTIAL FULFILLMENT OF THE REQUIREMENTS
FOR THE DEGREE OF MASTER OF ENGINEERING

UNIVERSITY OF FLORIDA

1986

ACKNOWLEDGMENTS

The author would like to express his sincere appreciation to Dr. Barry Benedict, committee chairman, for his patient teaching and guidance throughout this program. The author would also like to thank Dr. Bent A. Christensen and Dr. T. Gray Curtis for their assistance in the thesis. Above all, the author appreciates the knowledge and satisfaction gained in the teachings of Dr. Benedict, Dr. Christensen, and Dr. Curtis.

Appreciation is extended to Lisa Rossignol, Debbie Butler, Lynne Parten, and Candace Leggett for their quality typing.

Appreciation is also extended to the people of Jones, Edmunds and Associates who provided valuable support throughout the program.

Special thanks go to the author's close friends, colleagues, and family, who through their friendship have made completion of this program possible.

TABLE OF CONTENTS

LIST OF TABLES

LIST OF FIGURES

Figure		Page
7.4	Injection test at South Cross Bayou........................	74
7.5	Injection test at Southwest St. Petersburg.................	76
7.6	South Cross Bayou Simulation at a Point Near the Injection Well Using the Fully Numerical Model.............	80
7.7	South Cross Bayou simulation using fully numerical model...	81
7.8	Simulation of South Cross Bayou injection using the modified model...	85
7.9	Simulation of Southwest St. Petersburg injection using the modified model.................................	86

LIST OF SYMBOLS

B_{sc}	thickness of semi-confining layer
B_2	thickness of aquifer 2
B_1	thickness of aquifer 1
C	salt concentration
C_0	characteristic concentration
D	dispersion coefficent
d	days
$F(\eta)$	distribution function for horizontal specific discharge
h	depth below or above sea level
$\tilde{K}$	hydraulic conductivity tensor
K_1	hydraulic conductivity of aquifer 1 (horizontal)
K_2	hydraulic conductivity of aquifer 2 (horizontal)
K_{sc}	hydraulic conductivity of the semi-confining layer (vertical)
K_z	vertical hydraulic conductivity in aquifer 1
$L(\eta)$	distribution function for concentration
m	time level
n	porosity of the aquifer
p	pressure
q	specific discharge
r	radius of a point from a well
s	drawdown or head build up
S	storativity of the aquifer
T	transmissivity of an aquifer

t	time
U	characteristic specific discharge in the x-direction
u	component of specific discharge in the x-discharge
V	characteristic specific discharge in the y-direction
v	component of specific discharge in the y-direction
w	vertical component of specific discharge
z	vertical coordinate
α	constant relating salt concentration with unit weight
β	defined in Equation (4.36)
γ	unit weight of water
γ_o	unit weight of reference
δ	thickness of the transition zone
η	dimensionless coordinate within the transition zone
λ	leakage coefficient
ξ	bouyancy term defined in Equation (4.18b)
ρ	density
ϕ	potentiometric head
Ω	defined in equation (5.10)

Subscripts

b	bottom of transition zone
f	freshwater
i	x-direction coordinate
j	y-direction coordinate
o	initial or reference condition
s	salt
t	top of transition zone

Superscripts

$\rightarrow$	vector
$\sim$	tensor
m	time level

Abstract of Thesis Presented to the Graduate School
of the University of Florida in Partial Fulfillment of the
Requirements for the Degree of Master of Engineering

DEVELOPMENT OF A NUMERICAL MODEL OF INJECTION
INTO A THREE-DIMENSIONAL DENSITY-STRATIFIED AQUIFER

By

Steven J. Laux

December, 1986

Chairman: Dr. Barry A. Benedict
Major Department: Civil Engineering

An extension of the integral method was made to model the case of injection into a two-layer system of aquifers with injection into the top of the lower layer. An alternating direction implicit (ADI) finite-difference model was developed to solve the equations describing this system. The need for small time steps for model convergence and the rapid stabilization of the drawdowns led to the alternative use of an analytical method (the Hantush equation for leaky aquifers) to calculate drawdowns and drastically reduce computer time.

Attempts were made to fit the model to data from injection wells in Pinellas County, Florida. Data from the injection tests are sparse and of questionable quality; however the basic extent of the injected water field was reproduced fairly well. Neglect of vertical flows in the well region may be of importance here. The complicated system here, with saltwater both above and below the injected water, makes it difficult to estimate well concentrations currently.

The model developed in this work produces a tool for analysis of injections of wastes which should prove useful for preliminary assessments. Work should continue to further the development and test against other data.

Barry A. Benedict

Chairman

CHAPTER 1
INTRODUCTION

Description of Problem

Many coastal areas have density-stratified, artesian groundwater fields due to underlying saltwater and overlying freshwater, all held in a series of aquifers and semi-confining beds. In recent years, these saline aquifers have been used in deep injection disposal of treated sewage and industrial waste. Potential benefits or hazards to groundwater resources could result from this practice.

Treated freshwater sewage could possibly be injected into coastal areas in an effort to stop the landward movement of saltwater intrusion. This also provides a convenient method of disposing of treated sewage. Also, surface runoff and excess potable surface water could be injected into a saline aquifer during rainy seasons and periods of excess surface water. Later, during dry periods with little rainfall, the previously injected water would be pumped from the aquifer for potable use. This practice may prove beneficial in many coastal areas of Florida where saltwater intrusion has currently eliminated groundwater as a potable water resource.

There are also potential hazards associated with deep-well injection. This is a management technique where the technology is still very young and the long-term effects of injecting pollutants into an aquifer are still not well known.

Experts in this field still feel that they are working in an unknown area when they pump pollutants into an aquifer. In aquifers of low permeability, where water velocities are very low, undesirable changes to an aquifer due to injection may go undetected until the damage is already extensive. Also, in aquifers of low permeability, any changes may be essentially "irreversible", making it impossible to undo any undesirable effects of pollutant injection within a reasonable time.

Today, in Florida, there are over fifty injection wells that are owned and operated by municipal water treatment plants, power plants, industrial plants, and agricultural cooperatives. The majority of injection wells in Florida are used for disposal of sanitary sewage. There are also numerous gravity-driven drainage wells in Florida. With these wells in existence and with the increasing popularity of injection disposal of waste, the risk of extensive damage to potable water aquifers increases. If migration of pollutants is not anticipated correctly, the pollutants could appear in areas where they are undesirable.

It has long been recognized that a tool is needed to predict the effects of injecting a light fluid into a heavier fluid. It is the objective of this work to discuss several modeling methods available and to develop one or more of these techniques for use by persons involved in deep-well injection.

The goal is to develop a numerical, or semi-numerical, scheme for the prediction of effects of an injection well, or a series of injection wells, on an aquifer. It is desired to create such a program that would be usable by consulting firms and regulatory agencies; to this end, it is desired that the computer capacity requirements are small enough that modeling could take place on a micro-computer. This would put advanced modeling techniques within the grasp of persons previously not able to utilize them. It is important to realize that such technology may be misused by persons who do not understand the physical background of the model and its limitations. For this reason, a complete description of the model development has been included in this thesis.

Methodology

To develop a usable model of an injection well in a salt-water aquifer it will first be necessary to review the existing groundwater modeling literature. There is much information about the saltwater intrusion problem, which is analogous to the injection situation. Unfortunately, even most current stratified groundwater-flow models make the simplifying assumption of a sharp interface between the freshwater and saltwater. The actual change from fresh to saltwater occurs through a transition zone of varying density and salt concentration. It is desirable to locate the transition zone and use it to calculate salt concentrations within the pumping region.

Benedict, Rubin, and Means [1983] developed a three-dimensional saltwater upconing model that accounted for the transition zone using an integral technique. This model could be modified and the theory extended to simulate the injection problem. Although this model uses much less computer time than large-scale numerical models, several simplifying assumptions, based on analysis of the basic equations, could be made to further reduce its run-time cost. It has been observed that in the upconing model there are some numerical problems encountered in the transition zone calculations (see Chapter 5). These and other problems must be worked out before a modification of the upconing model could be considered.

Once a model has been developed, it will be necessary to compare its output to actual injection well field-data. Suitable data has been obtained from a U.S. Geological Survey report on several injection wells in the Pinellas County, Florida area.

Once the validity of the model has been verified, the model will be tested to establish limits for numerical convergence and stability, as well as model sensitivity to input parameters, as well as defining limits of model applicability. The final model should provide a useful tool for assessment of injection well impact, while at the same time being of a scale and cost as to be useful to many professionals.

CHAPTER 2
LITERATURE REVIEW

Introduction

In this chapter a review will be made of available literature covering stratified groundwater flow as it applies to the injection situation. Injection of freshwater into a saltwater aquifer is a phenomenon that is somewhat analogous to that of saline intrusion due to pumping. For this reason, and because there is less specific information available about injection modeling, part of the literature review will be of the saltwater intrusion situation.

Magnitude of Problem

Injection wells have been of interest in this country for years. They have been conceived as a means of waste disposal; as a means of recharging aquifers; as a means of increasing local potentiometric heads, thereby reducing potential for saltwater intrusion; or as some combination of these. Of particular concern is Florida, where the large coastal region offers many possibilities for injection into saline regions. Helpling [1980] noted that in 1980 at least ninety-one injection wells were being considered, planned, or were in operation in Florida. CH_2M Hill [1983] lists a large number of such sites, probably representing about 75 percent of existing injection sites in Florida. Table 2.1 lists wells in Florida to give an indication of the types of injection wells existing.

Table 2.1 Some injection wells in the State of Florida

Location	Number of Wells, (Diameter) Injection	Number of Wells, (Diameter) Monitor	Well Depth (ft)	Year Completed	Remarks
Sugar Cane Growers Cooperative of Florida	2 (8")	1 (6")	2,000	1966	Operated 1966-76 Superceded by wells for The Quaker Oats Co. (See listing below) Industrial effluent
General Waterworks Corporation	2 (16")	-	3,100	1970 1971	Sunset Park & Kendale Lakes Operating since 1971 in Dade Co. Secondary treated sanitary effluent Replaced by Miami-Dade Water and Sewer Authority system February 1983 (See listing below)
American Cyanamid	1 (6")	-	1,547	1971	Santa Rosa Plant Test well for industrial effluent
The Quaker Oats Company	3 (10")	3 (6")	3,300	1977	Operating since 1978 Industrial effluent
City of Margate	1 (24")	1 (9-5/8")	3,200	1974	Operating since 1974 Secondary treated sanitary effluent
Florida Power & Light Co.	1 (12")	-	1,500	1974	Willow Plant Exploratory well Underground storage
Florida Power & Light Co.	1 (12")	-	1,600	1974	Palatka Plant Exploratory well Industrial effluent
City of Sarasota	1 (16")	-	3,000	1974	Exploratory well Secondary treated sanitary effluent
City of Stuart	1 (16")	1 (8")	3,000	1975	Secondary treated sanitary effluent

Table 2.1--continued

Location	Number of Wells, (Diameter) Injection	Monitor	Well Depth (ft)	Year Completed	Remarks
City of Gainesville	4 (30")	10 (4")	800'-1,000	1976	Operating since 1976 Advanced treated sanitary effluent
City of St. Petersburg	3 (16")	5 (8")	1,000	1977	S.W. Plant Operating since 1977 Secondary treated sanitary effluent with filtration
City of St. Petersburg	3 (20")	5 (8")	1,000	1978	N.E. Plant Operating since 1980 Secondary treated sanitary effluent with filtration
City of St. Petersburg	2 (20")	1 (6")	-	-	N.W. Plant Design completed-construction scheduled for 1983 Secondary treated sanitary effluent with filtration
Hercules, Inc.	1 (10")	1 (6")	3,005	1979	Operating since 1979 Industrial effluent
Miami-Dade Water and Sewer Authority (MDWSA)	8 (24") 1 (20")	3 (6")	3,100 3,100	1981 1981	South District Plant Secondary treated sanitary effluent
General Development Utilities	1 (12")	1 (6")	3,400	1983	Port St. Lucie Secondary treated sanitary effluent
City of Sunrise	2 (24")	1 (6")	3,200	1984	Secondary treated sanitary effluent

Analytical Studies

An analytical technique for calculating the shape of a sharp, fresh-saline water interface was developed by Ghyben [Ghyben 1888] and Herzberg [Herzberg 1901]. The Ghyben-Herzberg relationship assumes horizontal streamlines in the freshwater and no movement in the saltwater. It has been widely applied to problems where vertical movement of the freshwater can be neglected. The Ghyben-Herzberg relationship uses a hydrostatic balance to show that the saltwater-freshwater interface is located at a depth below sea level approximately forty times that of the corresponding height of freshwater above sea level. Specifically, the relation is developed that

$$h_s = \frac{1}{\frac{\rho_s}{\rho_f} - 1} h_f \tag{2.1}$$

in which

h_f = height of freshwater above sea level

h_s = depth of salt-fresh interface below sea level at the same location

ρ_s, ρ_f = density of salt and freshwater, respectively.

Since the density of sea water is typically about 1.025 times that of freshwater, Equation 2.1 suggests $h_s \simeq 40h_f$. This also leads to the conclusion that decreasing the freshwater head by a unit value causes a resulting saltwater interface rise of about 40 units.

Hubbert [1940], among others, has shown that where streamline curvature is pronounced, Equation 2.1 gives values somewhat in error; however, the Ghyben-Herzberg relation still provides a useful point of reference.

The actual change from fresh to saltwater occurs through a transition zone of varying density and salt concentration. Bear [1979] notes that the extent of the transition zone is dependent on local conditions. He shows data from Kohout [1960] and Israel showing extensive and small transition zones, respectively. One expects that interfacial mixing and dispersion, existing in a given region, will determine the transition zone characteristics. These mixing features are in turn controlled by pumping rates, existing groundwater flows, and aquifer characteristics. As Bear [1979] notes, even when the assumption of a sharp interface is reasonable valid, a transition zone exists.

If the scale of the overlying freshwater lens is large with respect to the transition zone, it may be reasonable to assume that there is a sharp interface separating the fresh and saltwater. Studies along this line were done by Hantush [1968] and Dagan and Bear [1968].

Bear [1979] summarizes these and other sharp-interface approximations. Strack [1976] utilized a single harmonic potential to define interface movement inland due to pumping. Many sharp interface studies attempt only two-dimensional approaches, simulating a line of wells parallel to the coast. Only a few deal with the three-dimensional field around single wells or overlapping fields of wells. As an example, Muskat and Wychoff [1935] presented a model attempting to account for partial penetration of a pumping well by superposition of sinks.

Using the sharp interface assumption, traditional groundwater flow theory can be applied to both sides of the sharp interface between the fresh and saltwater, thus simplifying the calculation. However, in such calculations, salinity dispersion is neglected, and there is no direct method of estimating its effect on the dynamics of the flow and salinity distribution.

In more recent studies the effects of salinity dispersion at the interface are accounted for. Dagan [1971] formulated the equation of dispersion for a neutrally buoyant tracer in a steady flow by applying a coordinate system based on the potential and the stream function [Bachmat and Bear, 1964]. Then, by applying singular perturbations as suggested by Wooding [1963; 1964] they analyzed the migration of a tracer being initially tangent or nontangent to a streamline. In a later study Eldor and Dagan [1972] extended the analysis to include radioactive decay and absorption.

Gelhar and Collins [1971] applied a boundary layer approximation to develop general solutions for one-dimensional problems involving longitudinal despersion of neutrally buoyant tracers in porous media.

Koh [1964] and List [1965; 1968] analyzed the problem of flow induced by axially symmetric and two-dimensional sinks in a stratified flow through a porous medium. They showed that boundary layer approximations can be applied for the simulation of flow conditions in the aquifer.

Rubin and Pinder [1977], utilizing a perturbation technique, studied the effect of salinity dispersion on the dynamics of groundwater flow as well as on the salinity distribution in a porous medium. The phenomenon is described as a migration of a sharp interface perturbed by small disturbances due to salinity dispersion. The creation of the mixing zone between fresh and saline water is described as a formation of a boundary layer in the vicinity of a sharp interface. This method is primarily recommended for flow fields in which simple representation of the sharp interface migration is obtainable. This model was modified to form the basis for calculation of indices indicating sensitivity to potential saltwater intrusion by Calderon [1981].

Numerical Studies

Simulations of flow conditions in an aquifer subject to density stratification due to salinity distribution can be done by applying complete numerical schemes for the performance of the simultaneous solution of the equations of motion and salinity transport.

Numerical techniques have an advantage over analytical techniques since they are able to handle complex boundary conditions, varying aquifer thicknesses, heterogeneous and anisotropic permeabilities, varying pumping rates, multiple wells, and recharge. However, such numerical flexibility requires substantially better field data for input and verification. Finite difference, finite element, and boundary element techniques have been used. Each has some limitations. For example, the finite difference solution is a numerical technique that uses a linear approximation of the differential terms in an equation. As a result, problems arise with stability and convergence to a solution in actual non-linear phenomena such as the stratified flow situation. Considering leaky aquifers, variability of the aquifer's permeability and that of the semiconfining formations leads to a significant increase in the grid size for regions in which the flow is very slow. Incorporation of multiple aquifers and aquicludes in a three-dimensional model cannot be practically done by the application of a complete numerical scheme. Problems of numerical dispersion stemming from the use of the finite grid size must also be considered. These problems can be minimized by various methods, but they cannot be avoided in complete numerical models.

A numerical approach was applied by Pinder and Cooper [1970], who developed a two-dimensional model based on a finite difference characteristic method for the simulation of the movement of a saltwater front in an aquifer. For the same purpose Segol et al. [1975] developed a finite element procedure that provides a complete solution of the two-dimensional equations of motion and salinity transport.

Christensen [1978] presented a finite element method for analysis of freshwater lenses in the coastal zones of the Floridan Aquifer. This was applied to a large area in Pinellas County but with no data available then for verification. It was based on assumption of no buoyant forces or dispersion, with a piston-type displacement of saltwater by injected freshwater.

Rubin and Christensen [1982] and Rubin [1982] extended the integral approach to the simulation of unsteady state flow conditions in a two-dimensional aquifer subject to mineralization. Both studies use the integral boundary layer method whereby the solute transport equation is integrated over the vertical thickness of the transition zone subject to certain similarity conditions. The resulting equatrion is then solved simultaneously with the equations of continuity and motion by a finite difference scheme. This approach was extended by Means [1982] for the simulation of initial stages of saltwater intrusion in a three-dimensional flow field.

Wheatcraft and Peterson [1979] used a finite difference scheme to create a two-dimensional model simulating movement of a treated sewage due to injection in a saline aquifer.

Merritt [1983], in a joint United States Geological Survey and United States Corp of Engineers Project, studied the feasibility of recovering freshwater injected and stored underground in South Florida. An attempt was made to use the subsurface finite-difference waste disposal model [INTERCOMP 1976] to simulate the cyclic injection required by the injection-recovery project.

Summary

While analytical models are easy to apply and give solutions to simple aquifer situations, they have the disadvantage of not being able to accurately simulate complex flow phenomena. Numerical models can simulate complex flow phenomena but encounter problems with stability and convergence. Also, numerical models have large memory requirements and use considerable amounts of computer time, making them inaccessible to many professionals.

To overcome problems with stability, convergence, and computer requirements associated with numerical models, it may be necessary to make some simplifying assumptions, or even combine the model with analytical techniques.

CHAPTER 3
REVIEW OF PREVIOUS WORK

Introduction

Simulation of flow conditions in a saline aquifer subject to the injection of freshwater can be done by solving simultaneously the equations of continuity, motion, and solute transport. However, this procedure leads to a set of highly non-linear equations, thus causing problems with stability and convergence in a numerical solution.

By extending Rubin's [Rubin 1982] work, Means [1982] used an integral boundary layer technique whereby the solute transport equation was integrated over the vertical thickness of the transition zone subject to certain similarity conditions. By integrating through the transition zone, equations describing flow in that area were greatly simplified, thus making a numerical solution possible.

It is the intent of this report to modify the equations and extend the theory of the Means report in an effort to simulate the injection situation.

Before developing the equations to be used in the injection situation, it will first be helpful to briefly review the saltwater intrusion simulation done by Means.

The Approximate Method of Stratification Analysis

Figure 3.1 describes the typical flow field for the upconing situation in an inland aquifer. According to the figure, the flow field is divided into the following three zones:

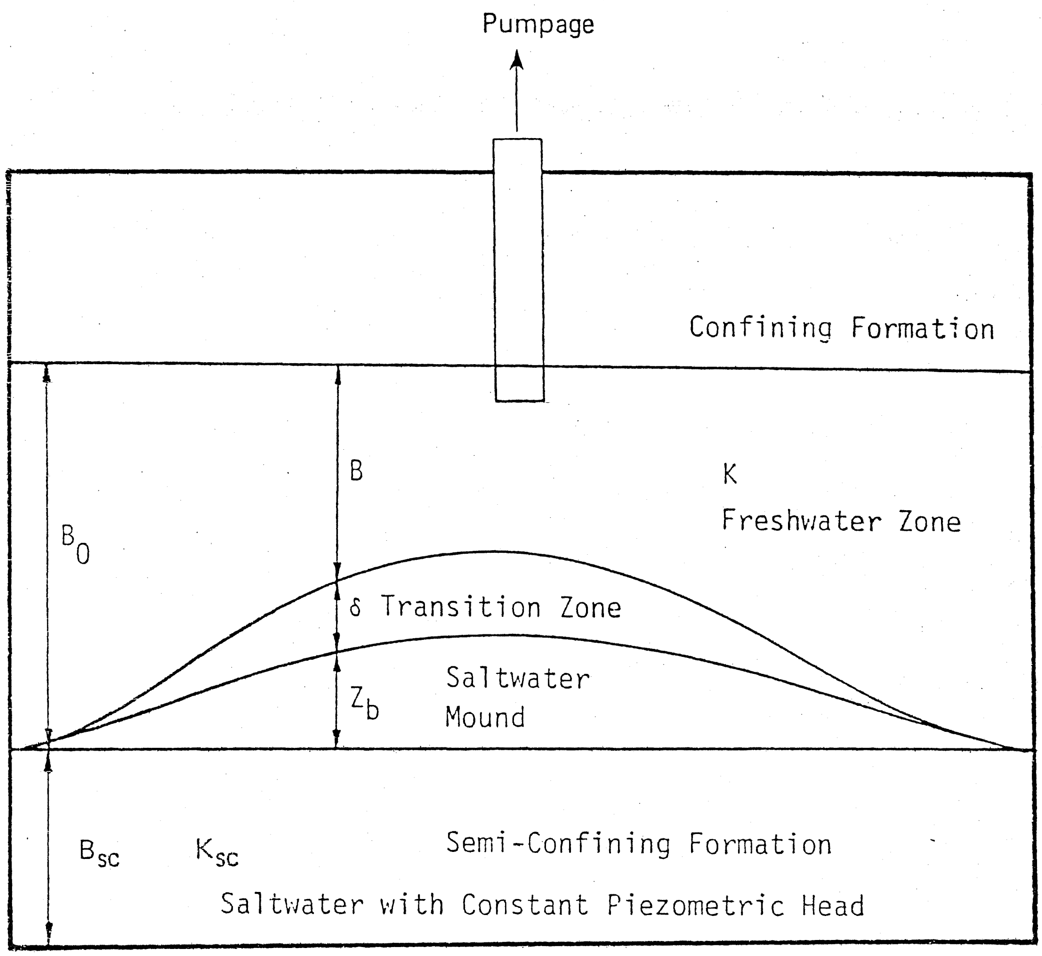

Figure 3.1 Schematic description of the development of a transition zone due to pumpage

(a) the upper zone of freshwater,

(b) the transition zone,

(c) the underlying saltwater zone.

The flow in the freshwater zone is assumed to be horizontal; flow in the transition zone is assumed horizontal and of varying salt concentration; displacement in the saltwater zone is assumed vertical.

The basic equations used for the simulation of stratified flow in an aquifer are the equations of continuity, motion, solute transport, and state represented respectively as follows:

$$\nabla \cdot \vec{q} + \frac{\partial n}{\partial t} = 0 \tag{3.1}$$

$$\vec{q} = -\tilde{K}\nabla\phi \tag{3.2}$$

$$n \frac{\partial C}{\partial t} + \nabla \cdot (\vec{q}C) = \nabla \cdot (\tilde{D} \cdot \nabla C) \tag{3.3}$$

$$\gamma = \gamma_o \ (1 + \alpha C) \tag{3.4}$$

in which

q = specific discharge

n = porosity

t = time

$\tilde{K}$ = hydraulic conductivity tensor

ϕ = potentiometric head

C = mineral concentration = mass of salt divided by the mass of the saltwater mixture at any finite point within the control volume = ρ_s/ρ

ρ = density of saltwater mixture = $\rho_s + \rho_F$

ρ_s = density of salt within the mixture = mass salt in sample divided by volume of measured sample

ρ_F = density of freshwater

$\tilde{D}$ = dispersion tensor

γ = unit weight

γ_0 = unit weight of reference

α = constant relating mineral concentration with unit weight

Equation (3.4) does not account for the effect of temperature on the unit weight of the fluid. Since temperature can have a major effect on the unit weight, and thus the bouyancy of a fluid, Equation (3.4) will be incorporated into the model (Chapter 4) in a form which will account for temperature effects.

It is assumed in this analysis that only the three principal components (those components acting in the x-x, y-y, and z-z directions) of the hydraulic conductivity tensor, $\tilde{K}$, are non-zero. All other components are assumed to be equal to zero.

The Integral Method of Boundary Layer Approximation

The integral method was applied to the problem of description of fluid boundary layers adjacent to solid boundaries. Boundary layer theory was first introduced by Prandtl [1904]. Blasius [1908] was the first to discuss the concept of similar velocity profiles within a boundary layer. It is the concept of similar velocity profiles which is the base of the integral method. The integral method simplifies the appropriate equations by integrating over the boundary layer thickness. This procedure has been extended to many other types of problems in which integration occurs over some physical region of interest. Due to its original applications, this is often called a boundary layer approximation. This method has been widely used in treatment of the flow of jets and plumes in stratified or unstratified media.

In the integral method, one assumes mathematical forms for the profiles of parameters of interest, such as velocity and concentration, across the "boundary layer." The profiles are called similar profiles because the mathematical form is the same at each section, and some writers refer to these as similarity techniques. Once a similarity profile is introduced, this is the same as specifying the solution form within the "boundary layer" region. The integration of the basic equation, with these similarity profiles included, effectively reduces the dimensionality of the problem being solved. For example, in a circular jet discharge, specification of axisymmetric similar profiles and subsequent integration reduces the three-dimensional problem to one-dimensional.

As noted by Morton [1961] and Benedict et al. [1974], the effect of assuming similar profiles is to suppress analytical solution of the details of the structure through the "boundary layer." Therefore, any reasonable profile could be assumed. While different assumed profiles might lead, for example, to different values for various empirical parameters, the prediction of the overall behavior of the phenomenon being modeled is presumed not highly sensitive to the form of profile chosen. However, if one is interested in using the profile form to predict concentrations or velocities at specific points in the flow field, then the form needs to be selected as accurately as possible. It should further be noted that any such integral approach decreases in accuracy as regions are reached where the assumption of similar profiles breaks down.

By integrating Equations (3.2) and (3.3) through the transition zone and solving simultaneously Equations (3.1), (3.2), (3.3) and (3.4), Means [1982] obtained a simplified description of the stratified flow situation. In the solution, two different polynomials were used for variation of salt concentration and specific discharge across the transition zone. The constraints were essentially the following:

(a) For concentration - saltwater at the bottom of the transition zone, freshwater (zero concentration) at the top.

(b) For specific discharge in the horizontal direction - zero at the bottom of the transition zone, with the velocity from the freshwater region at the top of the transition zone.

The integration yields three equations with three unknowns: s, (drawdown), z_b (bottom of the transition zone), and δ (thickness of the transition zone). These equations are solved by an iterative ADI (Alternating Direction Implicit) finite difference scheme. The iteration is necessary because of the nonlinearity of the equations. Some features of the solution procedure will be useful to this work, but others will need substantial reworking. For example, some apparent anomalies exist in transition zone thickness beneath the center of the large pumping region studied by Means [1982]. These would be significant for a single well, as in the injection problem.

CHAPTER 4
ANALYSIS OF INJECTION

Introduction

In this chapter, Equations (3.1), (3.2), (3.3), and (3.4) will be applied to the injection situation.

Figure 4.1 shows a profile of the injection situation. The flow field in a situation where freshwater is injected into a saline aquifer is the reverse of the flow field caused by upconing of saltwater under a pumping well. Instead of flow moving radially in toward the well, flow is now moving radially outward away from the well. Instead of having a saltwater mound under a pumping well, there is now a freshwater lens underneath an injection well.

The flow in the freshwater lens is assumed horizontal; flow in the transition zone is assumed horizontal and of varying salt concentration; and flow in the saline region is assumed vertical.

Development of Equations

The integral method simplifies the development of the model by assuming similar profiles to represent the velocities and solute concentration in the transition zone. This allows Equation (3.2) to be used to describe the velocities in the zones of constant density while using the Integral Technique in the transition zone. By assuming that flow in the transition zone is horizontal ($q_z = 0$), the hydrostatic law of varying pressure may be applied

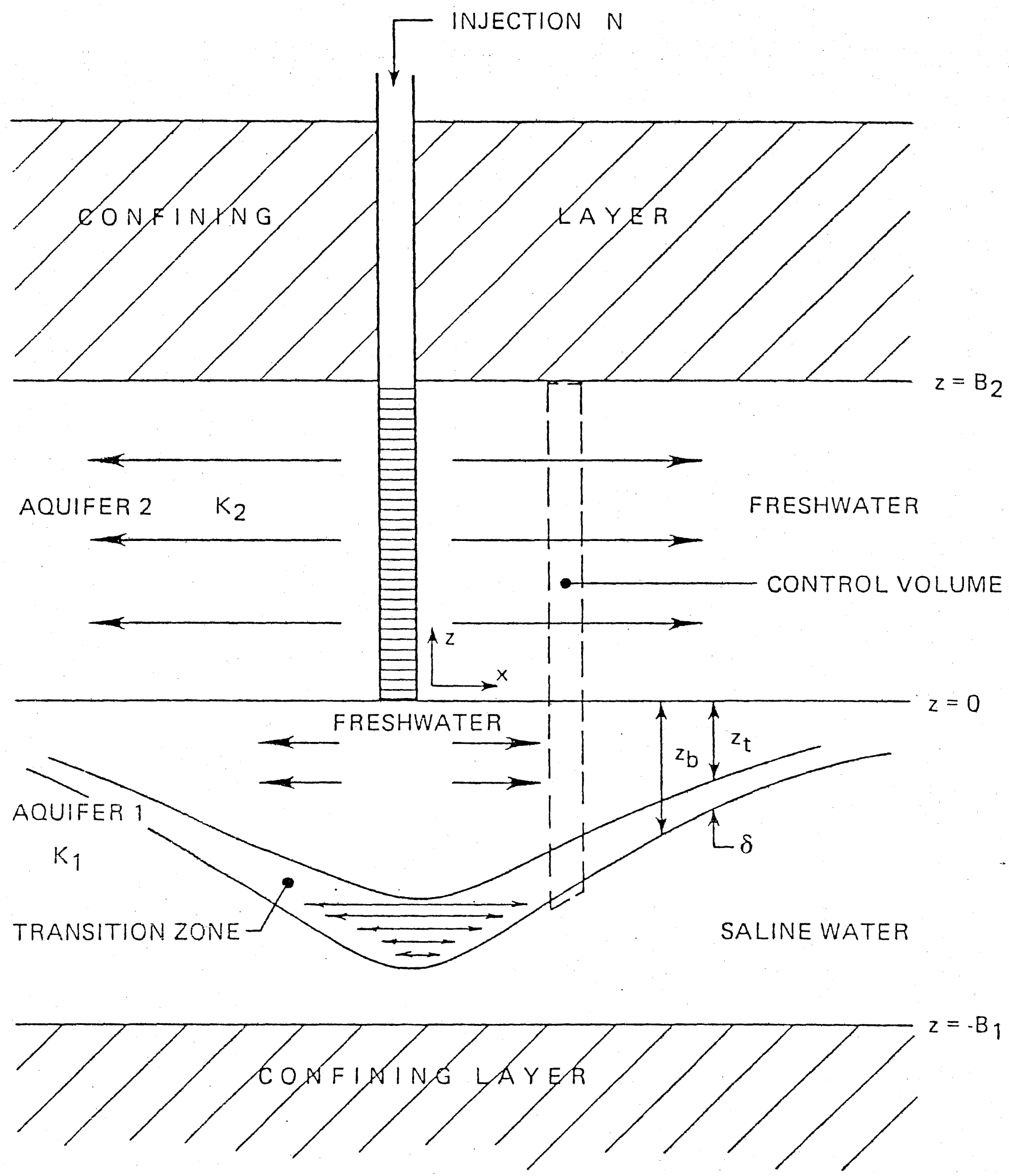

Figure 4.1 Schematic description of the development of a transition zone due to a freshwater injection into a saline aquifer

$$\partial p = -\gamma dz \tag{4.1}$$

Integrating (4.1) through the vertical thickness of the transition zone yields

$$p_t - p_b = -\int_{-z_b}^{-z_t} \gamma dz \tag{4.2}$$

where indices t and b represent the top and bottom of the transition zone, respectively. Potentiometric head, ϕ is defined as

$$\phi = \frac{P}{\gamma} + z$$

where P is the pressure of some point and z is the distance from some datum to the point. Applying (4.3) points at the top and bottom of the transition zone results in

$$\phi_{ft} = \frac{p_t}{\gamma_f} - z_t \tag{4.4}$$

$$\phi_{sb} = \frac{p_b}{\gamma_s} - z_b \tag{4.5}$$

where ϕ_{ft} and ϕ_{sb} are the potentiometric head at the top of the transition zone and bottom of the transition zone, respectively and indices f and s represent fresh and saline water, respectively. Rearranging (4.4) and (4.5)

$$p_t = \gamma_f(\phi_{ft} + z_t) \tag{4.6}$$

$$p_b = \gamma_s(\phi_{sb} + z_b) \tag{4.7}$$

Substituting (4.6) and (4.7) into (4.2), and dividing by $-\gamma_o$, where γ_o is the unit weight of reference, yields

$$\frac{\gamma_s}{\gamma_o}(\phi_{sb} + z_b) - \frac{\gamma_f}{\gamma_o}(\phi_{ft} + z_t) = \int_{-z_b}^{-z_t} \frac{\gamma}{\gamma_o} dz \tag{4.8}$$

From (3.4) it can be seen that

$$\gamma_s = \gamma_o(1 + \alpha C_s) \tag{4.9a}$$

$$\gamma_f = \gamma_o \tag{4.9b}$$

Inserting (3.4), (4.9a) and (4.9b) into (4.8)

$$(1 + \alpha C_s)(\phi_{sb} + z_b) - (\phi_{ft} + z_t)$$

$$= \int_{-z_b}^{-z_t} (1 + \alpha C)dz \tag{4.10}$$

It is assumed that the transition zone is a boundary layer which is isotropic in the x and y directions, and where the specific discharge and the solute concentration profiles satisfy the following similarity conditions

$$u = UF(\eta) \tag{4.11a}$$

$$v = VF(\eta) \tag{4.11b}$$

$$C = C_o L(\eta) \tag{4.11c}$$

where u and v are the components of specific discharge in the horizontal x and y direction, respectively; U and V are the reference specific discharge in the horizontal x and y direction, respectively: C_o is the reference concentration: F and L are the distribution functions for specific discharge and solute concentration, respectively; η is the dimensionless vertical coordinate within the transition zone and is defined as

$$\eta = \frac{[z - (-z_b)]}{\delta} = \frac{z + z_b}{\delta}\text{, and} \tag{4.12a}$$

$$\delta = -z_t - (-z_b) = z_b - z_t \tag{4.12b}$$

where, δ is the thickness of the transition zone.

Means (1982), suggested polynomials for the distribution functions F and L which will be employed in this work. These functions are defined as

$$F(\eta) = 2\eta - \eta^2 \tag{4.13a}$$

$$L(\eta) = 1 - 2\eta + \eta^2 \tag{4.13b}$$

It is assumed that the distribution functions are applied along the vertical axis. Actually these functions would be applied along an axis normal to the boundaries of the transition zone. The assumption of a vertical profile is probably valid as long as the slope of the transition zone is small. Differentiating (4.12a), with respect to the vertical coordinate z, yields

$$\frac{\partial\eta}{\partial z} = \frac{1}{\delta} \tag{4.14}$$

Introducing (4.11c), (4.12a), and (4.14) into (4.10) yields

$$\begin{aligned}(1 + \alpha C_s)(\phi_{sb} + z_b) - (\phi_{ft} + z_t)\\ = \int_0^1 [1 + \alpha C_o L(\eta)]\delta d\eta\end{aligned} \tag{4.15}$$

By introducing (4.12b) into (4.15), canceling δ on both sides of the equation and rearranging

$$\begin{aligned}(1 + \alpha C_s)\ \phi_{sb} - \phi_{ft} + \alpha C_s z_b\\ = \alpha C_o \delta \int_0^1 L(\eta) d\eta\end{aligned} \tag{4.16}$$

Introducing the salt concentration in saline water, C_s as $C_s = C_o$ and rearranging (4.16)

$$\phi_{ft} = (1 + \xi)\phi_{sb} + \xi z_b - \xi\delta \int_0^1 L(\eta) d\eta \tag{4.18a}$$

where

$$\xi = \alpha C_o = (\gamma_s - \gamma_f)/\gamma_f \tag{4.18b}$$

It is assumed that only constant vertical flow exists in the saltwater below the transition zone; as a result, if the porosity is assumed constant in time, (3.1) becomes

$$\frac{\partial w}{\partial z} = 0 \tag{4.19}$$

Consequently, w, the vertical velocity cannot vary vertically, and it must be equal to the value it attains at the bottom of the transition zone, which is given by

$$\frac{\partial(z_b)}{\partial t} = \frac{q_z}{n} = -\frac{K_z}{n}\frac{\partial\phi}{\partial z} \tag{4.20}$$

Rearranging and integrating through the saltwater region

$$\int_{-B_1}^{-z_b} \partial\phi = n\frac{\partial z_b}{\partial t}\int_{-B_1}^{-z_b} \frac{\partial z}{K_z} \tag{4.21}$$

Carrying out the integration, (4.21) becomes

$$\phi_{sb} - \phi_{B1} = n\frac{\partial z_b}{\partial t}\left[\frac{-z_b + B_1}{K_z}\right] \tag{4.22}$$

Initially, $\phi_{B_1} = \phi_{so}$, where ϕ_{so} is the potentiometric head at the bottom of aquifer 1 at time = 0; substituting for ϕ_{B1} and rearranging (4.22).

$$\phi_{sb} = \phi_{so} + n\frac{\partial z_b}{\partial t}\left[\frac{B_1 - z_b}{K_z}\right] \tag{4.23}$$

It is assumed that before injection occurs, vertical equipotentials exist throughout the aquifer, whereby applying continuity of pressure gives

$$\phi_{so}\gamma_s = \phi_{fo}\gamma_f \tag{4.23b}$$

where ϕ_{fo} is the potentiometric head at z = 0, time = 0.

Introducing (4.23) and (4.23b) into (4.18a) gives

$$\phi_{ft} = \phi_{fo} + (1 + \xi)n \frac{\partial z_b}{\partial t} \left[\frac{B_1 - z_b}{K_z}\right] + \xi z_b$$

$$- \xi\delta \int_0^1 L(\eta)d\eta \qquad (4.24)$$

where ϕ_{ft} is the potentiometric head in the freshwater zone at any time, t.

The increase of potentiometric head at a point due to injection into an aquifer is defined as

$$s = \phi_{ft} - \phi_{fo} \qquad (4.25)$$

where s is the head build-up. Introducing (4.25) into (4.24) and rearranging yields

$$\frac{\partial z_b}{\partial t} = \frac{K_z}{n(B1 - z_b)(1 + \xi)} \left(s - \xi z_b + \xi\delta \int_0^1 L(\eta)d\eta\right) \qquad (4.26)$$

which is the equation describing the rate of growth of the freshwater lens.

The injection of freshwater into saline water creates a nonhomogeneous, binary process involving a mixture of freshwater and salt. For a nonhomogeneous fluid, the conservation of mass principle must be satisfied for each component of the fluid mixture. Figure 4.2 is a control volume for the conservation of freshwater taken from the top of aquifer 2 to the bottom of the transition zone in aquifer 1. The convection and diffusion terms are shown as inflows and outflows of the control volume.

The conservation of freshwater mass equation will be derived first. The sum of all freshwater mass inflows are equal to the rate of

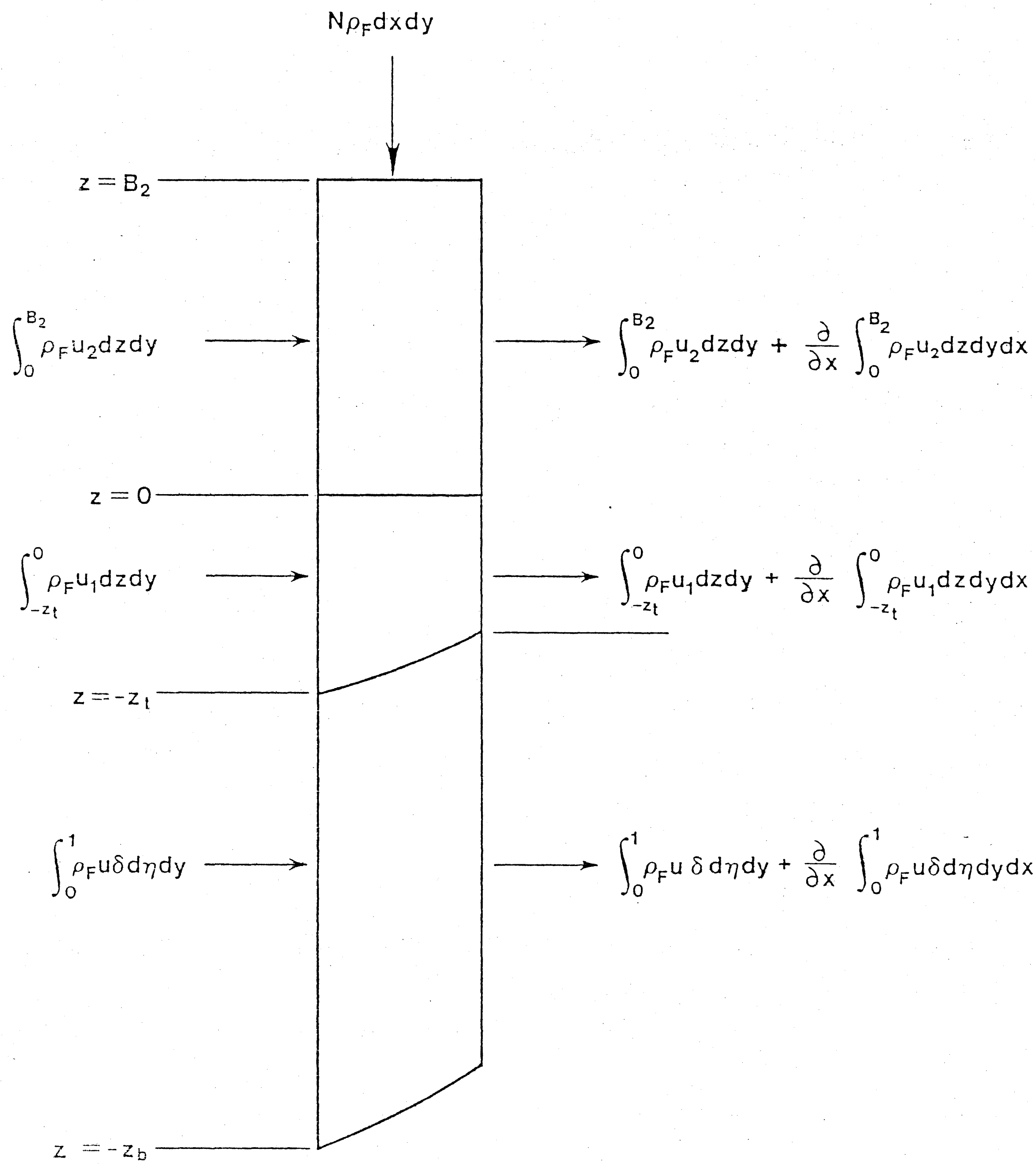

Figure 4.2 Control volume for conservation of mass of freshwater

change of storage of freshwater in the control volume. This fact can be written as follows:

$$
\begin{aligned}
&- \frac{\partial}{\partial x}\int_{0}^{B_2} \rho_F u_2 dzdxdy - \frac{\partial}{\partial y}\int_{0}^{B_2} \rho_F v_2 dzdydx \\
&- \frac{\partial}{\partial x}\int_{-z_t}^{0} \rho_F u_1 dzdxdy - \frac{\partial}{\partial y}\int_{-z_t}^{0} \rho_F v_1 dzdydx \\
&- \frac{\partial}{\partial x}\int_{0}^{1} \rho_F u\delta d\eta dxdy - \frac{\partial}{\partial y}\int_{0}^{1} \rho_F v\delta d\eta dydx \\
&+ N\rho_F dxdy = \frac{\partial}{\partial t}\int_{-z_b}^{B_2} \rho_F ndzdxdy
\end{aligned}
\tag{4.27}
$$

where u and v are components of specific discharge in the x and y directions, respectively, ρ_F is the density of freshwater and n is the porosity of the aquifer.

The term on the right hand side of the equality sign in Equation 4.27 is the storage term. Any net inflows or outflows to or from the control volume are accounted for in this term. It is assumed that ρ_F, n, dx, and dy are constant with depth of the aquifer. Rewriting the storage term in Equation 4.27 yields:

$$
\frac{\partial}{\partial t}\int_{-z_b}^{B_2} \rho_F ndzdxdy = \frac{\partial}{\partial t}\left(\rho_F ndxdy\int_{-z_b}^{B_2} dz\right) \tag{4.28}
$$

Integrating 4.28 and differentiating with respect to time yields

$$
\frac{\partial}{\partial t}\int_{-z_b}^{B_2} \rho_F ndzdxdy = \frac{\partial \rho}{\partial t} ndxdy + \frac{\partial z_b}{\partial t} \rho_F ndxdy \tag{4.29}
$$

where ρ is the density of the saltwater mixture.

The first term on the right side of the equality sign of Equation 4.29 refers to the changing mass of freshwater with time within the control volume due to the compressibility of the fluid and the aquifer. The second term on the right side of the equality sign of Equation 4.29 refers to the change in mass of freshwater due to a change in size of the control volume. A change in the control volume size is effected by the growth of the freshwater lens. Equation 4.29 may now be written as follows:

$$\frac{\partial}{\partial t}\int_{-z_b}^{B_2} \rho_F n\,dz\,dx\,dy = \frac{\partial M_s}{\partial t} + \frac{\partial z_b}{\partial t}\rho_F n\,dx\,dy \tag{4.30}$$

where the term $\frac{\partial M_s}{\partial t}$ is the change in mass of freshwater in the control volume due to the compressibility of the aquifer. The subscript s in this term indentifies the mass change as a change due to the storativity of the aquifer and fluid.

Substituting (4.12) and (4.13) and (4.30) into Equation (4.27), and using (4.11a) and (4.11b) to represent the velocity terms in the transition zone of Equation (4.27) and dividing Equation (4.27) by ρ_F, dx and dy yields

$$- \frac{\partial}{\partial x}\int_0^{B_2} u_2 dz - \frac{\partial}{\partial y}\int_0^{B_2} v_2 dz - \frac{\partial}{\partial x}\int_{-z_t}^{0} u_1 dz - \frac{\partial}{\partial y}\int_{-z_t}^{0} v_1 dz$$

$$- \frac{\partial}{\partial x}\int_0^{1} u_1 F(\eta)\delta d\eta - \frac{\partial}{\partial y}\int_0^{1} v_1 F(\eta)\delta d\eta + N$$

$$= \frac{\partial M_s}{\partial t}\frac{1}{\rho_F dx dy} + n\frac{\partial z_b}{\partial t} \tag{4.31}$$

The first storage term on the right side of Equation (4.31) may be rewritten as

$$\frac{\partial M_s}{\partial t}\,\frac{1}{\rho_F dxdy} = \frac{\partial M_s}{\partial t}\,\frac{(B_2 + Z_b)}{\rho_F dv} \tag{4.32}$$

The storage due to the compressibility of the aquifer and its fluid is defined as follows:

$$\frac{\partial M_s}{\partial t}\,\frac{(B_z + z_b)}{\rho_F dv} = \rho g n \alpha_A (B_2 + z_b)\left(1 + \frac{\alpha_F}{n\alpha_A}\right)\frac{\partial s}{\partial t} = S\,\frac{\partial s}{\partial t} \tag{4.33}$$

where v is the volume of the control volume, g is the gravitational acceleration of the earth, α_A and α_F are the reciprocal of the bulk-modulus of elasticity of the aquifer and fluid, respectively, s is the head buildup of the fluid in the aquifer, and S is the storativity of the aquifer.

It can be seen from (3.2) that

$$u = -K\frac{\partial s}{\partial x} \tag{4.34a}$$

$$v = -K\frac{\partial s}{\partial y} \tag{4.34b}$$

where K is the hydraulic conductivity of the aquifer. Once again, the sign of the derivatives is consistent with the definition of s given in Equation (4.25).

Introducing (4.32), (4.33), (4.34a) and (4.34b) into Equation (4.31) yields

$$\frac{\partial}{\partial x}\int_0^{B_2} K_2\,\frac{\partial s}{\partial x}\,dz + \frac{\partial}{\partial y}\int_0^{B_2} K_2\,\frac{\partial s}{\partial y}\,dz + \frac{\partial}{\partial x}\int_{-z_t}^{0} K_1\,\frac{\partial s}{\partial x}\,dz + \frac{\partial}{\partial y}\int_{-z_t}^{0} K_1\,\frac{\partial s}{\partial y}\,dz$$

$$+ \frac{\partial}{\partial x}\int_0^1 K_1\,\frac{\partial s}{\partial x}\,F(\eta)\delta d\eta + \frac{\partial}{\partial y}\int_0^1 K_1\,\frac{\partial s}{\partial y}\,F(\eta)\delta d\eta + N$$

$$= S\,\frac{\partial s}{\partial t} + n\,\frac{\partial z_b}{\partial t} \tag{4.35}$$

Integrating and rearranging Equation (4.35) yields

$$\frac{\partial}{\partial x}\left[K_1\left(\beta + \delta\int_0^1 F(\eta)d\eta\right)\frac{\partial s}{\partial x}\right] + \frac{\partial}{\partial y}\left[K_1\left(\beta + \delta\int_0^1 F(\eta)d\eta\right)\frac{\partial s}{\partial y}\right]$$

$$+ N - n\frac{\partial z_b}{\partial t} = S\frac{\partial s}{\partial t} \tag{4.36}$$

where

$$\beta = \frac{B_2K_2}{k_1} + z_b - \delta \tag{4.37}$$

Equations (4.36) and 4.37) describe the conservation of mass of freshwater. Next, the conservation of mass of salt equation will be written. Figure 4.3 is a control volume for the conservation of salt taken from the top of aquifer 2 to the bottom of the transition zone in aquifer 1. Note that in Figure 4.3 it is assumed that all dispersed salt comes from the saltwater region, and that no diffusion of the salt occurs across the top of the transition zone. The rate of change of storage of the salt in a given volume is equal to the sum of all inflows and outflows of the material, plus any internal sources and sinks (such as radioactive decay, biological degradation, etc., none of which exist for salt).

The conservation of mass of salt equation is written as follows:

$$- \frac{\partial}{\partial x}\int_0^1 \rho\, u_1F(\eta)C\delta d\eta dxdy$$

$$- \frac{\partial}{\partial y}\int_0^1 \rho\, v_1F(\eta)C\delta d\eta dydx$$

$$+ \left(-D\frac{\partial C}{\partial z}\bigg|_{z=z_b} \rho\, dxdy\right) = \frac{\partial}{\partial t}\int_{-z_b}^{-z_t} \rho C n dzdxdy \tag{4.38}$$

where C the concentration of salt and D is the diffusion coefficient. In the transition zone, Equation (4.11c) describes the concentration of

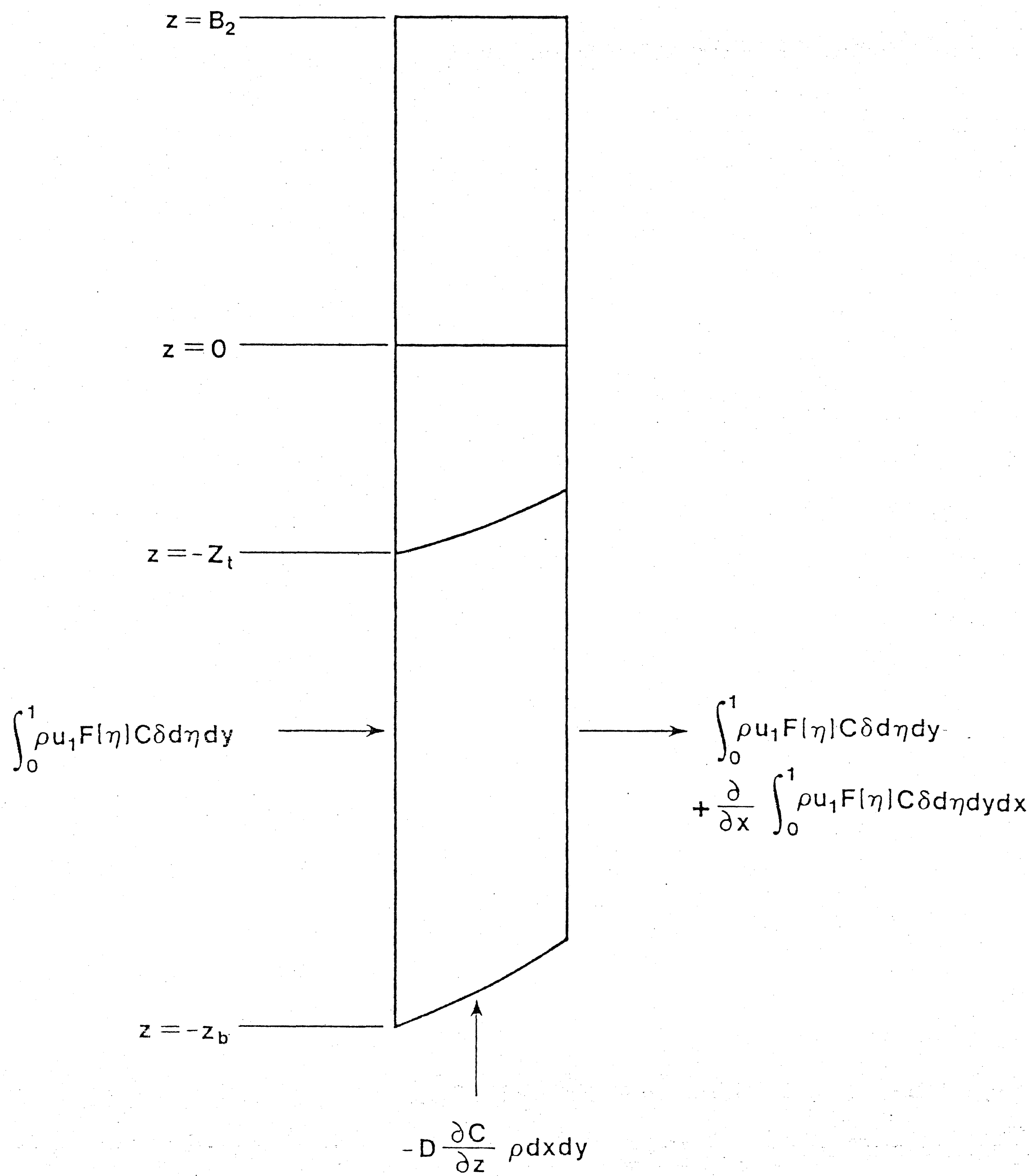

Figure 4.3 Control volume for conservation of mass of salt

salt as $C = C_0L(\eta)$. Substituting Equation (4.11c), (4.12), (4.13), and (4.14) into Equation (4.38) and dividing by ρ, dx, and dy yields

$$- \frac{\partial}{\partial x}\int_0^1 u_1 F(\eta) C_0 L(\eta)\delta d\eta - \frac{\partial}{\partial y}\int_0^1 v_1 F(\eta) C_0 L(\eta)\delta d\eta$$

$$- \frac{D}{\delta}\left.\frac{\partial(C_0L(\eta))}{\partial\eta}\right|_{\eta=0} = \frac{\partial}{\partial t}\int_0^1 nC_0 L(\eta)\delta d\eta \qquad (4.39)$$

Dividing Equation (4.39) by C_0 and multiplying by δ and re-arranging yields

$$(\frac{n}{2}\int_0^1 L(\eta)d\eta)\,\frac{\partial\delta^2}{\partial t} + [\delta^2(\frac{\delta u_1}{\delta x} + \frac{\delta v_1}{\partial y}) + \frac{1}{2}\,(u_1\frac{\partial\delta^2}{\partial x} + v_1\,\frac{\partial\delta^2}{\partial y})]\int_0^1 F(\eta)L(\eta)d\eta$$

$$= -DL'(0) \qquad (4.40)$$

where D is generally accepted to be proportioned to the absolute value of the specific discharge, or

$$D = a(u_1{}^2 + v_1{}^2)^{1/2} \qquad (4.41)$$

where a is equal to the transverse dispersivity of the aquifer.

Introducing Equations (4.41), (4.34a) and (4.34b) into Equation (4.40), one obtains

$$\frac{n}{2}\,(\int_0^1 L(\eta)d\eta)\,\frac{\partial\delta^2}{\partial t} - [\delta^2 K_1(\frac{\partial^2 s}{\partial x^2} + \frac{\partial^2 s}{\partial y^2})$$

$$+ \frac{1}{2}\,K_1\,(\frac{\partial s}{\partial x}\,\frac{\partial\delta^2}{\partial x} + \frac{\partial s}{\partial y}\,\frac{\partial\delta^2}{\partial y})]\int_0^1 F(\eta)L(\eta)d\eta$$

$$= -aK_1\,[(\frac{\partial s}{\partial x})^2 + (\frac{\partial s}{\partial y})^2]^{1/2}\,L'(0) \qquad (4.42)$$

The pertinent equations to solve now become Equations (4.26), (4.36), (4.37) and (4.42). These equations could be solved by perturbation techniques (e.g. Rubin and Pinder, 1977), but the possibilities of multiple wells and aquifer inhomogeneities suggest that a numerical solution will provide more flexibility. Such a solution procedure will be outlined in Chapter 5.

The equations developed in this chapter should provide a sound basis for analysis of many injection problems. Numerous assumptions have been made to simplify the equations while still maintaining the basic character of the physical system.

CHAPTER 5
NUMERICAL SIMULATION

Development of the Numerical Model

Equations (4.26), (4.36) and (4.42) completely describe the flow process due to a freshwater injection into a saline aquifer. Equation (4.37) allows continuous updating of the flow thickness. In this chapter a method will be devised in which these equations can be solved simultaneously to provide a description of the injection process. Since Equations (4.26), (4.36) and (4.42) are non-linear and expressed by three independent variables (two spatial variables and a time variable), a numerical scheme will provide the most direct solution. Since finite element and boundary integral models are generally more site-specific and useful for only one application, a finite difference numerical scheme will be used. The finite difference scheme has the advantage of being applicable to a wide variety of boundary situations, requiring somewhat less input data, and requiring somewhat less computer time and space.

Since Equations (4.26), (4.36) and (4.42) must all be solved simultaneously, it is advantageous to use an iterative alternating direction implicit (IADI) finite difference method. The main advantage of using an ADI method is that for each time step it reduces large sets of simultaneous equations into smaller sets [Bear, 1979]. The ADI method is accomplished by breaking the desired forward stepping in time into two steps. First, the unknowns are solved for in the x-direction at the advanced time step using the known terms being set in the y-direction at the previous time step. In the second half advancing time step, the situation reverses. The unknown values at the advanced time step are now written in the y-direction and are solved using the values in the x-direction at the previous time step. Since Equations (4.26), (4.36) and (4.42) are all interdependent on each other, it is necessary to solve them iteratively. This means that the ADI process is repeated for each time step, using in each iteration updated values.

A Finite Difference Approximation of Equation (4.36)

In formulating a finite difference approximation for Equation (4.36), an ADI method is used so that there are only three unknown variables at one node (the three variables at the advanced time step). Using only three unknowns at each node, a tridiagonal matrix can be generated for each column or row of a time step. This is the main reason for going to an ADI method, for reduction to a tridiagonal matrix allows use of the highly efficient Thomas algorithm for solution of the system of equations.

An implicit ADI finite difference scheme for the calculation of head build up, (4.36), is presented as follows:

First, the calculations are made for the unknowns in the x-direction at the (m+1) time step using known values in the y-direction at the (m) level.

$$-s_{i-1,j}^{(m+1)}\left[\left(\beta+\delta\int_0^1 F(\eta)d\eta\right)\frac{K_1\Delta t}{(\Delta x)^2}\right]_{i-0.5,j}^{(m+0.5)}+s_{i,j}^{(m+1)}\Big\{S$$

$$+\left[\left(\beta+\delta\int_0^1 F(\eta)d\eta\right)\frac{K_1\Delta t}{(\Delta x)^2}\right]_{i+0.5,j}^{(m+0.5)}+\left[\left(\beta+\delta\int_0^1 F(\eta)d\eta\right)\frac{K_1\Delta t}{(\Delta x)^2}\right]_{i-0.5,j}^{(m+0.5)}\Big\}$$

$$- s_{i+1,j}^{(m+1)}[(\beta + \delta\int_0^1 F(\eta)d\eta)\frac{K_1\Delta t}{(\Delta x)^2}]_{i+0.5,j}^{(m+0.5)} = S\ s_{i,j}^{(m)} - n\ (\frac{\partial z_b}{\partial t})_{i,j}^{(m+0.5)}\Delta t$$

$$+ N_{i,j}\ \Delta t + (s_{i,j+1}^{(m)} - s_{i,j}^{(m)})[(\beta + \delta\int_0^1 F(\eta)d\eta)\ \frac{K_1\Delta t}{(\Delta y)^2}]_{i,j+0.5}^{(m+0.5)}$$

$$+ (s_{i,j-1}^{(m)} - s_{i,j}^{(m)})[(\beta + \delta\int_0^1 F(\eta)d\eta)\ \frac{K_1\Delta t}{(\Delta y)^2}]_{i,j-0.5}^{(m+0.5)} \tag{5.1}$$

where

$$\beta = \frac{B_2K_2}{K_1} + Z_b - \delta \tag{5.2}$$

In Equation (5.1), the notation m implies known values from the previous time step, while (m+0.5) represents an average over the time step from time (m) to time (m+1). Similarly, the notation (i-0.5) and (i+0.5) implies use of appropriate average values over the space increment from i-1 to i and from i to i+1, respectively. The notation j+0.5 has a similar meaning. For example, the value of δ used in such averaged terms will be the average of the δ values at the two end points of the indicated region. Note that this also allows one to conveniently specify K values which vary spatially.

Next, the calculations are made for the unknowns in the y-direction at the (m+2) time step using the previously calculated values in the x-direction at the (m+1) time step.

$$-s_{i,j-1}^{(m+2)}\ [(\beta + \delta\int_0^1 F(\eta)d\eta)\frac{K_1\Delta t}{(\Delta y)^2}]_{i,j-0.5}^{(m+1.5)} + s_{i,j}^{(m+2)}\ \{S + [(\beta$$

$$+ \delta\int_0^1 F(\eta)d\eta)\ \frac{K_1\Delta t}{(\Delta y)^2}]_{i,j+0.5}^{(m+1.5)} + [(\beta + \delta\int_0^1 F(\eta)d\eta\frac{K_1\Delta t}{(\Delta y)^2}]_{i,j-0.5}^{(m+1.5)}\}$$

$$-s_{i,j+1}^{(m+2)}[(\beta + \delta\int_0^1 F(\eta)d\eta\ \frac{K_1\Delta t}{(\Delta y)^2}]_{i,j+0.5}^{(m+1.5)} = S\ s_{i,j}^{(m+1)}\ -n\ (\frac{\partial z_b}{\partial t})_{i,j}^{(m+1.5)}\Delta t$$

$$+ N_{i,j}\Delta t + (s_{i+1,j}^{(m+1)} - s_{i,j}^{(m+1)})[(\beta + \delta\int_0^1 F(\eta)d\eta)\frac{K_1\Delta t}{(\Delta x)^2}]_{i+0.5,j}^{(m+1.5)} + (s_{i-1,j}^{(m+1)}$$

$$- s_{i,j}^{(m+1)})[(\beta + \delta\int_0^1 F(\eta)d\eta)\frac{K_1\Delta t}{(\Delta x)^2}]_{i-0.5,j}^{(m+1.5)} \qquad (5.3)$$

where β is defined by (5.2)

In Equation (5.3), the 0.5 superscripts again mean averages over the pertinent temporal or spatial increment. The superscript (m+1.5) implies a time average over the step from (m+1) Δt to (m+2)Δt. The spatial subscripts such as (i+0.5), (i+0.5), and (j-0.5) represent spatial averages as in Equation (5.1).

A Finite Difference Approximation to Equation (4.42)

It was observed that when Means [1982] used a centered difference scheme for representation of the velocities in his pumping model, several anomalies occurred in the vicinity of the well.

It is generally accepted that a centered difference scheme gives the most accurate finite difference description of gradients in the vicinity of a point. It has been observed in this report however, that the centered difference scheme does not work when representing velocities (head gradients) in the vicinity of a well. At a relative maximum or minimum on a head-curve, a centered difference scheme will give a gradient of zero. This is technically the correct gradient when Δx approaches to zero, but for a finite grid size there actually is a relatively large gradient in the increment adjacent to the well. It is for this reason that a backward difference scheme is used when representing velocity terms in the transition zone thickness calculation. The following is a backward difference representation of the squared thickness of the transition zone in the x-direction:

$$(\frac{n}{2}\int_0^1 L(\eta)d\eta)\ \frac{\delta^{2\,(m+1)}_{i,j} - \delta^{2\,(m)}_{i\,j}}{\Delta t} - [\delta^{2\,(m+1)}_{i,j}\ K_{1,i,j}(\frac{s^{(m+1)}_{i+1,j} - 2s^{(m+1)}_{i,j} + s^{(m+1)}_{i-1,j}}{(\Delta x)^2})$$

$$+ \delta^{2\,(m)}_{i,j}\ K_{1,i,j}(\frac{s^{(m)}_{i,j+1} - 2s^{(m)}_{i,j} + s^{(m)}_{i,j-1}}{(\Delta y)^2}) + \frac{1}{2}K_{1,i,j}\ (\frac{s^{(m+1)}_{i,j} - s^{(m+1)}_{i-1,j}}{\Delta x})$$

$$(\frac{\delta^{2\,(m+1)}_{i,j} - \delta^{2(m+1)}_{i-1,j}}{\Delta x}) + \frac{1}{2}K_{1,i,j}(\frac{s^{(m)}_{i,j} - s^{(m)}_{i,j-1}}{\Delta y})(\frac{\delta^{2\,(m)}_{i,j} - \delta^{2\,(m)}_{i,j-1}}{\Delta y})]\int_0^1 F(\eta)L(\eta)d\eta$$

$$= - ak_{1,i,j}\ [(\frac{-s^{(m+1)}_{i,j} + s^{(m+1)}_{i-1,j}}{\Delta x})^2 + (\frac{-s^{(m+1)}_{i,j} + s^{(m+1)}_{i,j-1}}{\Delta y})^2]^{1/2}\ \ L'(0) \qquad (5.4)$$

The equation can now be solved implicitly for $\delta^{2\ (m+1)}_{i,j}$.

Likewise, for the calculation of the squared thickness of the transition zone in the y-direction at time step (m+2), Equation (4.42) can be written as follows:

$$(\frac{n}{2}\int_0^1 L(\eta)d\eta)\ \frac{\delta^{2\,(m+2)}_{i,j} - \delta^{2\,(m+1)}_{i,j}}{\Delta t} - [\delta^{2\,(m+1)}_{i,j}\ K_{1,i,j}(\frac{s^{(m+1)}_{i+1,j} - 2s^{(m+1)}_{i,j} + s^{(m+1)}_{i-1,j}}{(\Delta x)^2})$$

$$+ \delta^{2\,(m+2)}_{i,j}\ K_{1,i,j}(\frac{s^{(m+2)}_{i,j+1} - 2s^{(m+2)}_{i,j} + s^{(m+2)}_{i,j-1}}{(\Delta y)^2}) + \frac{1}{2}K_{1,i,j}(\frac{s^{(m+1)}_{i,j} - s^{(m+1)}_{i-1,j}}{\Delta x})$$

$$(\frac{\delta^{2\,(m+1)}_{i,j} - \delta^{2\,(m+1)}_{i-1,j}}{\Delta x}) + \frac{1}{2}K_{1,i,j}(\frac{s^{(m+2)}_{i,j} - s^{(m+2)}_{i,j-1}}{\Delta y})(\frac{\delta^{2\ (m+2)}_{i,j} - \delta^{2\ (m+2)}_{i,j-1}}{\Delta y})]$$

$$\int_0^1 F(\eta)L(\eta)d\eta = -aK_{1,i,j}\left[\left(\frac{-s_{i,j}^{(m+1)} + s_{i-1,j}^{(m+1)}}{\Delta x}\right)^2 + \left(\frac{-s_{i,j}^{(m+2)} + s_{i,j-1}^{(m+2)}}{\Delta y}\right)^2\right]^{1/2} L'(0) \tag{5.5}$$

This equation can also be solved for $\delta_{i,j}^{2(m+1)}$.

A Finite Difference Approximation to Equation (4.26)

The equation for calculation of the change in thickness of the freshwater lens with respect to time is written simply as follows:

$$\left(\frac{\partial z_b}{\partial t}\right)_{i,j}^{m+0.5} = \left[\frac{K_z}{n(B1-z_b)(1+\xi)}\left(s - \xi z_b + \xi\delta\int_0^1 L(\eta)d\eta\right)\right]_{i,j}^{(m+0.5)} \tag{5.6}$$

General Solution Procedure

First a grid is created in the x-y plane. On the grid there are n number of nodes in the x-direction each spaced Δx distance apart. There are m number of nodes in the y-direction that are each spaced Δy distance apart. Arrays containing the permeabilities, storativities, and well magnitudes for each point are superimposed on the finite difference grid so that each point on the grid is represented by its corresponding points on the arrays.

As the solution procedure begins, the head buildups are first calculated using the ADI method. Depending on the time step, Equation (5.1) or (5.3) is used. At the first time step, Equation (5.1) is used going in the x-direction one row at a time. At the end of each row a tri-diagonal matrix has been formed and is solved using the Thomas Algorithm. After Equation (5.1) has been solved, the values of the head build-up will be used in the solution of the thickness of the transition zone, Equation (5.4).

With the values calculated in the head build-up and the transition zone thickness, the solution of the change in size of the freshwater lens with respect to time can be calculated from Equation (5.6). As stated previously, the solution of the governing equations must be iterative since the equations are nonlinear. The iterations continue until some specified level of tolerance is met; that is, the difference in the parameter from one iteration to the next must be less than the specified allowable difference.

Once the required tolerance has been met in the x-direction portion of the ADI prodecure, the next time step proceeds. Drawdowns are calculated using Equation (5.3), with δ^2 being obtained from Equation (5.5). The bottom of the transition zone can be found by use of Equation (5.6). Figure 5.1 shows a concise flow chart illustrating the calculation strategy.

Stability and Convergence Characteristics of Numerical Scheme

Because the equations being used here are nonlinear, it is difficult to perform one of the standard stability analyses on the equations to determine their expected stability and convergence as a function of time and distance steps and the pertinent physical parameters. However, some preliminary estimates can be made based on available literature on solution of the groundwater and diffusion equations by similar schemes. Bear (1979), Holly (1975), and numerous others present such material. The basic drawdown equation, Equation (4.33), with finite difference counterparts (5.1) and (5.3), should be influenced only slightly by values of δ and z_b. The stability criterion for it, as well as an indicator of convergence (or accuracy), should be something like

$$\frac{T}{S}\frac{\Delta t}{\Delta x^2} \leqslant C_1 \qquad (5.7)$$

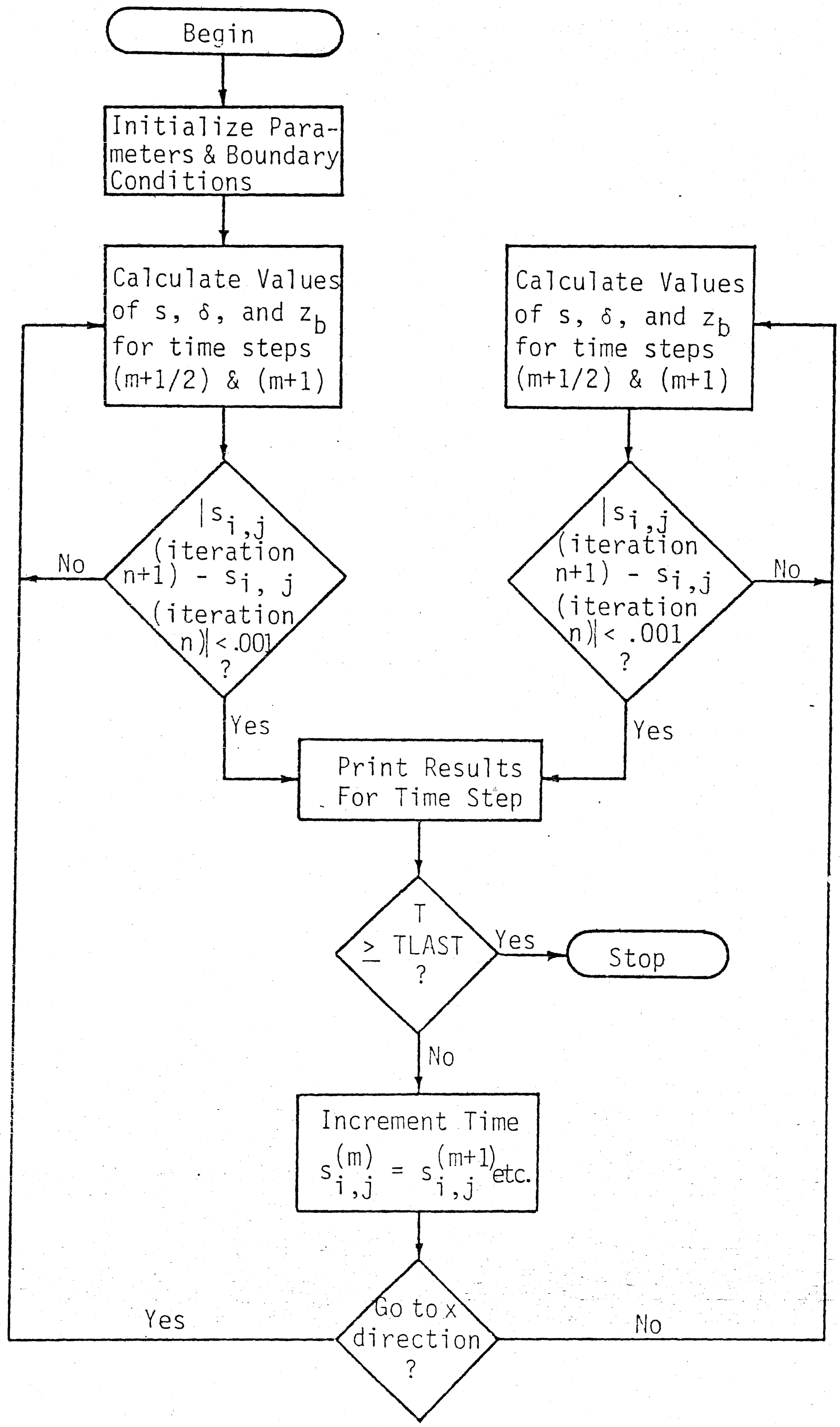

Flow Chart

Figure 5.1 Flow chart of numerical model in which C_1 = constant depending on the exact scheme used, but probably about 0.5.

Similarly, the dispersion equation, represented by Equation (4.47) and its finite difference representation Equation (5.4) or (5.5), will likely adhere to a constraint something like

$$D \frac{\Delta t}{\Delta x^2} \leqslant C_2 \tag{5.8}$$

in which C_2 = a constant which may or may not be equal to C_1.

There may be other constraints placed on model performance as well. For example, numerical experimentation suggested that for the very first time steps some relationship between the rate of growth of z_b and the other terms exists which may require even smaller time steps than given by Equation (5.7) and proved to always be the controlling factor in determining an acceptable time step. For typical values of T/S of 10^8 - 10^9 m/day, the time step required by Equation (5.7) was in the order of 0.0001 days or less for typical values of Δx of 100-500 meters.

While such time steps may in fact be necessary for some problems requiring the complete model capabilities, these small time steps begin to increase computational time substantially, especially if one is interested in times on the order of months or years. Therefore, in trying to be consistent with one of the stated objectives of this project, to minimize computer time and storage requirements, alternative approaches were sought for use in appropriate cases. It is expected that drawdown will stabilize much more quickly than the other parameters. In fact, drawdown is expected to stabilize in about a day or so; in fact, for the Pinellas County situation in Chapter 6, the drawdown will stabilize within an hour. This rapid convergence of the drawdown, coupled with its severe constraint on allowable time step suggests two possible alternatives in the calculation procedure. First, one can proceed with the numerical scheme as is, but with provisions to begin bypassing Equations (5.1) and (5.3) when the drawdown reaches steady state (as measured by the rate of change falling below some specified level). A second approach would involve bypassing Equations (5.1) and (5.3) altogether and using an analytical method for calculation of the drawdowns. The particular method would depend on the aquifer situation in the area being modeled. Either one of these methods would relax the time step constraints, although the first method would still require small steps for a period of time. In the following paragraphs, the use of the second scheme will be outlined. Subsequent results will show that time steps of at least one day can be tolerated with the analytical scheme.

A Simplified Injection Model

By replacing Equation (4.36) with an analytical drawdown relationship, some simplifying assumptions must be made. It is assumed that the stratified conditions in the aquifer do not affect the drawdowns. This assumption was checked with field data from the United States Geological Survey report on injection wells in the Pinellas County, Florida area [Hickey, 1982] and was found to be valid.

Analytical Calculation of Head Build-up

There are many analytical methods available for the calculation of drawdowns due to the influence of a well. Theis [1935] developed a drawdown equation for unsteady flow in a confined aquifer.

$$\phi_o - \phi = \frac{Q}{4\Pi T}\int_{y=\Omega}^{\infty} \frac{e^{-y}dy}{y} \qquad (5.9)$$

where Q = discharge or injection rate of the well, T = transmissivity of the aquifer, and Ω is given by the following relationship:

$$\Omega = \frac{r^2 S}{4Tt} \tag{5.10}$$

where r = radius from the well to the point evaluated, S = storativity of the aquifer, and t = time since the injection or pumping began.

The exponential integral in Equation (5.9) can be approximated by an infinite series

$$\int_{\Omega}^{\infty} \frac{e^{-\Omega} d\Omega}{\Omega} = 0.5772 - \ln \Omega + \Omega - \frac{\Omega^2}{2 \cdot 2!} + \frac{\Omega^3}{3 \cdot 3!} - \cdots \tag{5.11}$$

for a small value of Ω, the sum of the series beyond Ω becomes negligible [Cooper and Jacob, 1946].

Although Equation (5.9), using (5.10) and (5.11), provides an accurate solution for a confined aquifer, it does not account for leakance in the confining layer. Since most practical applications would encounter leakance, it is desirable to account for leakance in the drawdown calculations.

Hantush and Jacob [1955] developed the following relationship describing the drawdown due to unsteady flow to a well in an infinite leaky confined aquifer.

$$\phi_o - \phi = \frac{Q}{4\Pi T} \int_{y=\Omega}^{\infty} \frac{1}{y} \exp\left(-y - \frac{(r/\lambda)^2}{4y}\right) dy \tag{5.12}$$

$$= \frac{Q}{4\Pi T} W(\Omega, r/\lambda) \tag{5.13}$$

where Ω is defined in Equation (5.10), r is the radius from the well, and

$$\lambda = \left(\frac{B'T}{K'}\right)^{1/2} \tag{5.14}$$

where λ is the leakage factor; T is the transmissivity of the aquifer; and K' is the thickness and permeability of the semiconfining layers, respectively.

For a large r/λ value, the integral in Equation (5.12) can be approximated by a Taylor series expansion [Hunt, 1978]. A more simple and accurate representation is an asymptotic expansion by Wilson and Miller [1982].

$$W(\Omega,\ r/\lambda) = \left(\frac{\Pi\lambda}{2r}\right)^{1/2} \exp\left(\frac{-r}{\lambda}\right) \operatorname{erfc}\left(-\frac{\frac{r}{\lambda} - 2\Omega}{2\Omega^{1/2}}\right) \qquad (5.15)$$

where erfc is the complementary error function.

The previous approximation was used extensively in this report. A problem occurs, however, in aquifers of high transmissivities, especially at locations close to the well where r/λ values are small and the assumption of large r/λ values is violated.

An alternate solution of Equation (5.12) is to numerically integrate the integral using a numerical integration technique. This method yielded excellent results for calculation of drawdowns, and worked for a wide variety of injection situations.

In an effort to conserve computer resources, a relationship developed by Hantush was used to approximate Equation (5.12). The assumption for the following relationship is that $\Omega < r^2/20\lambda^2$ if $\Omega < 1$ [Bear, 1979]

$$W(\Omega,\ r/\lambda) = 2K_0(r/\lambda) - I_0(r/\lambda)\ W(Tt/S\lambda^2) \qquad (5.16)$$

Where K_0 and I_0 are Bessel Functions that can be approximated using polynomial expansions. $W(Tt/S\lambda^2)$ is an exponential integral of a well function $W(\Omega)$ where $\Omega = Tt/S\lambda^2$.

An advantage of applying analytical drawdown calculations is that there are many types of equations that apply to many situations. In his book, Muskat and Wychoff [1935] describes an analytical means for accounting for partial penetration of the well in steady state drawdown calculations. Hantush also derived an infinite-series expansion equation that accounted for partial penetration in a leaky aquifer for unsteady flow [Bear 1979].

A Simplification of Equations (5.4) and (5.5)

If an analytical method is being used to calculate drawdowns, the finite difference approximation of head gradients can be eliminated or refined. Specific discharge is proportional to the head gradient. If the head gradient could be calculated analytically by differentiating the drawdown equation, an exact solution for the specific discharge could be obtained.

If differentiation of the drawdown equation is not practical, a more refined finite difference approximation can still be attained. Since drawdown can be calculated at any point, finite difference points for velocity calculation are not restricted to the points on the overall finite difference grid. To find head gradients at a point, drawdowns very close to that point at distances independent of the overall grid size, can be found and head gradients calculated using a finite difference scheme.

It was observed in the report by Means [1982] and in this report that drawdowns attain steady state conditions rapidly. For this reason it is reasonable to use in Equation (4.42) drawdowns at the previous time step, thus making an explicit solution to Equation (4.42) possible.

By calculating the slopes directly, and by using slopes at the previous time step, Equation (4.42) is now approximated by

$$\left(\frac{n}{2}\int_0^1 L(\eta)d\eta\right)\frac{\delta_{i,j}^{2(m+1)}-\delta_{i,j}^{2(m)}}{\Delta t}-\left[\delta_{i,j}^{2(m)}\,K_{i,j}\left(\frac{\partial^2 s}{\partial x}+\frac{\partial^2 s}{\partial y}\right)\right.$$

$$\left.+\frac{1}{2}\,k_{i,j}\left(\frac{\partial s}{\partial x}\,\frac{\delta_{i,j}^{2(m)}-\delta_{i-1,j}^{2(m)}}{\Delta t}+\frac{\partial s}{\partial y}\,\frac{\delta_{i,j}^{2(m)}-\delta_{i,j-1}^{2(m)}}{\Delta x}\right)\right]\int_0^1 F(\eta)L(\eta)d\eta$$

$$=-a\left(\left(-\frac{\partial s}{\partial x}\right)^2+\left(-\frac{\partial s}{\partial y}\right)^2\right)^{1/2}L'(0) \qquad (5.17)$$

Equation (5.17) can be solved for $\delta_{i,j}^{2(m+1)}$ explicitly.

<u>General Solution Procedure</u>

Since the modified version of the injection model calculates drawdowns analytically and calculates the transition zone thickness explicitly, only the equation for the thickness of the freshwater lens is solved iteratively. Figure 5.2 shows this procedure in a flow chart.

By reducing the number of equations to be iterated, and by solving Equation (4.42) explicitly, computer resources are conserved greatly.

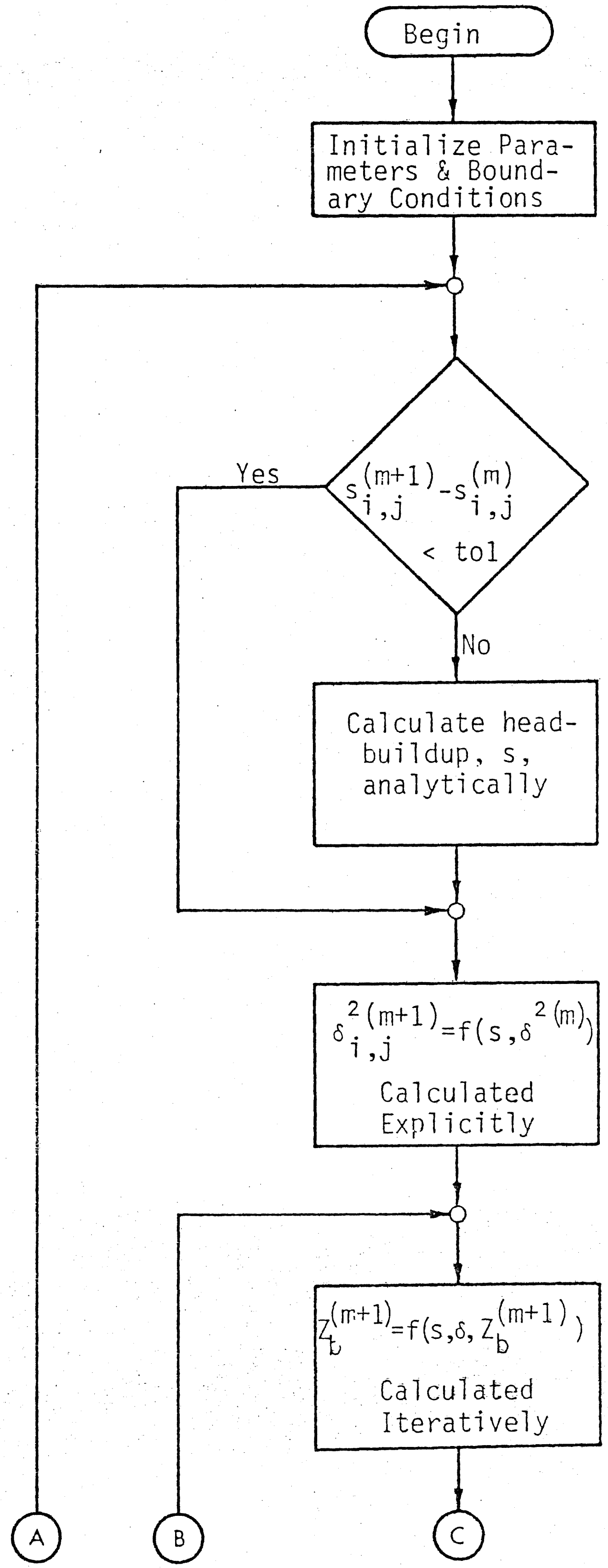

Figure 5.2 Flow chart of modified model

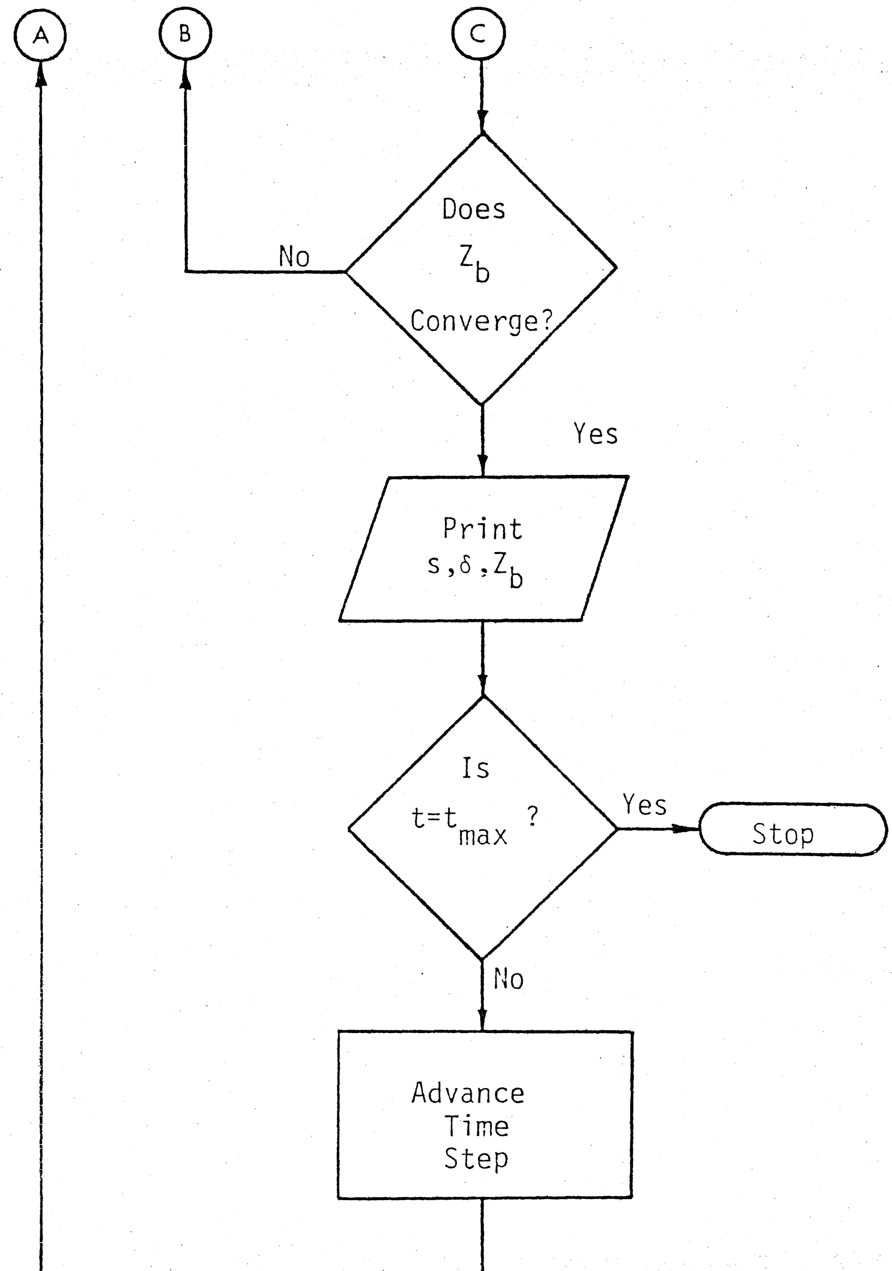

Figure 5.2 (Continued)

CHAPTER 6
MODEL BEHAVIOR

Introduction

In this chapter the fully numerical model is tested extensively using various input parameters. The objective of this chapter is to observe model behavior and determine its sensitivity to certain input parameters.

General Behavior of the Fully Numerical Model

Inspection of Equation (4.36) reveals that it is simply a form of the continuity equation. An important feature of this equation is that it utilizes a variable transmissivity.

Transmissivity is the product of the hydraulic conductivity and the thickness of the aquifer. Equation (4.36), however, sees the aquifer thickness as only the thickness of the freshwater region minus a fraction of the transition zone. The thickness of the freshwater region (determined from Equation 4.26) grows in response to the head buildup associated with the injection process. Because these equations are solved iteratively at each time step, a freshwater zone thickness will be obtained that satisfied each of the equations.

As an injection into the unstratified aquifer continues, the hydraulic head of the aquifer will steadily increase. This is not the case in the stratified aquifer. Initial head increases may be higher in the stratified situation, however, head build-up will quickly stabilize. Any head build-up in the aquifer will cause the thickness of the freshwater zone to be increased. This in effect increases the transmissivity of the aquifer, thus reducing the head build-up resulting from the injection process.

At the beginning of the simulation, when the freshwater lens is very thin, the transmissivity is small, causing the injection to create a large head build-up. As the freshwater lens increases in size, the transmissivity becomes larger, thus reducing the effect of the injection. This reduction in head build-up is somewhat offset by the increase in head with time.

Observation shows that for deeper saline aquifers and relatively low injection rates, the freshwater lens grows very slowly. This causes the head build-up to reach a "temporary" steady state. As the freshwater lens grows significantly enough, the freshwater zone thickness, and thus, the transmissivity increases, and a new temporary "steady state" is approached. This cycle continues until a final steady state is reached. This steady state can be derived using Equation (4.26). At steady state,

$$\frac{\partial Z_b}{\partial t} = 0 \tag{6.1}$$

Substituting Equation (6.1) into Equation (4.26) and solving for Z_b yields

$$Z_b = \frac{S}{\xi} + \delta \int_0^1 L(\eta)d\eta \tag{6.2}$$

The integrated concentration profile that is assumed for this report is

$$\int_0^1 L(\eta)d\eta = 0.33$$

The buoyancy term (ξ) for freshwater in saltwater is typically 0.025. Substituting these values into Equation (6.2) yields

$$Z_b = 40S + \frac{\delta}{3} \qquad (6.3)$$

Figure 6.1 shows the head build-up, freshwater lens thickness, and transition zone thickness as they vary with time for a given set of input parameters.

To speed up the behavior of the model, and to make trends more obvious, the porosity of the aquifer is lowered to 0.05. This is not a realistic value for most aquifers; however, the higher velocities associated with small pore spaces increases the rate at which the freshwater lens grows and thus speeds up the climb toward steady-state conditions.

Analysis of the behavior shown in Figure 6.1 using Equation 6.3 reveals that steady state is being approached. Shown in Figure 6.1 is the actual value of Z_b as it grows with time. Also shown in the figure is the calculated value (from Equation 6.3) that Z_b should have, given the actual head build-up and transition zone thickness for each time step, if it were to be at steady state at that particular time step. It can be seen from this analysis that the system is approaching steady-state conditions.

Model Response to Input Parameters

In an effort to analyze the fully numerical model's response to certain input parameters, some of the parameters were varied and the corresponding model behavior was recorded.

Grid Spacing

When hydraulic gradients are changing rapidly in space, small grid spacings are necessary to give an accurate solution. Near the well,

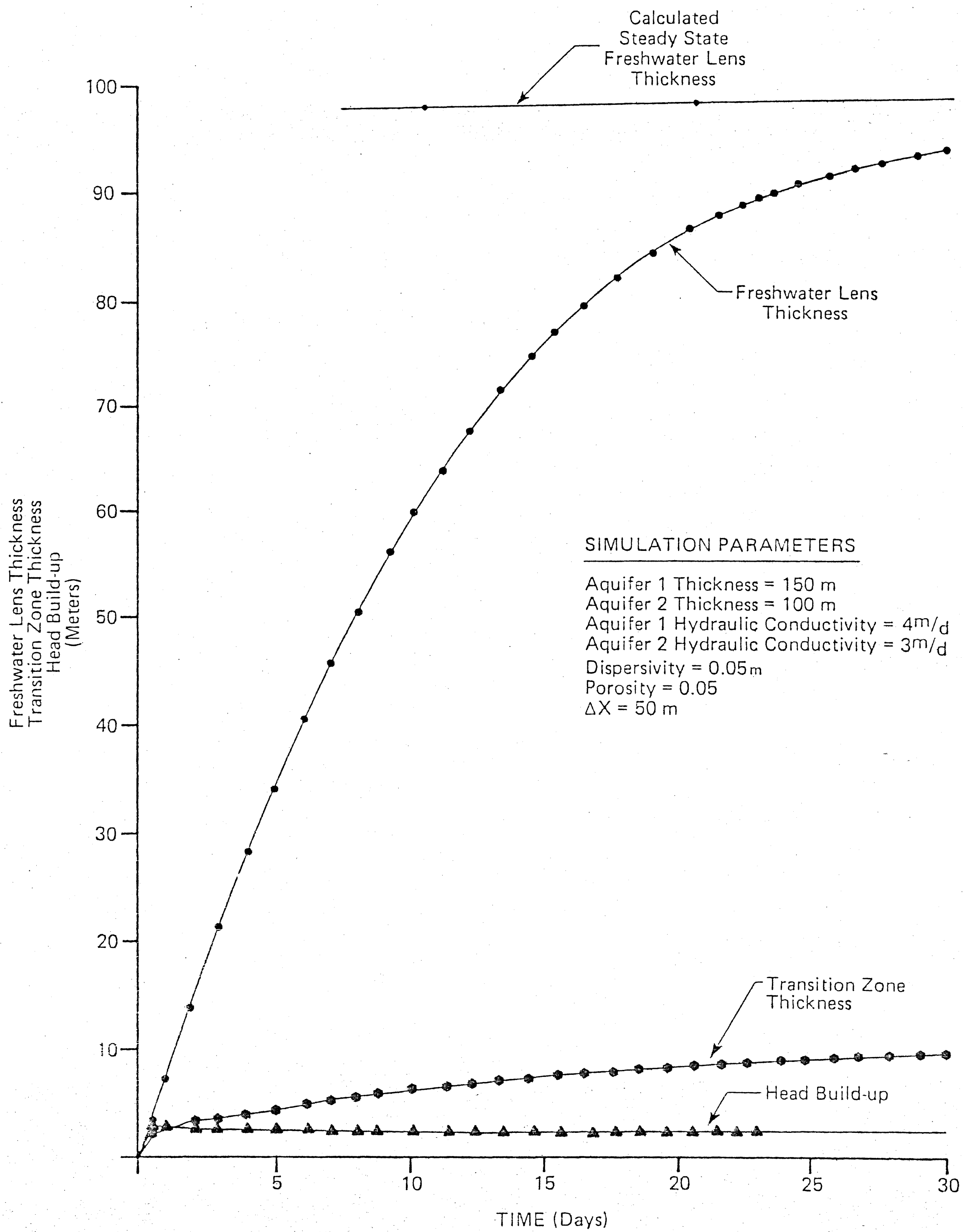

Figure 6.1 Plot of simulation results at the well

where the hydraulic gradient is very steep grid sizes must be chosen carefully. To simulate behavior at the well using a finite difference scheme, a grid size must be chosen that will accurately reflect the well geometry.

It has been noted by Prickett and Lonnquist (1971) that model accuracy can be improved by spatially varying grid sizes throughout a simulation. This could be accomplished by using smaller grids at points of steep hydraulic gradient. Some amount of experience is necessary in defining the magnitude of the variable sized grids, and this experience can be gained only by making a few computer runs with different grid configurations.

An ADI model of an unstratified, confined aquifer with leakance was used for the grid size analysis. This model was used to observe the effect of grid size on the accuracy of finite difference models near the well. This model has the advantage of being less demanding of computer resource and is easy to compare to analytical solutions.

The summarized response of the ADI finite difference approximation to various grid spacings is shown in Figures 6.2 and 6.3.

A head build-up of 4.5 feet was calculated using the analytical solution of the same aquifer parameters for a point at the edge of a two-foot diameter well, using the Theis method as modified by Hantush and Jacob (1955) for leaky aquifers.

A comparison of the numerically approximated solution and the analytical solution at the well reveals that as the grid sizes are made smaller, the numerical approximation results approach those of the analytical solution.

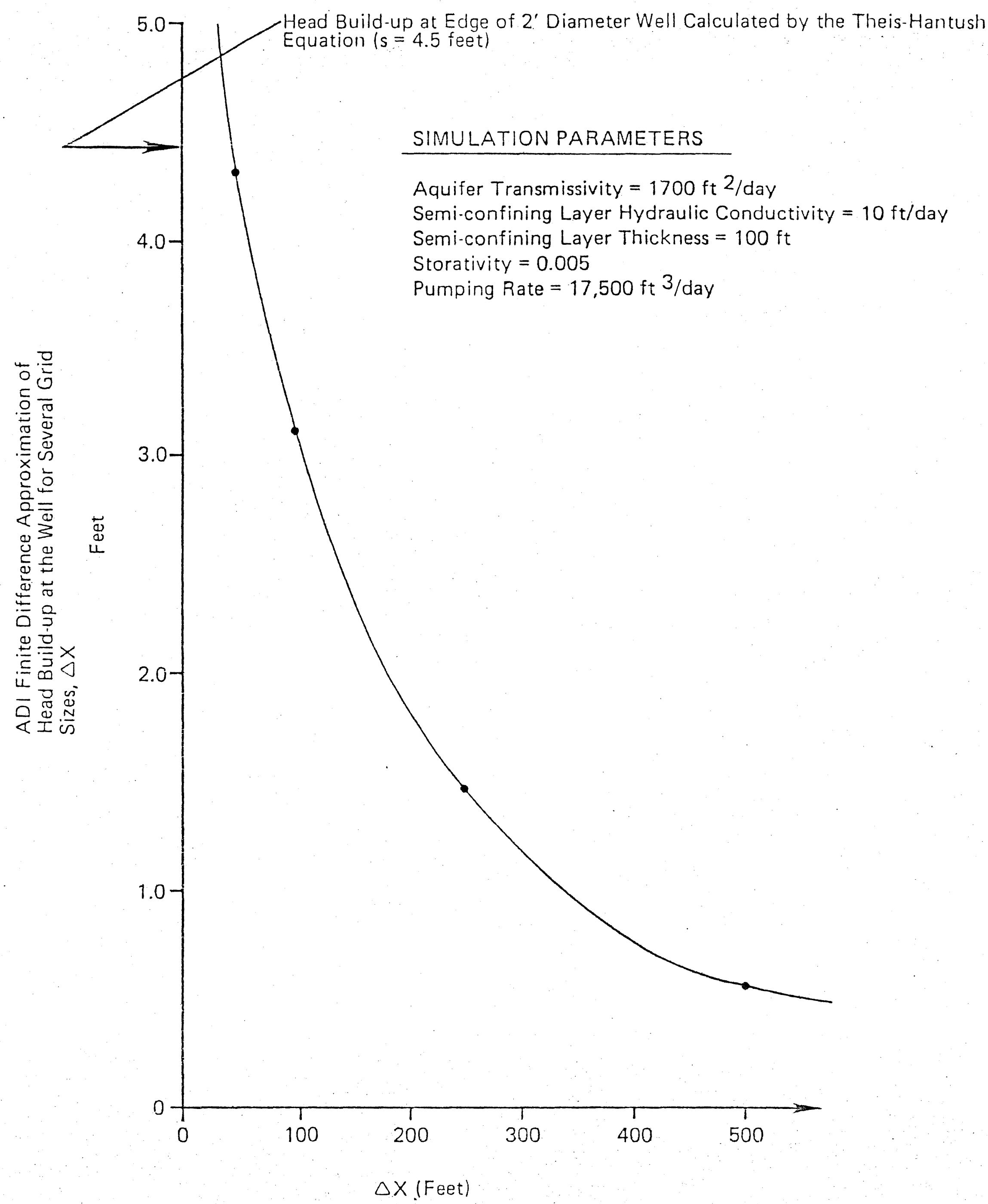

Figure 6.2 Simulated head build-up at the well using an ADI finite difference model at various grid spacings

SIMULATION PARAMETERS

Aquifer Transmissivity = 1700 ft ^{2}/day
Semi-confining Layer Hydraulic Conductivity = 10 ft/day
Semi-confining Layer Thickness = 100 ft
Storativity = 0.005
Pumping Rate = 17,500 ft ^{3}/day

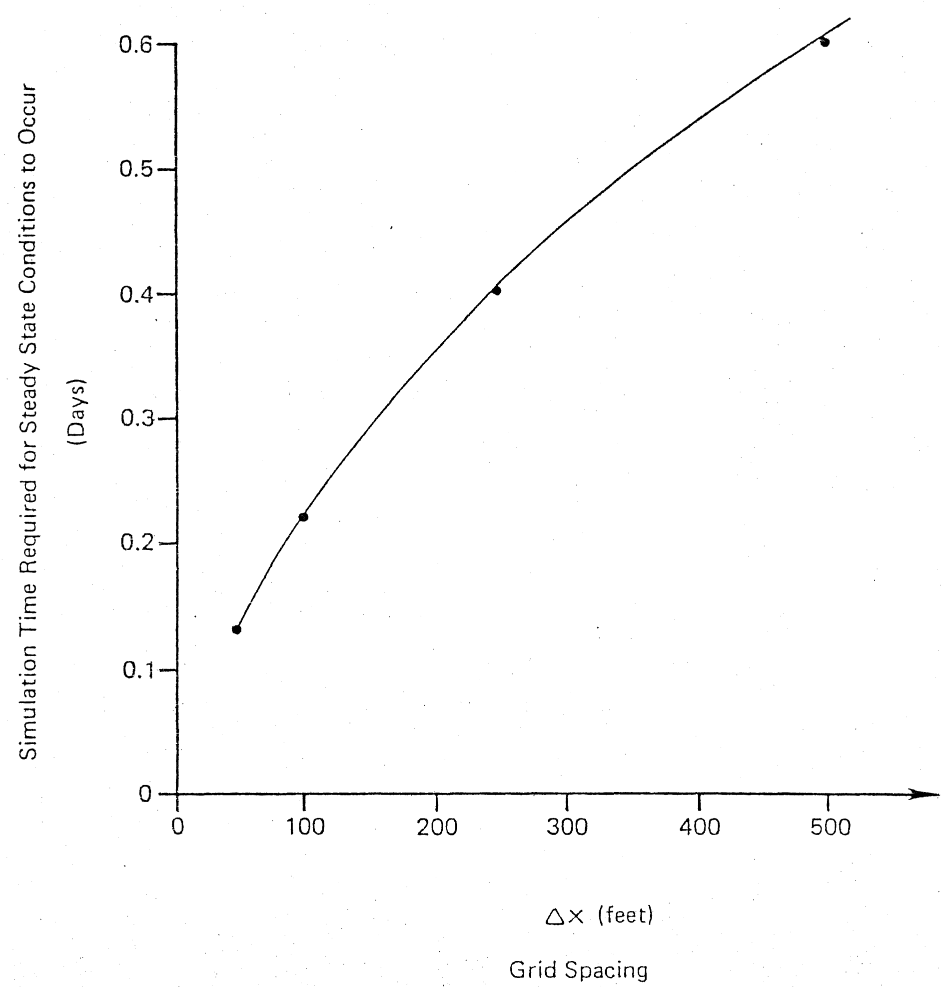

Figure 6.3 Simulated time to steady state using an ADI finite difference model at various grid spacings

It was also noticed in this analysis that points away from the well are not much affected by the change in grid size.

It can be seen that for this simulation, a reasonable numerical representation of flow conditions about a well of 1 foot radius will require grid sizes near the well of approximately 15 feet. If reasonable accuracy is required near the well, a variable size grid must be utilized. For this case, the grid must be as small as 15 feet. For other simulations, the grid size may be smaller or larger. For each case, an analysis similar to the one performed in this section for the desired aquifer parameters should be done.

Dispersivity

Equation (4.42) describes the transition zone growth. The principal component of this equation is the dispersion term. The dispersion term is dependent on the average speed of the groundwater flow. Because the velocity terms in the transition zone are assumed horizontal, and the transition zone grows vertically, the coefficient of importance is the transverse dispersivity.

Simulations using different dispersivities, but otherwise identical data, are shown in Figures 6.4, 6.5, and 6.6. It can be seen from these figures that an order of magnitude increase of the input dispersivity triples the transition zone thickness. This is consistent with Equation (4.42). It can be seen from this equation that the dispersion term D is proportional to the square of the transition zone thickness δ and that an increase of D by 10 times will increase δ by the square root of 10, which is approximately 3. Such an increase, however, does not cause any noticeable change in the head build-up, and causes only a slight increase in the thickness of the freshwater lens.

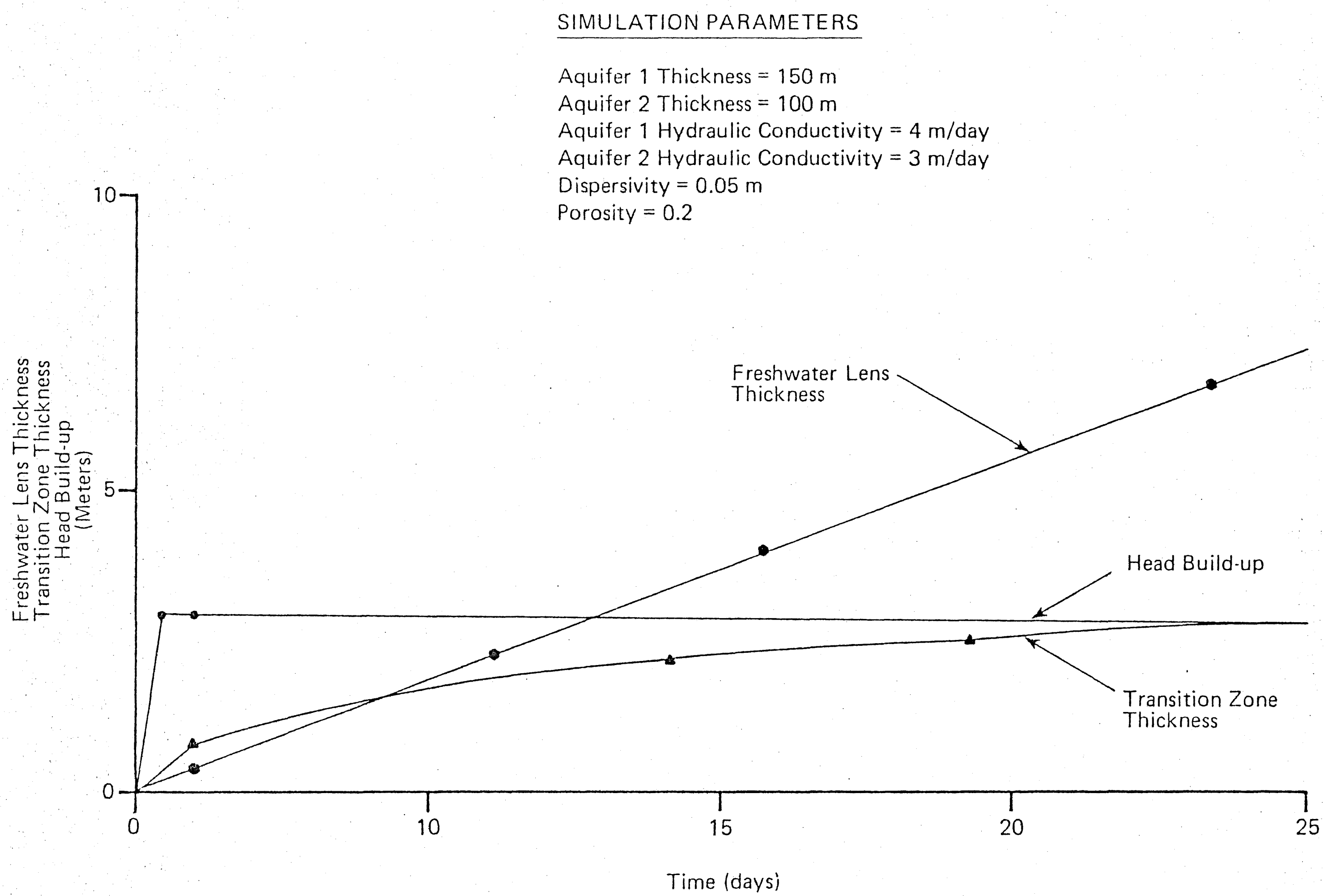

Figure 6.4 Injection simulation using dispersivity of 0.05m

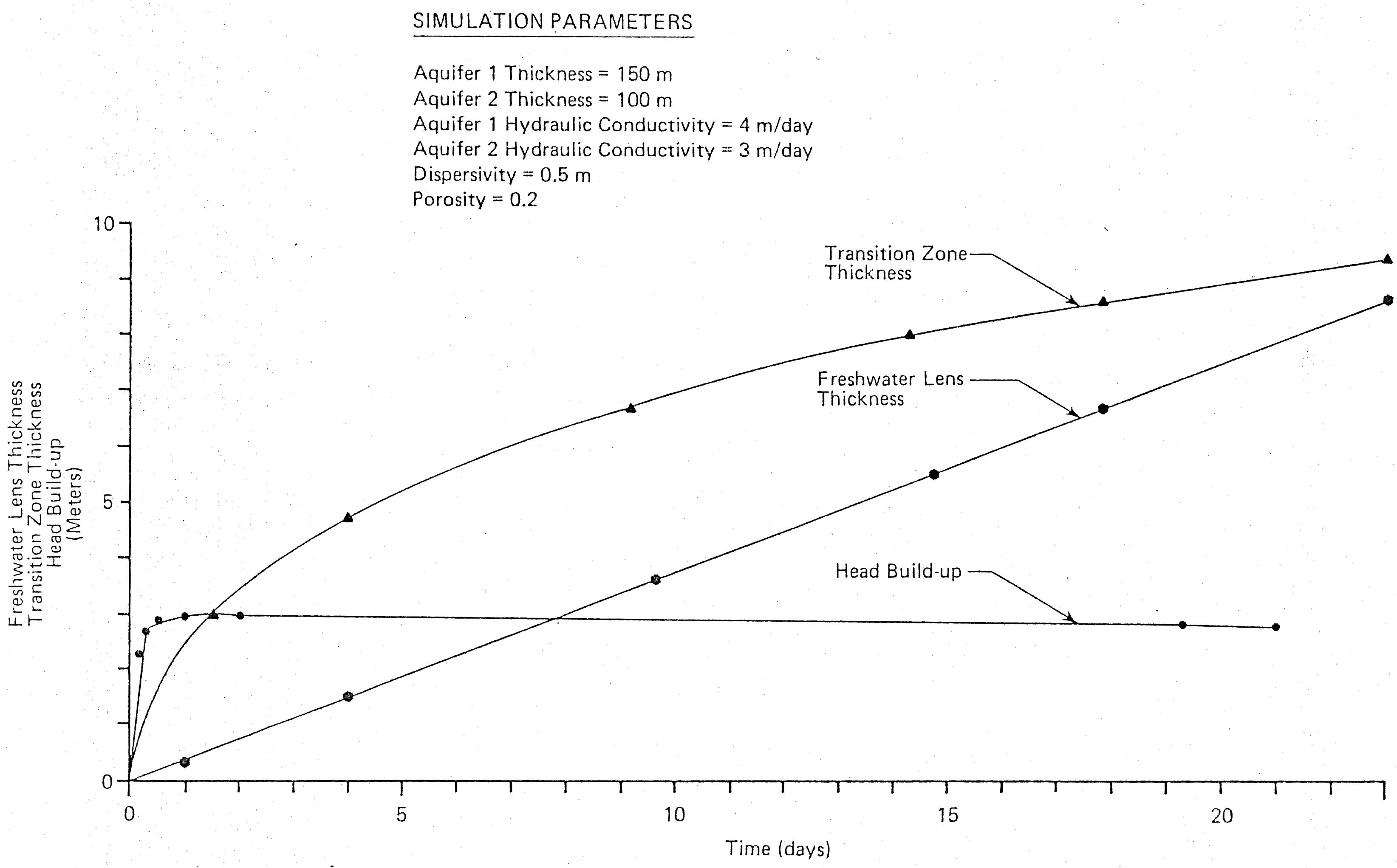

Figure 6.5 Injection simulation using a dispersivity of 0.5m

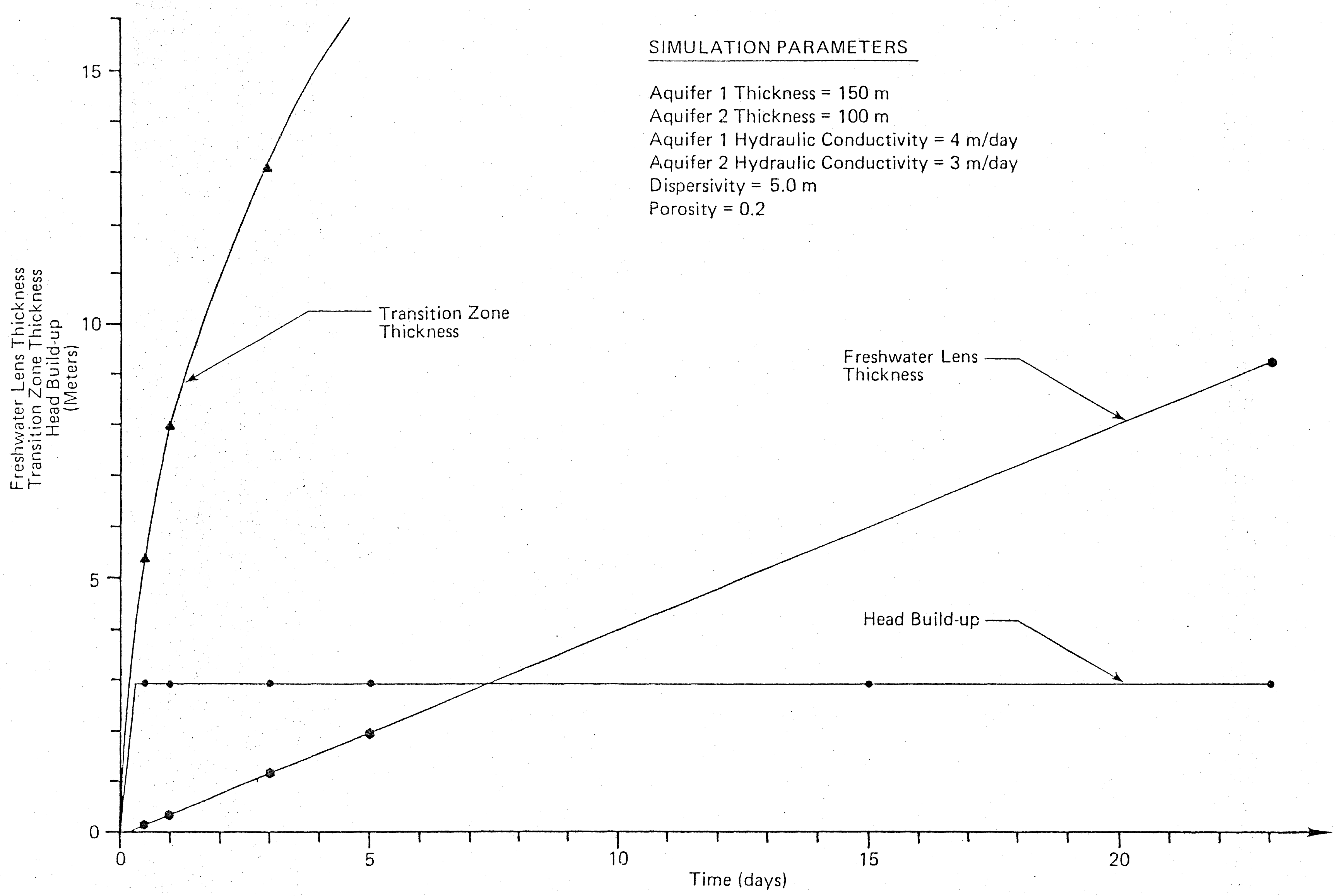

Figure 6.6 Injection simulation using a dispersivity of 5.0m

It can be seen in Figures 6.4, 6.5, and 6.6 that the transition zone is sometimes larger than the freshwater lens thickness. The model is still valid in this situation as long as the hydraulic conductivities of aquifer 1 and aquifer 2 are equal and β remains greater than zero. Once β becomes equal to zero, the effective thickness of the freshwater zone is zero and the model is no longer valid. For the modeled situation, the effective thickness of the freshwater lens is much greater than zero. The simulations shown in Figures 6.4, 6.5 and 6.6 use hydraulic conductivities which differ from aquifer 1 to aquifer 2 and the transition zone sometimes enters aquifer 2 making the simulation technically invalid. However, the effect of this problem is small here since the difference in hydraulic conductivity between the two aquifers is small.

Field determination of dispersivity is very difficult, making it easy to misjudge its actual value. It may be necessary to determine the dispersivity by calibration of simulated results to actual field observations.

Porosity

Figures 6.7 and 6.8 show the results of two simulations using different porosities, but otherwise identical input parameters. Because of the higher flow velocities associated with lower porosities in an aquifer, the effect caused by a lower porosity is a more rapid movement toward steady-state. By examining Equation (4.26) and observing Figures 6.7 and 6.8, it can be seen that he freshwater lens will grow more rapidly if the porosity of the aquifer is lowered. It can also be seen in the figures and by examination of Equation (4.42) that an increased velocity caused by a reduction in pore volume will increase the

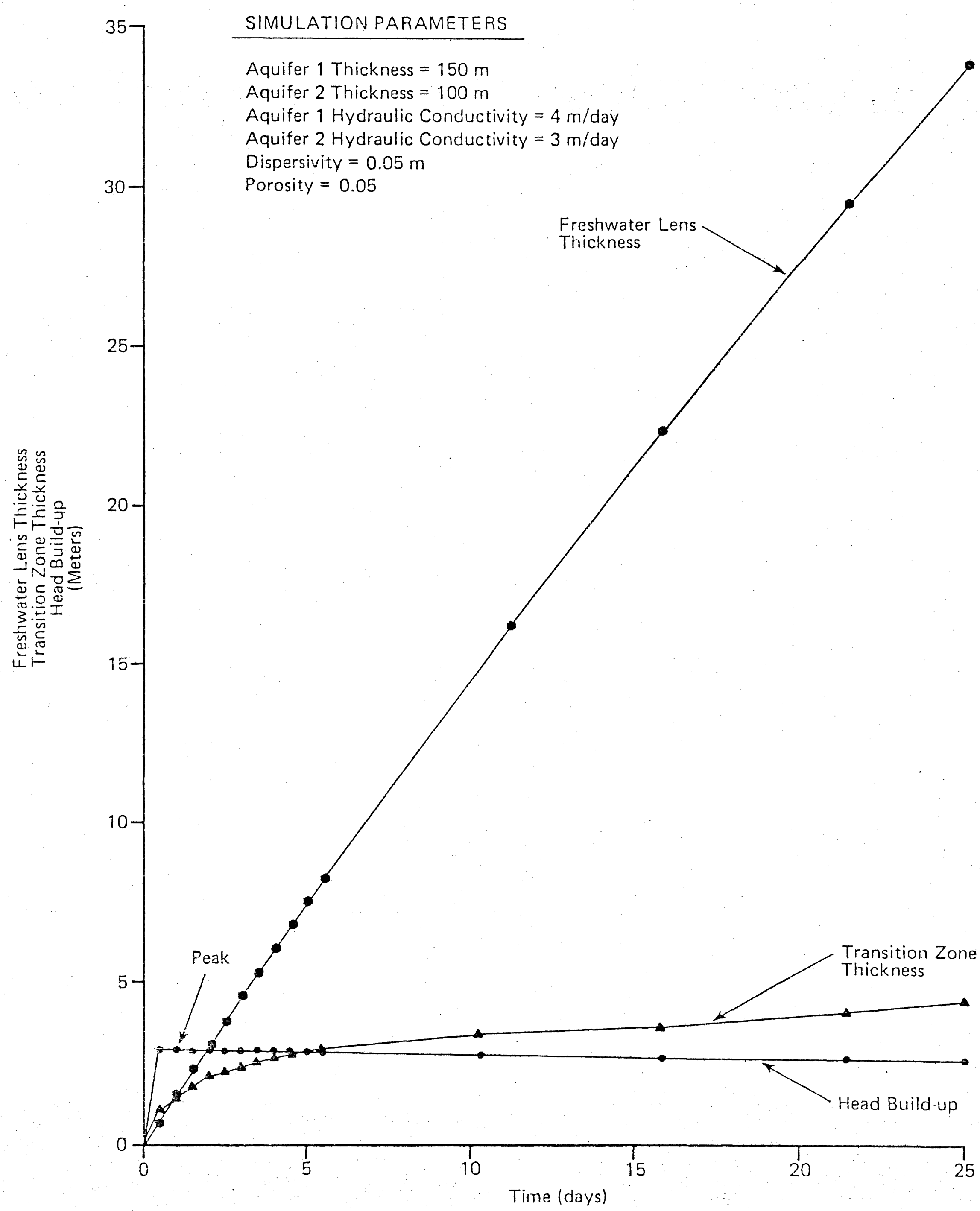

Figure 6.7 Aquifer simulation using a porosity of 0.05

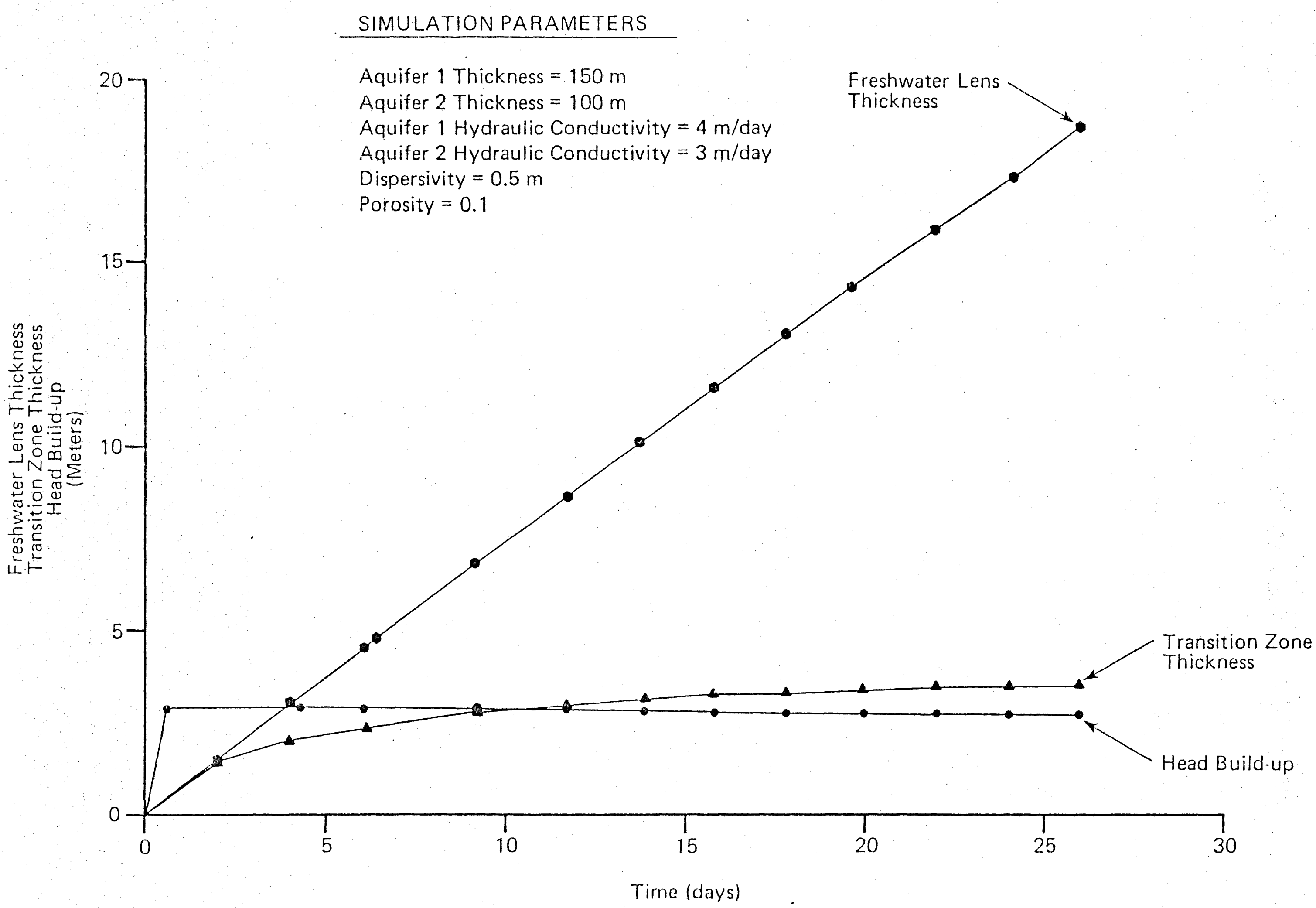

Figure 6.8 Aquifer simulation using a porosity of 0.10

dispersion rate in the transition zone and thus increase the transition zone thickness.

It is noted that in an actual aquifer the intrinsic permeability is a function of the aquifer's porosity and that an increase in porosity will cause an increase in the intrinsic permeability. It can then be concluded that change in porosity actually may have a large effect on the head build-up. The goal of this section, however, is to view the response of the model to varied input parameters.

Anisotropy

Figure 6.9 shows the result of two simulations (simulation A and simulation B). Simulation A uses input parameters for a hypothetical isotropic aquifer situation. Simulation B uses input parameters which are identical to the input parameters of simulation A (including horizontal hydraulic conductivity), except that the aquifer in simulation B is anisotropic. The vertical hydraulic conductivity value in this simulation is much less than the horizontal hydraulic conductivity.

It can be seen in Figure 6.9 that the head build-up is greater at any given time in the anisotropic simulation. This is due in part to the effective hydraulic conductivity being reduced by the lower vertical component of the hydraulic conductivity. It can also be seen from Figure 6.9 that the growth of the freshwater lens is much slower for the anisotropic simulation. As a result of the reduced effective hydraulic conductivity and the slow movement of the freshwater lens, the head build-up is somewhat larger at any given time in simulation B. This is partly because the thinner freshwater lens further reduces the transmissivity of the aquifer, thus causing the head build-up to be greater for the input injection rate.

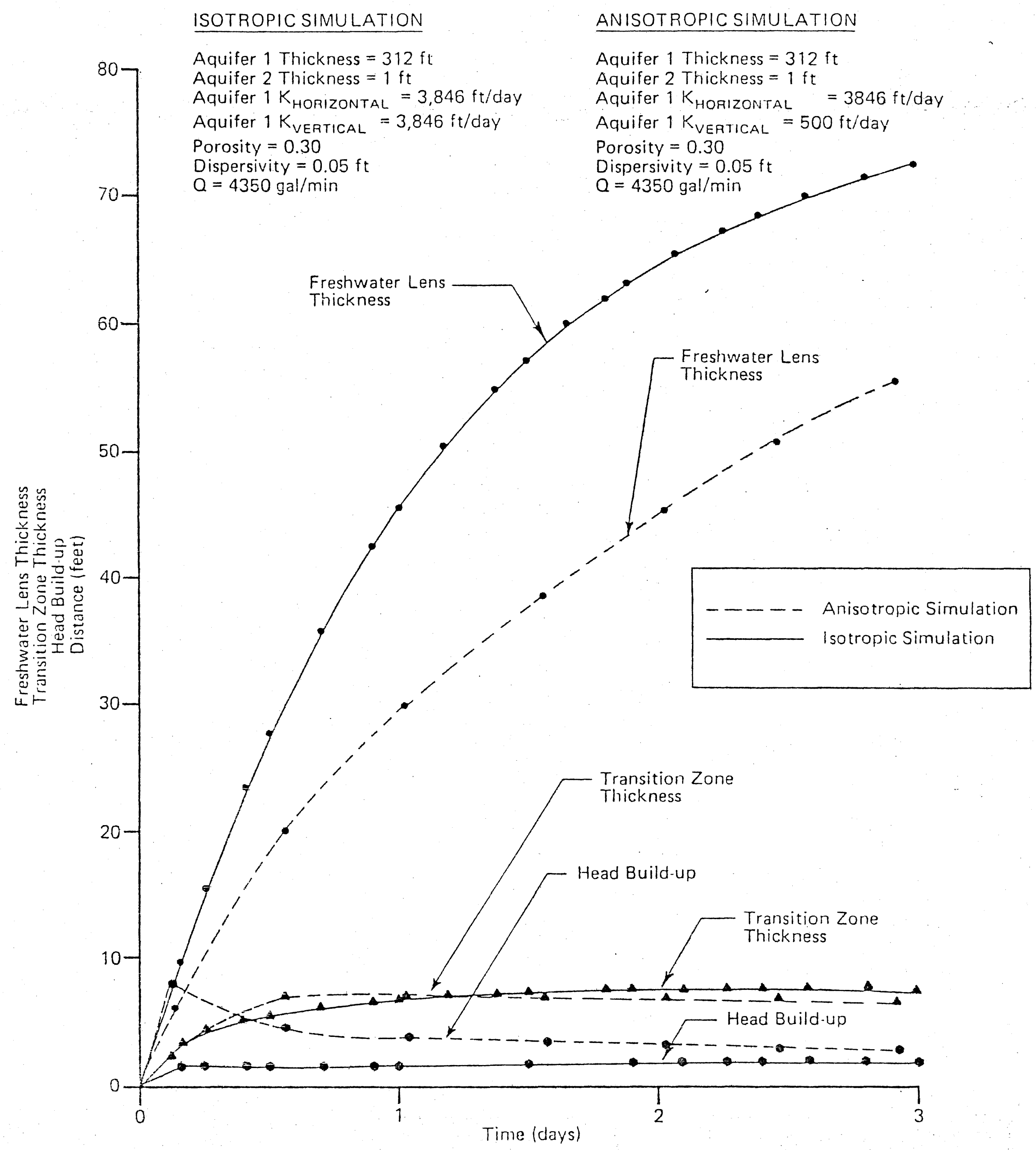

Figure 6.9 Comparison of simulations using isotropic versus anisotropic hydraulic conductivity

CHAPTER 7
VERIFICATION

Introduction

In this chapter final results from the previously developed injection models will be compared to a series of field injection-tests into a saline aquifer in Pinellas County, Florida. Field data is taken from a United States Geological Survey report entitled, "Hydrogeology and Results of Injection Tests at Waste-Injection Sites in Pinellas County, Florida" [Hickey 1982].

Geologic Framework of Pinellas County, Florida

Figure 7.1 shows the geologic formations beneath St. Petersburg. The aquifer system underneath Pinellas County is mainly composed of several layers of sedimentary rocks ranging in age from Cretaceous to Pleistocene. The sedimentary rocks that make up the aquifers are mostly dolomite and limestone, which reach vertical thicknesses of approximately 10,000 to 12,000 feet. The stratigraphy of Pinellas county consists of several layers of sedimentary rocks, deposited over several geologic periods. The youngest deposits are the surficial sand deposits, which were deposited during the Pleistocene Epoch. Below the surficial deposit is the Hawthorn Formation, which was formed during the middle Miocene. Older formations in order of increasing age, are Tampa Limestone (Lower Miocene), Suwannee Limestone (Oligocene), Ocala Limestone (Upper Eocene), Avon Park Limestone (Middle Eocene), Lake City Limestone (Middle Eocene), and Oldsmar Limestone (Lower Eocene). Pinellas County is located on the southwest edge of the Peninsular Arch,

ERATHEM	SYSTEM	SERIES		FORMATION
Cenozoic	Quaternary	Pleistocene		Surficial sand
	Tertiary	Miocene	Middle	Hawthorn Formation
			Lower	Tampa Limestone
		Oligocene		Suwannee Limestone
			Upper	Ocala Limestone
			Middle	Avon Park Limestone
				Lake City Limestone
			Lower	Oldsmar Limestone
		Paleocene		Cedar Keys Limestone
Mesozoic	Cretaceous	Undifferentiated for this report		
Pre-Mesozoic	Undifferentiated for this report			

Figure 7.1 Geologic formations beneath St. Petersburg, Florida

which is the geologic backbone of the Florida peninsula, and is that area's most dominant subsurface feature. Pinellas County is also located southwest of the Ocala Uplift, which is a gentle, anticlinal flexure, and runs axially parallel to the Peninsular Arch. Previous studies [Puri and Vernon, 1964] reveal that there are extensive fracture patterns in the Ocala Uplift in the northern part of Pinellas County.

All of the strata beneath St. Petersburg are permeable to some degree; however some rock layers are much less permeable than others. For this reason certain layers are classified as aquifers and others as confining beds. An aquifer is defined as a formation, group of formations or part of a formation that contains sufficient permeable material to yield significant quantities of water to wells and springs. They define a confining bed to be a body of "impermeable material" stratgraphically adjacent to one or more aquifers. Confining beds are much less permeable than aquifers and restrict the flow between aquifers.

Figure 7.2 shows the aquifer system beneath St. Petersburg. In the U.S.G.S. study, two aquifers were identified, the surficial aquifer and the Floridan aquifer. Two confining beds were also identified. There is the upper confining bed of the Floridan aquifer, which separates the surficial aquifer from the Floridan aquifer. There is also the lower confining bed of the Floridan aquifer, which is mostly made up of Lake City Limestone.

The Floridan aquifer can be further divided into four permeable zones, each separated by three semi-confining beds, where semi-confining beds are less permeable than the permeable zones. In this study the four permeable zones have been labeled alphabetically where zone A is

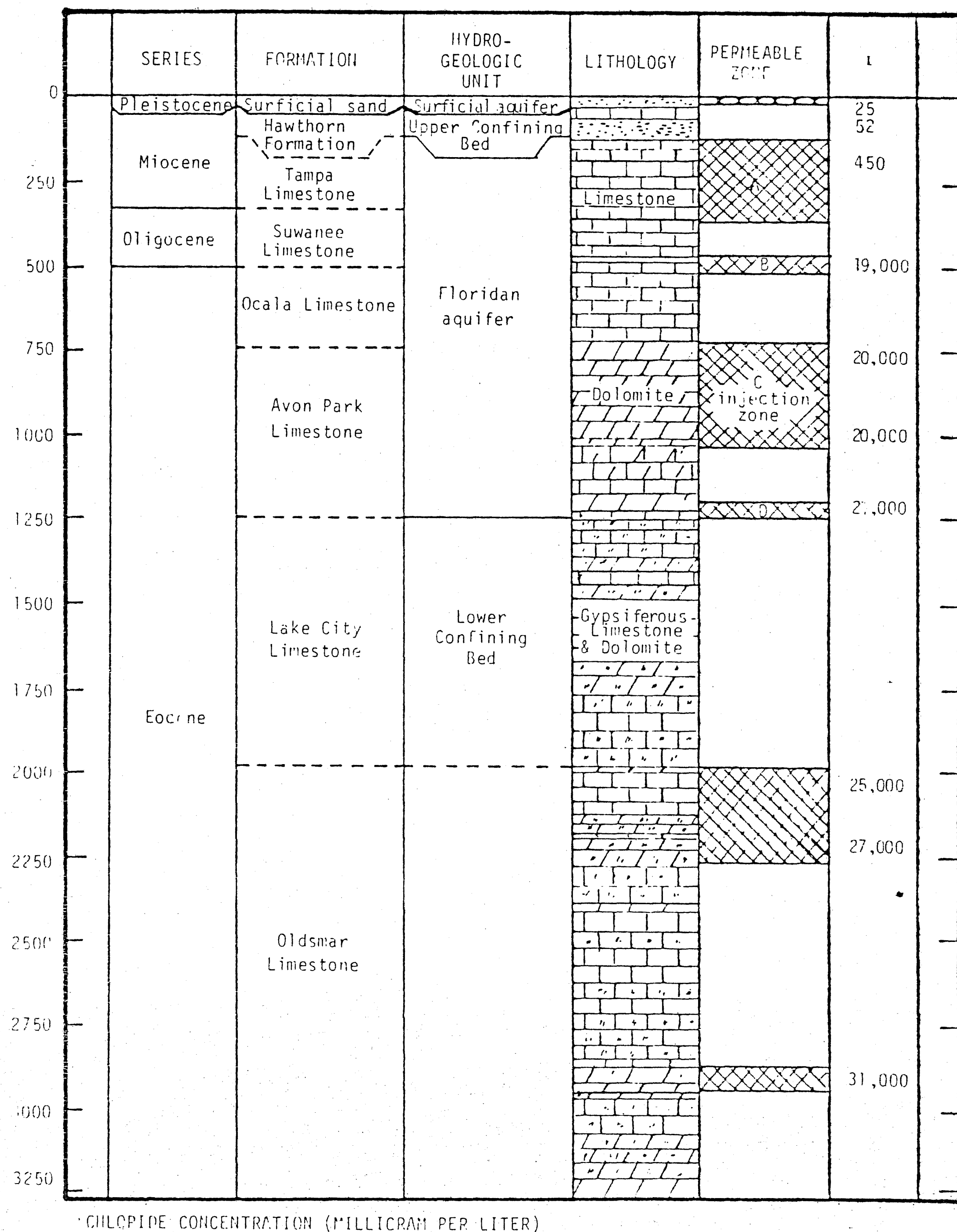

Figure 7.2 Aquifer system beneath St. Petersburg, Florida

the shallowest within the aquifer and zone D is the deepest. Zone C is the permeable zone in which the injection tests will take place.

Most of the aquifer parameters were obtained using pumping tests, whereby observed drawdowns were matched with the corresponding pumping rates.

The water in the previously described aquifers is mostly saline, with a small layer of freshwater in the overlying surficial aquifer. Sources of the deeper saline water are the Gulf of Mexico and Tampa Bay, whereas the source of freshwater near the surface is rainwater that infiltrates from the surface. The salinity content ranges from 6 mg/L in the surficial aquifer to approximately 21,000 mg/L below the bottom permeable zone.

Small amounts of freshwater are tapped from the surficial aquifer for irrigation and municipal supplies; however, all water distributed by Pinellas County and the city of St. Petersburg is pumped from as far as 40 miles inland from Pinellas County.

Injection Tests

Although the data for the injection tests are sparse and the quality of the data is questionable, it is believed that these tests provide the best available material for validation of the model. Injection tests were run at three locations: McKay Creek, South Cross Bayou, and southwest St. Petersburg. Well locations for the three tests are shown in Figure 7.3. Duration of tests ranged from 3 days at South Cross Bayou to 91.1 days at southwest St. Petersburg. Injection rates ranged from 650 gal/min at McKay Creek to 4,350 gal/min at South Cross Bayou.

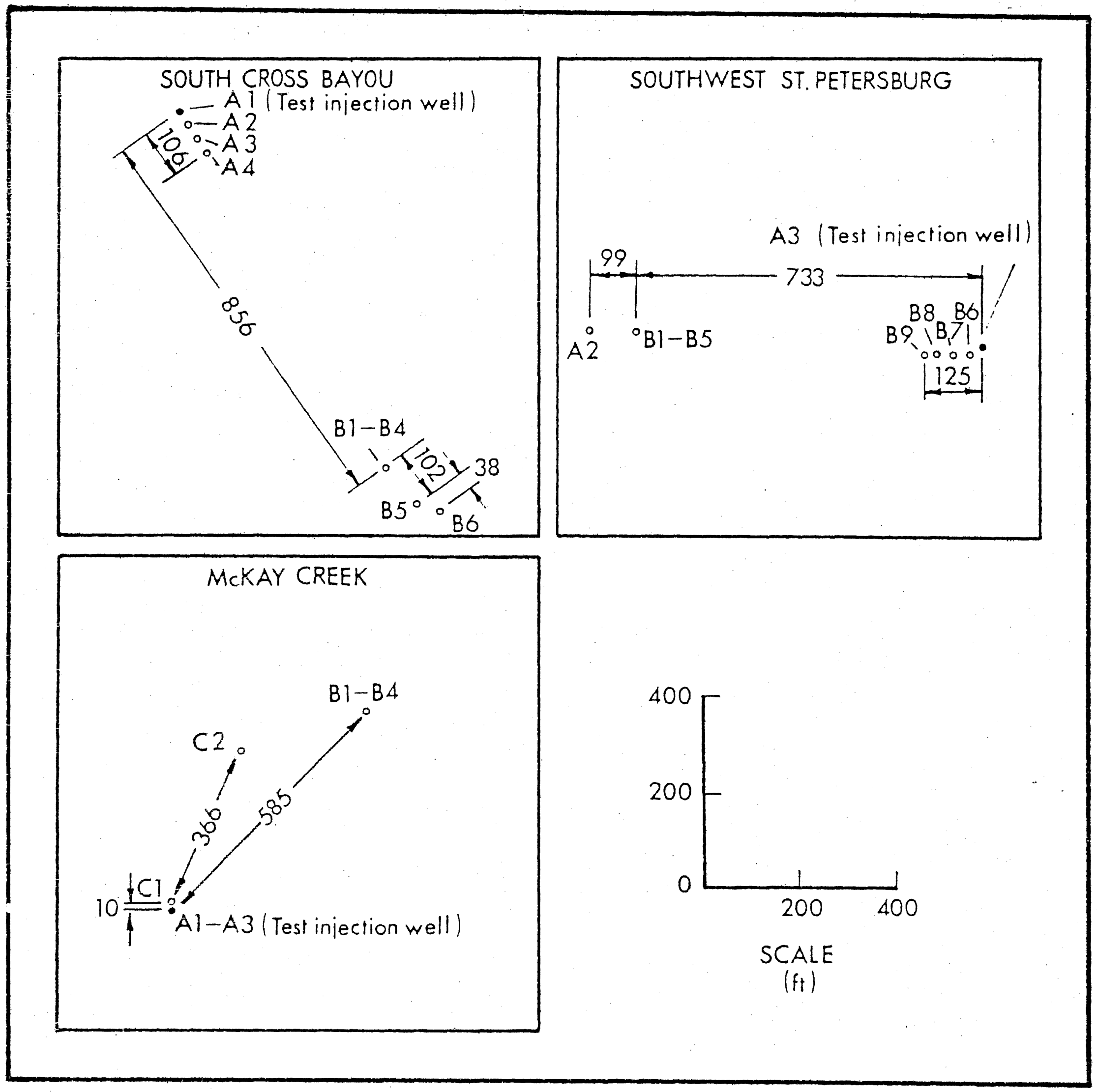

Figure 7.3 Well locations for injection tests at South Cross Bayou, Southwest St. Petersburg and McKay Creek

Injection Tests at McKay Creek

The injection test at McKay Creek was run for 57.1 days: water with a chloride content ranging from 93 to 110 mg/L was injected at an average of 650 gal/min into permeable zone A. The well casings at the McKay Creek test site were open for the top sixty percent of the aquifer's thickness for well C1, and over forty percent of the aquifer's thickness for well C2. Water quality and water level data were collected before, during and after the test. During the test, no substantial head increase was noticed; this is a result of the high tranmissivity of the injected aquifer. Chloride content in a well 585 feet from the injection well dropped from 20,000 mg/L before the test, to 18,000 mg/L after the test. A well directly above the injection interval experienced no change in chloride content, indicating inhomogeneity in the vertical permeability of zone A.

Injection Tests at South Cross Bayou

The South Cross Bayou injection test was run for three days by injecting water with an average chloride concentration of 710 mg/L at a rate of 4,350 gal/min into permeable zone C. The injection well's casing at South Cross Bayou was open over approximately the bottom 35% of the aquifer's thickness. The chloride concentration of the native water in the injection zone was 20,000 mg/L. Data such as head buildup and concentration changes caused by the injection are shown in Figure 7.4. It is noted that the head buildup at South Cross Bayou was very small, indicating a high transmissivity of the injected aquifer.

Injection Tests at Southwest St. Petersburg

The test at southwest St. Petersburg was run for 91.1 days. In this test, treated effluent from St. Petersburg's city wastewater

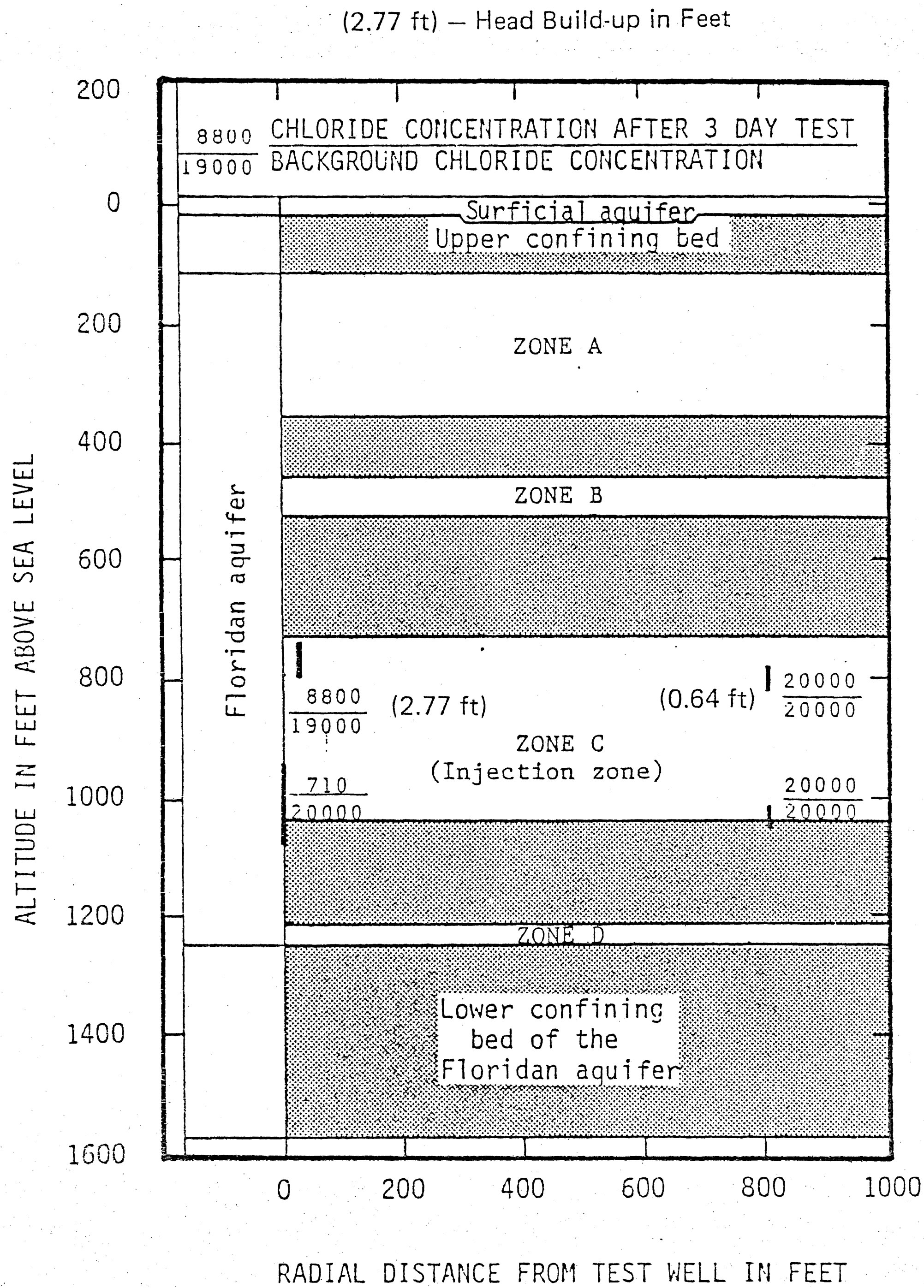

Figure 7.4 Injection test at South Cross Bayou

treatment plant was injected into permeable zone C along with a tracer (rhodamine WT). The tracer was used to make detection of injected water in observation wells easier. The injection rate averaged 3,380 gal/min (standard deviation = 80 gal/min) for the first 9.1 days. For the remaining 82 days the injection rate was lowered to 2,770 gal/min (standard deviation = 150 gal/min). The average injection rate for the entire test was 2,830 gal/min. The casing of the injection well in this test was open approximately over the lower sixty percent of the aquifer thickness.

Rhodamine WT was detected in a well directly above the injection point between 0.03 to 1.2 days from the start of the test. The tracer was also detected above the well in permeable zone B, indicating a "short circuit" in the vicinity of the injection well. The term "short circuit" is used since the tracer probably would not have leaked through the upper semi-confining layer had it not been disturbed. A well 733 feet from the injection well detected the tracer at the top of permeable zone C, but when used to sample the bottom portion of permeable zone C, no tracer was detected. This indicates that the injected water stratified due to density differences near the top of the injection zone. Data from the injection test can be seen in Figure 7.5.

Simulation of Injection Tests Using the Fully Numerical Injection Model

Using the fully numerical injection model, computer simulations of the injection tests at South Cross Bayou were made. Because of the prohibitive cost associated with a 91-day computer simulation using the current version of this model, a simulation of the Southwest St. Petersburg Injection Test was not done. The McKay Creek injection test also was not modeled since results from the test showed little effect of

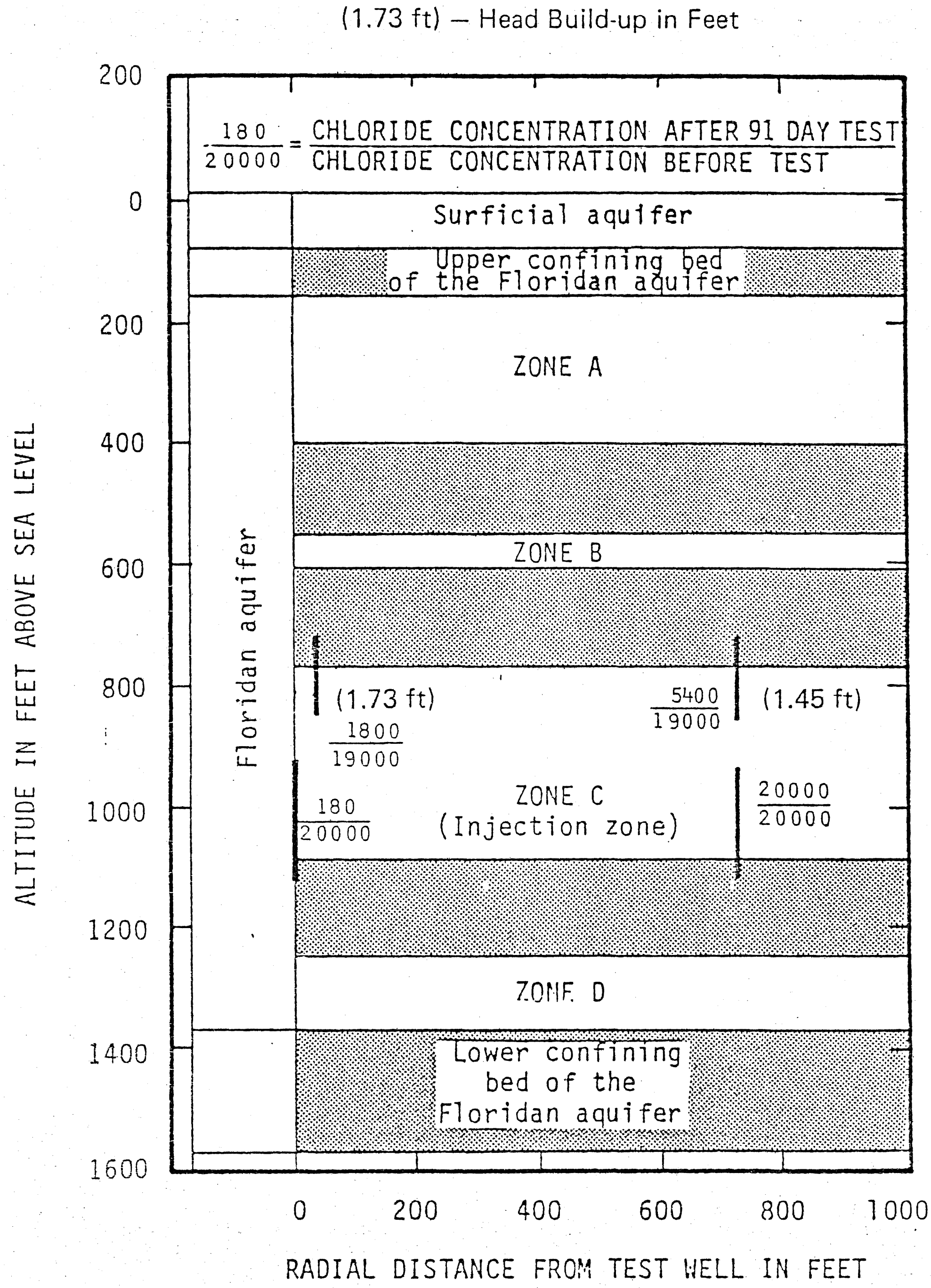

Figure 7.5 Injection test at Southwest St. Petersburg

the injection on the aquifer. Input parameters used in the simulation are described in the previous section and Table 7.1. Although a simulation was not run for the southwest St. Petersburg and Mckay Creek injection tests, parameters for the tests are listed for completeness.

South Cross Bayou Simulation

The South Cross Bayou simulation was three days in duration; Initial time steps for the numerical procedure were in increments of 0.00006 days. During the simulation, the time step was increased using a doubling routine. The doubling routine allows the time step to be increased during the simulation whenever the model becomes more stable as judged by the number of iterations required for convergence. This small time step is dictated by the stability constraints described in Chapter 5. It can be noted that the simulated aquifer is very permeable, and the grid sizes are relatively small. These two parameters cause the stability time constraint to be very small.

The grid spacing (for both the x and y directions) used in this simulation was 200 feet. The injection rate was 4,350 gallons per minute. This is incorporated into the model as 20.93 feet per day of vertical inflow over the entire area of one 200 foot by 200 foot grid square. The transmissivity of aquifer 1 is 1.2×10^6 square feet per day. The thickness of aquifer 1 is input as 312 feet. The horizontal hydraulic conductivity of aquifer 1 is calculated to be 3,846 feet per day (transmissivity divided by the depth of the aquifer). Although a vertical hydraulic conductivity was not reported, a value of 500 feet per day was assumed. This is based upon the assumption that the South Cross Bayou site and the southwest St. Petersburg site are similar and that the value of 500 feet per day reported at southwest St. Petersburg

Table 7.1 Estimated aquifer coefficients for zone C (injection zone) based on aquifer test analyses

Test Site	Transmissivity T (ft^2/d)	Storage coefficient S	Storage coefficient from laboratory compressibility tests S	Leakance coefficient k'/b' (1/d)	Diffusivity T/S (ft^2/d)
S.W. St. Petersburg*	1.2×10^6	3.3×10^{-4}	6.0×10^{-4}	2.2×10^{-4} to 1.9×10^{-3}	3.6×10^9
South Cross Bayou	1.2×10^6	2.2×10^{-4}	1.5×10^{-4}	3.7×10^{-4} to 1.5×10^{-3}	5.5×10^9
McKay Creek	0.9×10^6	0.8×10^{-4}	3.1×10^{-4}	6.6×10^{-3} to 1.5×10^{-2}	11.3×10^9

* vertical hydraulic conductivity = 500 ft/day, Hickey (1986)

applies at this site. The porosity of the aquifer is assumed to be equal to 0.30. The USGS study does not report any values for the dispersivity, however, a dispersivity of 0.05 feet seems to yield good results.

The assumed values for the integrated distribution function of the solute concentration, specific discharge, and the solute concentration multiplied by the specific discharge function are 0.33, 0.67, and 0.17, respectively, based on Equation 4.13.

Comparison of Simulation Results of the Fully Numerical Model to Test Data

Figure 7.6 shows the simulation output values for a point at the well for several times during the simulation. Observation of this figure reveals that, after three days, the simulation has not reached steady state. Analysis, using Equation 6.3, of Figure 7.6 at a time of 3.0 days shows that the simulation has not reached steady state. By inputting into Equation 6.3, the simulated head build-up (s = 2.85 feet) and transition zone thickness (δ = 6.70 feet) at time = 3.0 days, the expected steady state freshwater lens thickness for these values can be calculated (Z_b = 116.23 feet). Comparing this calculated steady state freshwater lens thickness to the actual simulated freshwater lens thickness (Z_b = 55.26 feet) reveals that the simulation has not reached steady state conditions. It can be seen from this simulation that the head build-up grows rapidly in the simulation, and, as the freshwater zone grows, the head build-up begins to slowly decrease until a steady state balance between the head build-up, freshwater lens, and the transition zone is reached.

Figure 7.7 shows the results at the end of the three-day South Cross Bayou simulation for several points along the x-axis. Observation

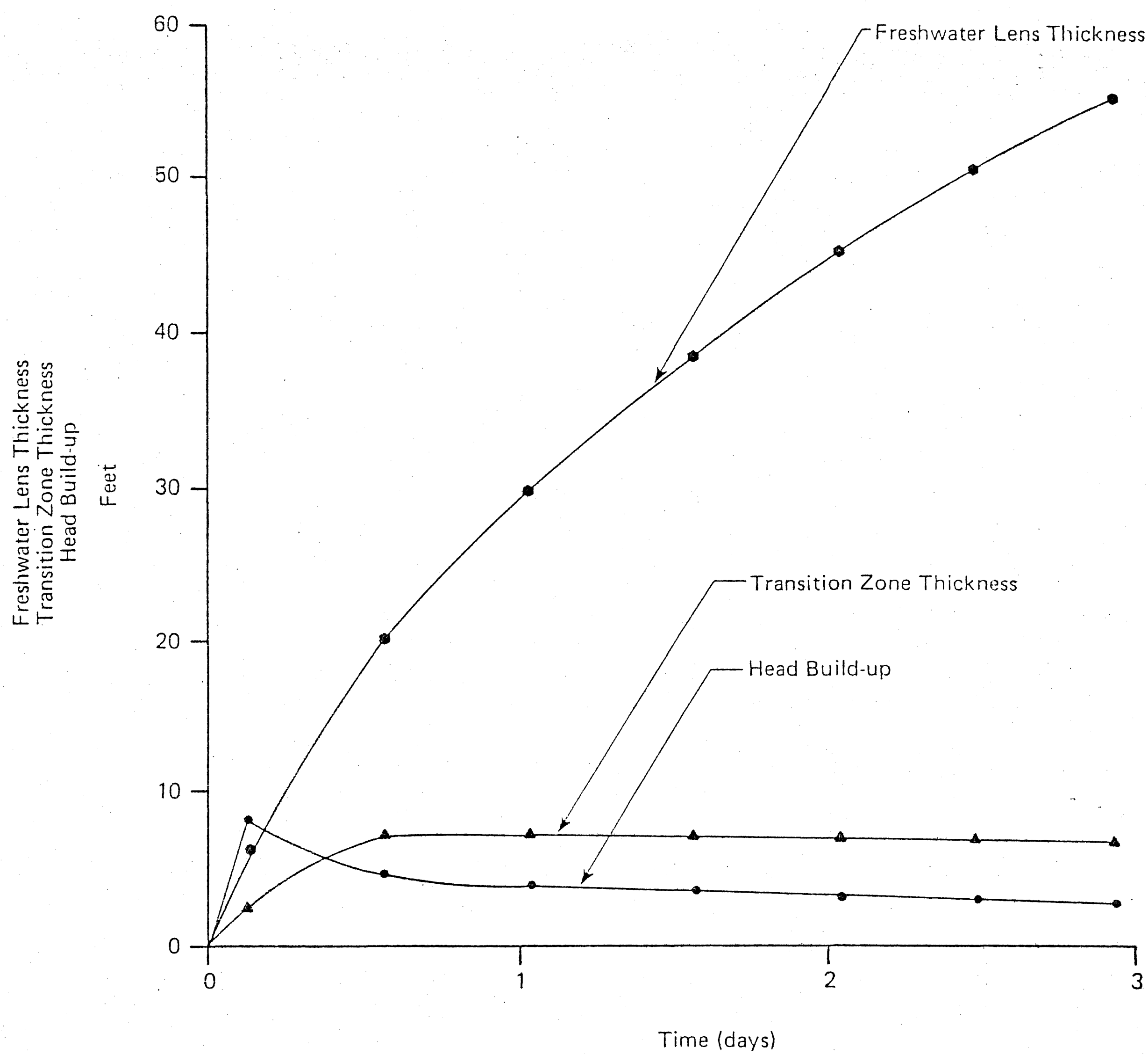

Figure 7.6 South Cross Bayou Simulation at a Point Near the Injection Well Using the Fully Numerical Model

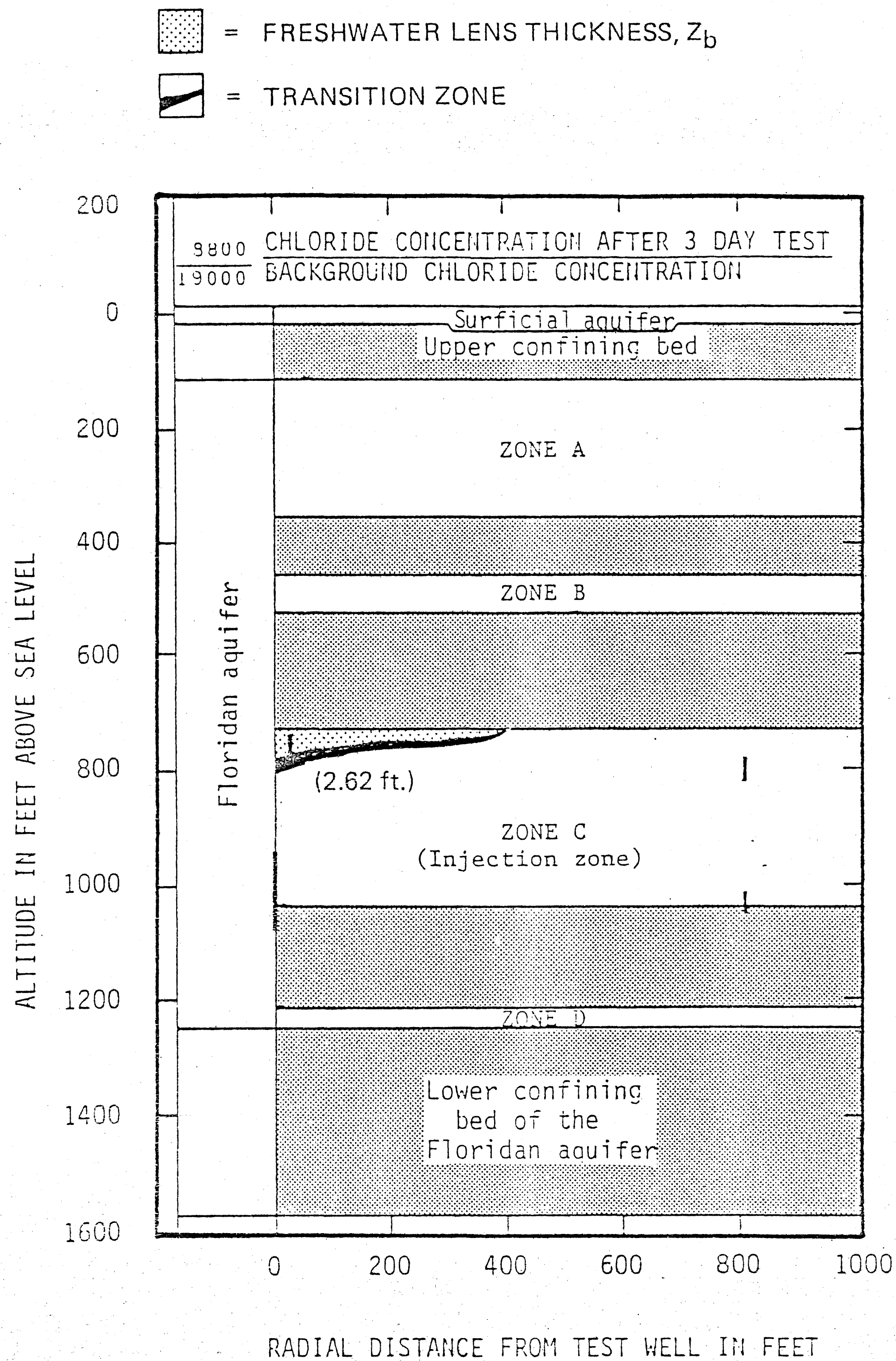

Figure 7.7 South Cross Bayou simulation using fully numerical model

of Figure 7.7 shows that the simulated results are very much like the actual field data.

The simulation for a point near the well (approximately 35 feet from the well) at 3.0 days shows a freshwater lens thickness of 49.23 feet, a transition zone thickness of 7.51 feet and a head build-up of 2.62 feet. This would mean that the freshwater lens thickness extends to a point 22.77 feet above the bottom of well A2. The injected water has a chloride content of 710 mg/l. The pre-injection chloride concentration of the aquifer is approximately 20,000 mg/l, and the distribution function of solute concentration through the transition zone of 0.33. Using these parameters, the simulated chloride concentration that would appear in well A2 is 9,600 mg/l. This value is slightly higher than is reported in the field observation (8,800 mg/l). The difference between the actual and simulated results is caused by several factors. The two factor affecting these results near the injection well is probably the assumed value of the dispersion coefficient.

The dispersion coefficient in the simulation is probably higher than the actual dispersion coefficient. By lowering this value, the transition zone size will decrease, thus decreasing the chloride concentration of the water entering the well.

Although the predicted chloride concentrations for this simulation are slightly higher than the actual field measured values, it has been demonstrated that good results can be produced by the model.

A small anomaly in the transition zone value at the well appeared in this simulation. While all other values in the transition zone grid display the expected values, the value near the well appears to be smaller than expected. This phenomenon was noticed in output from the upconing model presented by Means (1982) and in output presented by Rubin (1986). Although other investigators have not addressed this anomaly, it is believed that it is not an accurate representation of physical reality at the injection well. It is believed that this anomaly is a result of difficulties in accurately defining derivatives near the well where change is rapid. Future efforts could attempt to run the model with extremely small grid spacings. It is believed that a finer discretization would provide the accuracy needed to eliminate the anomaly at the well. Such runs could provide guidance to a proper treatment of the derivatives to allow a realistic spatial increment. In addition, other approximations could be considered. Currently, data is lacking to adequately define the actual behavior in this area and it may be difficult to judge the accuracy of any further refinements. The general shape of the freshwater lens and transition zone as they grow with time are reasonable. The almost steady state values from the simulation are also consistent with steady state estimates.

Simulation of Injection Tests Using the Simplified Injection Model

Using the simplified model described in Section 5, computer simulations of the injections tests at South Cross Bayou and southwest St. Petersburg were made. The McKay Creek injection was not modeled as results from the test showed little impact. Input parameters used in the simulation are described earlier in this chapter and in Table 7.1. Although a simulation was not run for the McKay Creek Injection test, parameters for the test are listed for completeness.

Both the South Cross Bayou and southwest St. Petersburg simulations with the modified model were run with isotropic conditions. At the time of the simulations, the anisotropic information from Hickey (1986) was not available. After reviewing the results from the modified model, it was felt that further modifications were needed before anisotropy was included, and therefore no additional runs were made for anisotropic conditions using the modified model. However, one can get a sense of the expected influence of anisotropy based on the comparison in Figure 6.9, which was actually generated using South Cross Bayou data.

South Cross Bayou Simulation

The South Cross Bayou simulation was three days in duration; time steps for the numerical procedure were in increments of 0.1 day. The injection rate was 4,350 gal./min. The lowest leakance coefficient value was chosen from the range given in Table 7.1. Using the smallest leakance coefficient will result in a calculation of the maximum possible head buildup which will provide the most conservative estimate of the injection well.

Results of the South Cross Bayou simulation are illustrated in Figure 7.8.

Southwest St. Petersburg Simulation

The simulation of the injection test at southwest St. Petersburg was 92 days in duration; time steps for the numerical procedure were in increments of 0.1 day for the first day and were increased to increments of 1 day after the first day of the simulation. Again the lowest leakance coefficient was chosen from the range given in Table 7.1 to provide the most conservative results possible.

Results of the southwest St. Petersburg simulation are illustrated in Figure 7.9.

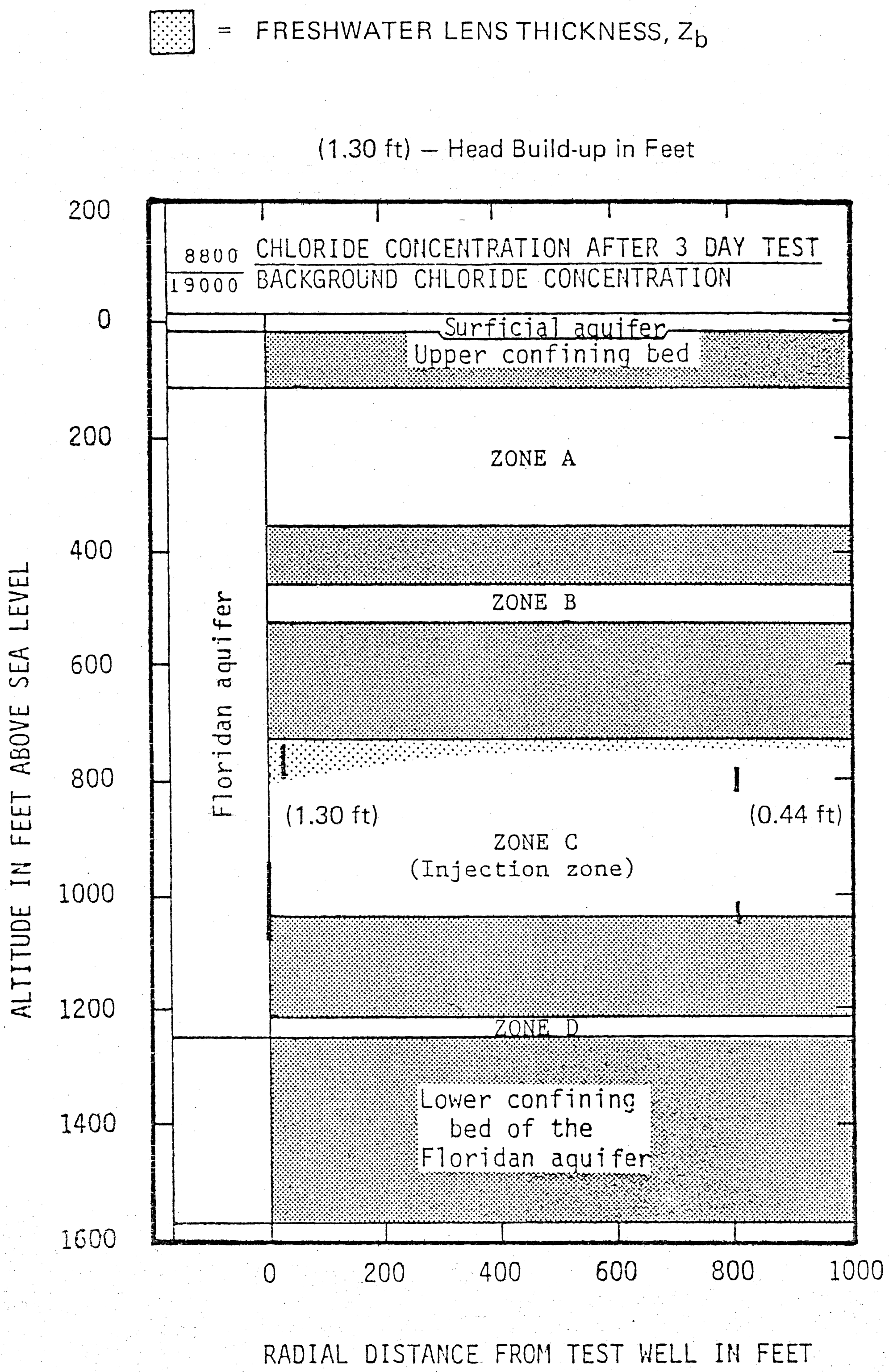

Figure 7.8 Simulation of South Cross Bayou injection using the modified model

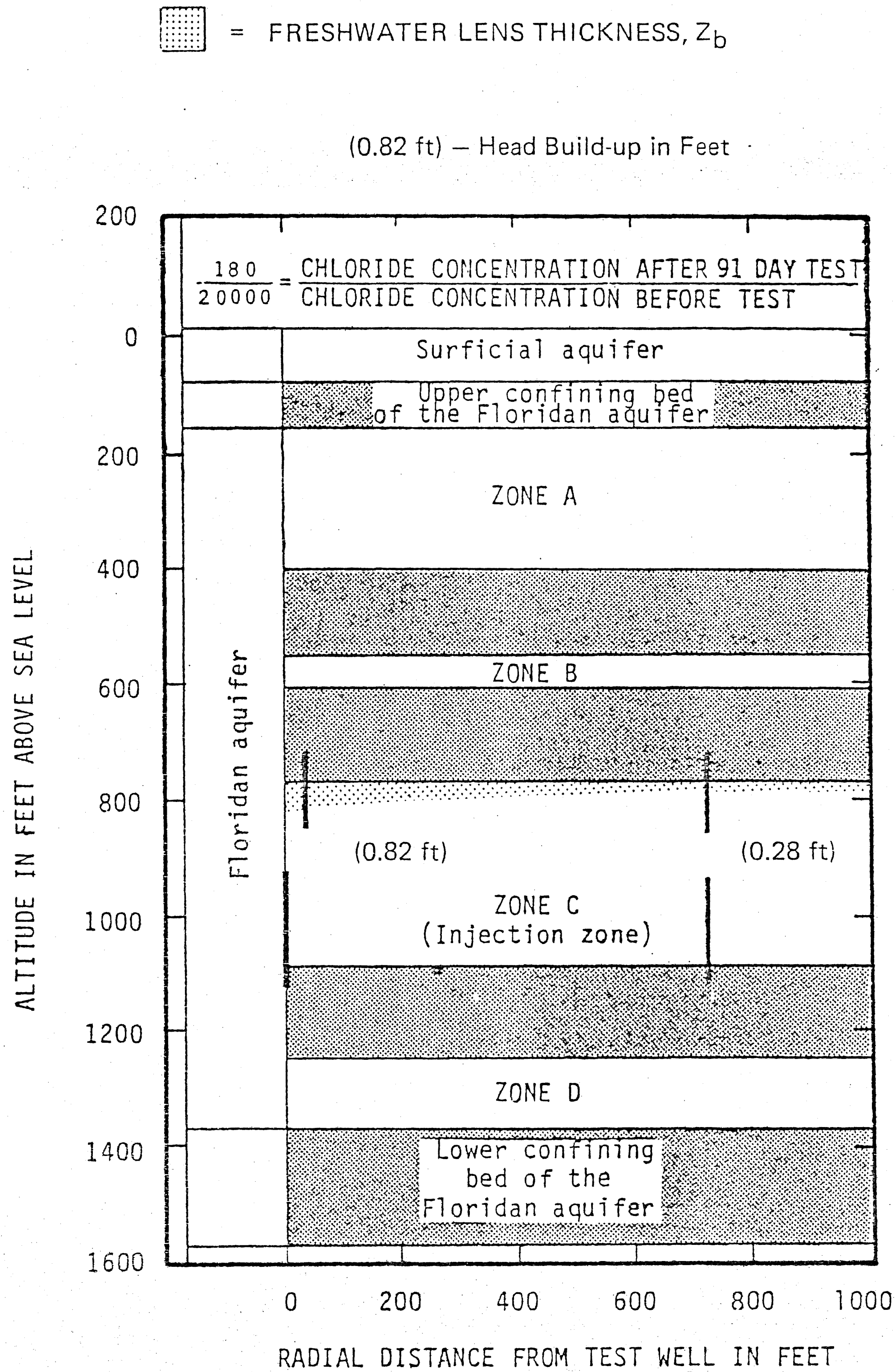

Figure 7.9 Simulation of Southwest St. Petersburg injection using the modified model

Comparison of Simulation Results of the Modified Model to Test Data

To compare the computer simulation to the field data, z_b (thickness of the freshwater lens) from the simulation is plotted on Figures 7.8 and 7.9 for South Cross Bayou and southwest St. Petersburg tests, respectively. Listed in Figures 7.4 and 7.5 is the data from the injection tests at South Cross Bayou and southwest St. Petersburg, respectively.

The results obtained from the simulation in both the South Cross Bayou and southwest St. Petersburg situations underestimate the influence of the injection well in the vicinity of the well. This discrepancy is probably due to the assumption of only horizontal flow in the freshwater region. By making the assumption of horizontal flow, the influence of vertical flow is neglected; in the vicinity of the well, vertical flow is likely to be of major influence. This is especially true due to the location of the injection wells at the bottom of the injection zone.

Some difficulties in convergence are encountered in the region of rapid head changes near and at the well.

It is possible that these difficulties can be eliminated if a more accurate description of the drawdown in the vicinity of the well is obtained. Work is continuing to refine the problems in the vicinity of the well.

Figures 7.8 and 7.9 indicate that the general extent of the injected water field is reasonably reproduced. Figure 7.8 (South Cross Bayou) indicates that the well nearest the injection well is partly in the injected water and partly in the saltwater. This seems consistent with the high chloride value observed there (8800 mg/l).

CHAPTER 8
CONCLUSIONS AND RECOMMENDATIONS

Conclusions

In this report, a three-dimensional model was developed for simulation of injection into a two-layered stratified aquifer. To account for effects in the flow field due to a transition zone of varying density and salt concentration between the fresh and saline layers an integral technique is used. By using an integral technique, the appropriate equations are simplified enough to be solved using an iterative ADI numerical scheme.

By taking advantage of the rapid stabilization of the head build-up, simplifications were made to the model which enhanced the stability characteristics and decreased the computer run time requirements of the model. Since the head build-up stabilizes quickly, it was possible to calculate the head build-up directly by using available analytical drawdown relationships. Because of the simplification of the head build-up calculation, the overall solution procedure was greatly simplified by eliminating the need for an overall iterative scheme. Also, because of the analytical calculation of the head build-up, flow velocities could be calculated directly, thus allowing for simplification of the calculation of the transition zone thickness.

To check accuracy of models, both the fully numerical and modified simulations were made with the model using input data from injection tests in Pinellas County, Florida. Simulation output was compared to the actual results of the injection tests. Data from the tests are sparse and of questionable quality, and therefore detailed comparisons are difficult. However, the general features of the injection field seem to be adequately represented, with the performance of the numerical model apparently superior to the modified model for these runs.

The numerical model appears to be behaving better in its current form, and it certainly has more potential for applications where hydraulic conditions (e.g., hydraulic conductivity) vary horizontally and vertically. However, the modified model also shows promise and further development should be useful. Both currently could be expected to provide useful analyses of injection sites with proper selection of parameters.

Recommendations

The models presented in this report provides a basis for future refinements. It should provide the ability for users to make preliminary estimates of the behavior of injection fields in settings similar to that modeled herein. There are several areas where further work is needed, some of which is continuing now. The following topics seem most deserving of attention in terms of their potential for most improvement of the model.

1. Techniques should be developed to refine the numerical portion of the model solution in the vicinity of the well. This may lead to guidelines for selection of time and distance steps, as well as possibly modified finite-difference expressions.

2. The model should be modified to account for partial penetration of the well, both in terms of the expected head buildup and in terms of the flow field attained by the injected fluid.

3. Vertical flow effects should be incorporated into the model in at least two ways: the assessment of chlorides added to the injected water by the rising plume, and achieving a better description of the actual injection field.

4. The use of analytical calculations shows a head buildup occurring at some distance from the well at very short times. The model then responds to these head buildups by showing immediate arrival of injected water. However, there is quite likely a lag time associated with the actual arrival of the injected water. Neglect of this feature may lead to inaccuracies of the model when used for short duration events. Attempts should be made to investigate this factor.

5. The effect of the assumed profiles on predictions should be investigated by numerical experimentation with other profiles. This effort should also be extended to allow integration of the profiles to estimate chloride (or other constituent) concentrations at various wells.

6. The effect of the assumed flow directions should be investigated.

7. Methods should be developed to eliminate the depression of the transition zone which occurs near the well. It is expected that this can be accomplished through improved estimates of gradients near the well.

8. Modify the model to handle the condition which occurs when the transition zone intrudes into an upper layer which has a different hydraulic conductivity.

It is believed that the model which has been developed provides a useful tool for preliminary analysis of injection problems. It is expected that completion of some of the recommended items described will enhance its use.

APPENDIX A

FULLY NUMERICAL MODEL PROGRAM LISTING

```
C       THREE DIMENSIONAL INJECTION MODEL * DENSITY STRATIFIED
C       CREATED 8/84 * S. LAUX, B. A. BENEDICT
C       MODIFIED 4/86 SJL
      COMMON/INIT/ N1,M1,IXP,IYP
      DIMENSION S(50,50),SN(50,50),SE(50,50),Z(50,50),ZN(50,50)
     *  ,ZE(50,50),DZ(50,50),XN(50,50),BI(50,50)
     *  ,A(50),B(50),C(50),D(50),X(50)
     *  ,DL(50,50),DLN(50,50),DLE(50,50),D2(50,50),DN2(50,50)
     *  ,DE2(50,50)
C      -----------------------------------------------------
C           THREE DIMENSIONAL INJECTION SIMULATION
C      -----------------------------------------------------
C            AQUIFER DETAILS
C            ===============
C      XK1=HORIZONTAL HYDRAULIC CONDUCTIVITY,AQUIFER 1(LOWER AQUIFER)
C      XK1Z=VERTICAL HYDRAULIC CONDUCTIVITY,AQUIFER 1
C      XK2=HORIZONTAL HYDRAULIC CONDUCTIVITY,AQUIFER 2(UPPER AQUIFER.)
C      B1=THICKNESS,AQUIFER 1   B2=THICKNESS,AQUIFER 2
C      PN=EFFECTIVE POROSITY    ST=STORAGE COEFFICIENT
C      A1=TRANSVERSE DISPERSIVITY
C      XKSI=PARAMETER OF DENSITY RATIO
C      N=NUMBER OF X NODAL POINTS    M= NUMBER OF Y NODAL POINTS
C      NM=NUMBER OF GRID POINTS(=N*M)
C      -----------------------------------------------------
C       ID=TYPE OF PRINTING ID=0 MEANS DRAWING
C      ----------------------------------------------------------------
      READ(5,2222) ID,IP,ITM,N,M,IXS,IXF,IYS,IYF
 2222 FORMAT(9I5)
      READ(5,2232) TMAX,DT1,TOL,DX,B2,B1,XK1,XK1Z,XK2,
     *PN,A1,ST,ALF,BET,AB,AL,XKSI,Q
 2232 FORMAT(F8.4,F8.6,4F8.4,3F8.3/8F8.4/F10.4)
      READ(5,8764) IPRI
 8764  FORMAT(I5)
C     READ(5,*) ZW1,ZW2
      TT=IPRI
C      IMA=0
      IXP=(IXS+IXF)/2
      IYP=(IYS+IYF)/2
      NM=N*M
      DB=0.
      IP=1
      WRITE(6,10)XK1,XK2,B2,B1,PN,ST,A1,XKSI,N,M,NM
   10 FORMAT(1H1,///,5X,'========================================='/
     *              ,5X,'INJECTION INTO A STRATIFIED 2-LAYERED AQUIFER'/
     *              ,5X,'   THREE DIMENSIONAL ANALYSIS'
     *             /,5X,'=========================================',
     *  //5X,'AQUIFER DETAILS'/5X, '---------------'//,5X,'XK1=',F9.3,
     *  5X,'XK2=',F9.3,5X,'B2=',F4.0,5X,'B1=',F4.0/,
     *  5X,'PN=',F4.2,5X,'ST=',F6.4,5X,'A1=',F6.4/,5X,'XKSI=',F5.3/,
     *  5X,'NODAL AND GRID POINTS  N=',I2,5X,'M=',I2,5X,'NM=',I4/)
C      ---------------------------------------------------------
C             CHRACTERISTICS OF THE TRANSITION ZONE
C             -------------------------------------
C     ALF=INTEGRAL OF F*DI(ETA)    BET=INTEGRAL OF L*DI(ETA)
```

```
C     AB=INTEGRAL OF F*L*DI(ETA)   AL=L'(0)
C     ---------------------------------------------------------
      AL1=AL*A1
      PNL=PN*BET*0.5
      WRITE(6,20)ALF,BET,AB,AL
   20 FORMAT(//,5X,'CHARACTERISTICS OF THE TRANSITION ZONE'/
     *         ,5X,'----------------------------------------'/
     *
     *      5X,'ALF=',F6.4,5X,'BET=',F6.4,5X,'AB=',F6.4,5X,'AL=',
     *     F6.3,
     *     5X)
C     ----------------------------------------------------------------
C                    PARAMETERS
C                    ==========
C     S(I,J),SN(I,J),SE(I,J)=INIT.,FI.,AVE HEAD BUILDUP
C     Z(I,J),ZN(I,J),ZE(I,J)=INIT.,FI.,AVE THICK. OF FRESHWATER LENS
C     DL(I),DLN(I),DLE(I)=INIT.,FI.,AVE.THICKNESS OF TRANS.ZONE
C     D2(I),DN2(I),DE2(I)=INIT.,FI.,AVE.SQUARE THICK. OF TRANS ZONE
C     BI(I,J)=AVERAGE THICKNESS OF THE FRESHWATER ZONE
C     DZ(I,J)=AVERAGE RATE OF GROWTH OF SALTWATER MOUND
C     XN(I,J)=RATE OF INJECTION PER UNIT AREA
C     ----------------------------------------------------------------
      DO 50 I=1,N
      DO 40 J=1,M
      S(I,J)=0.
      SN(I,J)=0.
      SE(I,J)=0.
      Z(I,J)=0.
      ZN(I,J)=0.
      ZE(I,J)=0.
      DZ(I,J)=0.
      BI(I,J)=B2*XK2/XK1
      XN(I,J)=0.
      DL(I,J)=0.
      DLN(I,J)=0.
      DLE(I,J)=0.
      D2(I,J)=0.
      DN2(I,J)=0.
      DE2(I,J)=0.
   40 CONTINUE
   50 CONTINUE
C     ----------------------------------------------------------------
C     INJECTION DISTRIBUTION
C     -----------------------------------------------------------------
      WRITE(6,60)
   60 FORMAT(5X,'INJECTION DISTRIBUTION',/5X,'===================='/)
      N1=N-1
      M1=M-1
       DO 80 I=IXS,IXF
        DO 70 J=IYS,IYF
         XN(I,J)=Q
   70  CONTINUE
   80 CONTINUE
      IF(ID.EQ.1) GOTO 88
```

```
      WRITE(6,82)
   82 FORMAT(///,10X,'MAP OF INJECTION'//)
      CALL DRAW1(XN,IP,DB)
      GOTO 132
   88 DO 130 I=20,30
      DO 120 K=1,2
      J=20+(K-1)*6
      J1=J+1
      J2=J+2
      J3=J+3
      J4=J+4
      J5=J+5
      IF(K.EQ.2) GOTO 100
      WRITE(6,90)I,J,XN(I,J),I,J1,XN(I,J1),I,J2,XN(I,J2),I,J3,XN(I,J3),
     * I,J4,XN(I,J4),I,J5,XN(I,J5)
   90 FORMAT(3X,'XN(',I2,',',I2,')=',F4.2,3X,'XN(',I2,',',I2,')=',F4.2
     *  ,3X,'XN(',I2,',',I2,')=',F4.2,3X,'XN(',I2,',',I2,')=',F4.2,
     *    3X,'XN(',I2,',',I2,')=',F4.2,3X,'XN(',I2,',',I2,')=',
     *  F4.2)
      GOTO 120
  100 WRITE(6,110)I,J,XN(I,J),I,J1,XN(I,J1),I,J2,XN(I,J2),I,J3,XN(I,J3)
     * ,I,J4,XN(I,J4)
  110 FORMAT(3X,'XN(',I2,',',I2,')=',F4.2,3X,'XN(',I2,',',I2,')=',F4.2,
     * 3X,'XN(',I2,',',I2,')=',F4.2,3X,'XN(',I2,',',I2,')=',F4.2,
     *    3X,'XN(',I2,',',I2,')=',F4.2)
  120 CONTINUE
  130 CONTINUE
C     ----------------------------------------------------------------
C     GRID INTERVALS
C     ----------------------------------------------------------------
  132 WRITE(6,140) DX
  140 FORMAT(/ 3X,'GRID INTERVALS DY=DX=',F4.0,' METERS')
      N1=N-1
      N2=N-2
      N3=N-3
      M1=M-1
      M2=M-2
      M3=M-3
      A(1)=0.
C     ----------------------------------------------------------------
C     INITIAL TIME STEP=DT1
C     ----------------------------------------------------------------
      WRITE(6,150)DT1
  150 FORMAT(//,5X,'TIME STEP DT=',F5.3,' DAYS',/5X,
     * '===================='/)
      T=0.
      WRITE(6,160)T
  160 FORMAT(//5X,'T=',F8.3,' DAYS'/,5X,'=================='/)
      WRITE(6,170)
  170 FORMAT(// 5X,'ALL PARAMETERS VANISH'/,5X,'----------------------')
      DT=DT1
      DX2=DX*DX
  180 CONTINUE
      XKK=XK1*XK2/(PN*(1.+XKSI))
```

```
      BK=B1*XK1
      IX=1
       ITRY=0
 210   CONTINUE
      ITRY=ITRY+1
       IF(ITRY.LE.10) GO TO 201
       IF(IT.LE.1) DT=2*DT
       ITRY=0
 201   CONTINUE
      T=T+DT
      IF(T.GT.TMAX) GOTO 660
C     ------------------------------------------------------------------
C     STARTING ITERATION PROCEDURE
C     ------------------------------------------------------------------
      R=DT/DX2
      XKT=XK1*R
  220 IT=-1
  222 IT=IT+1
       IF(IT.GT.ITM) GO TO 340
      BK=B1*XK1
      IF(IX.EQ.2) GOTO 590
C     ------------------------------------------------------------------
C     IMPLICIT SCHEME IN THE X DIRECTION
C     ------------------------------------------------------------------
      SBIG=0.
      DO 280 J=2,M1
      DO 230 I1=2,N2
      I=I1+1
      A(I1)=.5*XKT*(BI(I-1,J)+BI(I,J)+(DLE(I-1,J)+DLE(I,J))*ALF)
  230 CONTINUE
      DO 240 I1=1,N2
      I=I1+1
      B(I1)=ST+XKT*0.5*(BI(I+1,J)+2.*BI(I,J)+BI(I-1,J)
     *  +(DLE(I+1,J)+2.*DLE(I,J)+DLE(I-1,J))*ALF)
      D(I1)=ST*S(I,J)-PN*DT*DZ(I,J)+XN(I,J)*DT+XKT*0.5*((BI(I,J+1)+
     *  BI(I,J)+(DLE(I,J+1)+DLE(I,J))*ALF)*(S(I,J+1)-S(I,J))+(BI(I,J)
     *  +BI(I,J-1)+(DLE(I,J)+DLE(I,J-1))*ALF)*(S(I,J-1)-S(I,J)))
  240 CONTINUE
      DO 250 I1=1,N3
      I=I1+1
      C(I1)=0.5*XKT*(BI(I,J)+BI(I+1,J)+(DLE(I+1,J)+DLE(I,J))*ALF)
  250 CONTINUE
      CALL THOMAS(A,B,C,D,X,N2)
      DO 260 I=2,N1
      I1=I-1
      SN1=X(I1)
      SB=ABS(SN1-SN(I,J))
      IF(SB.GT.SBIG) SBIG=SB
      SN(I,J)=0.5*(SN1+SN(I,J))
  260 CONTINUE
      DO 270 I=2,N1
      SE(I,J)=(S(I,J)+SN(I,J))*0.5
  270 CONTINUE
  280 CONTINUE
```

```
      DO 284 J=2,M1
      DO 283 I=2,N1
      IF(Z(I,J).LT.0.0001) GOTO 283
      SCK=(SE(I,J)-SE(I-1,J))/DX
      SCK2=(SE(I,J)-SE(I,J-1))/DX
      JJ=J
      II=I
      IF(I.LT.IXS)GO TO 281
      IF(SCK.LT.0) II=I+1
 281  IF(J.LT.IYS)GO TO 282
      IF(SCK2.LT.0) JJ=J+1
 282  CONTINUE
C  TEMPORARY FIX TO REDUCE INFLUENCE OF 'DOUGHNUTING' ON DIFFERENCE SCHEME
      IF(I.GT.IXS)II=I+1
      IF(J.GT.IYS)JJ=J+1
C  END OF TEMPORARY FIX **************************************************
C***  BALANCED TRANS. X
      DEN=PNL-XKT*AB*(SE(I+1,J)+SE(I-1,J)-2.0*SE(I,J)+XSGN*0.5*
     *  SE(II,J)-XSGN*0.5*SE(II-1,J))
      DN2(I,J)=(D2(I,J)*PNL+XKT*AB*
     *  (-XSGN*0.5*DN2(III-1,J)*(SE(II,J)-SE(II-1,J))+D2(I,J)*
     *  (SE(I,J+1)+SE(I,J-1)-2.*SE(I,J))+.5*(SE(I,JJ)-SE(I,JJ-1))*
     *  (D2(I,JJ)-D2(I,JJ-1)))-DX*AL1*XKT*SQRT((-SE(II,J)+
     *  SE(II-1,J))**2+(-SE(I,JJ)+SE(I,JJ-1))**2))/DEN
C***  END BALANCED TRANS X
      IF(DN2(I,J).LT.0.) DN2(I,J)=0.
  283 CONTINUE
  284 CONTINUE
C     ------------------------------------------------------------------
C     CALCULATION APPLIED TO X AND Y DIRECTIONS
C     ------------------------------------------------------------------
  285 DBIG=0.
      DBI2=0.
      DO 288 I=2,N1
      DO 287 J=2,M1
      DLN(I,J)=SQRT(DN2(I,J))
      DLE(I,J)=.5*(DLN(I,J)+DL(I,J))
      DE2(I,J)=.5*(D2(I,J)+DN2(I,J))
      DB1=ABS(DLN(I,J)-DL(I,J))
      DB2=ABS(DN2(I,J)-D2(I,J))
      IF(DB1.GT.DBIG) DBIG=DB1
      IF(DB2.GT.DBI2) DBI2=DB2
  287 CONTINUE
  288 CONTINUE
      ZBIG=0.
      DO 300 J=2,M1
      DO 290 I=2,N1
      DZ(I,J)=XK1Z/((B1-ZE(I,J))*PN*(1+XKSI))*(SE(I,J)+XKSI*(-ZE(I,J)
     $ +BET*DLE(I,J)))
      ZN(I,J)=Z(I,J)+DT*DZ(I,J)
      IF(ZN(I,J).LT.0.) ZN(I,J)=0.
      IF(SN(I,J).EQ.0.) ZN(I,J)=0.
      ZE(I,J)=0.5*(ZN(I,J)+Z(I,J))
      BI(I,J)=B2*XK2/XK1+ZE(I,J)-DLE(I,J)
```

```
      IF(BI(I,J).LE.0.0) BI(I,J)=0.0
      ZB=ABS(ZN(I,J)-Z(I,J))
      IF(ZB.GT.ZBIG) ZBIG=ZB
  290 CONTINUE
  300 CONTINUE
C     IF(IT/10.NE.0.1*IT) GOTO 312
C     WRITE(6,310)T,IT,IX,SBIG,ZBIG,DBIG,DBI2
C310  FORMAT(//3X,F8.5,4X,'IT=',I3,3X,'IX=',I4,3X,'SBIG=',E8.2,3X,
C    &'ZBIG=',E8.2,
C    *  3X,'DBIG=',E8.2,3X,'DBI2=',E8.2)
C312    CONTINUE
C     IF (T.LT.0.01) GO TO 1080
C     WRITE (6,1050)
C     DO 1010 J=1,M
C      WRITE(6,9876) (SN(I,J), I=1,N)
C1010 CONTINUE
C     WRITE(6,1060)
C     DO 1020 J=1,M
C      WRITE(6,9876) (DN2(I,J), I=1,N)
C1020 CONTINUE
C     WRITE(6,1070)
C     DO 1030 J=1,M
C      WRITE(6,9876) (ZN(I,J), I=1,N)
C1030 CONTINUE
C1050 FORMAT(1X,'SN')
C1070 FORMAT(1X,'ZN')
C1080 CONTINUE
      IF(IT.EQ.0) GOTO 222
      IF(SBIG.GT.TOL) GOTO 222
      IF(IX-2) 320,330,330
  320 IX=2
      GOTO 380
  330 IX=1
      GOTO 380
  340 T=T-DT
      DT=0.5*DT
  350 DO 370 J=2,M1
      DO 360 I=2,N1
      SE(I,J)=S(I,J)
      DLE(I,J)=DL(I,J)
      DE2(I,J)=D2(I,J)
      ZE(I,J)=Z(I,J)
      BI(I,J)=B2*XK2/XK1+ZE(I,J)-DLE(I,J)
      IF(BI(I,J).LE.0.0) BI(I,J)=0.0
      DZ(I,J)=XK1Z/((B1-ZE(I,J))*PN*(1+XKSI))*(SE(I,J)+XKSI*(-ZE(I,J)
     *  +BET*DLE(I,J)))
  360 CONTINUE
  370 CONTINUE
      IF(IT.GT.ITM) GO TO 210
      GOTO 210
  380 DS=0.
      DO 400 J=2,M1
      DO 390 I=2,N1
      DSS=ABS(SN(I,J)-S(I,J))
```

```
      IF(DSS.GT.DS) DS=DSS
  390 CONTINUE
  400 CONTINUE
C     IF(DS.LT.0.00001) GOTO 660
      DB=0.
      DO 420 J=2,M1
      DO 410 I=2,N1
      S(I,J)=SN(I,J)
      Z(I,J)=ZN(I,J)
      DL(I,J)=DLN(I,J)
      IF(DL(I,J).GT.DB) DB=DL(I,J)
      D2(I,J)=DN2(I,J)
  410 CONTINUE
  420 CONTINUE
C     -----------------------------------------------------------------
C     PRINTING RESULTS
C     -----------------------------------------------------------------
  561 FORMAT(5X,'ALL ORDINATES ARE SMALLER THAN 0.05 METER'//)
C     -----------------------------------------------------------
C     CONCENTRATION CALCULATIONS
C     -----------------------------------------------------------
C     DLCC=DL(IXP,IYP)
C     IF(DLCC.EQ.0.0) GO TO 1563
C     ZB=Z(IXP,IYP)
C     ZT= ZB + DL(IXP,IYP)
C     IF(ZW1.GE.ZT) GO TO 1561
C     ETA1=(ZT-ZW1)/DL
C     ETA2=(ZW2-ZB)/DL
C     IF(ETA2.GT.1.0)GO TO 1563
C     CW=ETA1**2  - (5./3.)*ETA1**3 + ETA1**4 - .2*ETA1**5
C     CW= CW - ETA2**2 + (5./3.)*ETA2**3 - ETA2**4 + .2*ETA2**5
C     CW1=2.*ETA1 - ETA1**2 -2.*ETA2 + ETA2**2
C     CW=( CW/ CW1) * 19000
C     WRITE(6,1562)  CW
C1562 FORMAT(//,10X,' CURRENT  CONCENTRATION= ',F20.2)
C     GO TO 1563
C1561 ETA2=(ZW2-ZB)/DL
C     IF(ETA2.GT.1.0)GO TO 1563
C     CWD=((2./3.) - ETA2**2 - ETA2**3/3.) * DL
C     CWD=  CWD + ZCW1 -ZT
C     CWN= (2./15.) - ETA2**2 + (5./3.)*ETA2**3
C     CWN=  CWN - ETA2**4 +0.2*ETA2**4
C     CW=( CWN*DL  )/ CWD
C     CW= CW * 19000
C     WRITE(6,1562)  CW
 1563  CONTINUE
      IF(T.LT.TT)GO TO 586
      TT=TT+IPRI
C      IF(T.GT.6.0) DT1=0.5
C      IMA=IMA+1
C      IF (IMA.GT.IPRI) IMA=0
C      IF (IMA.LT.IPRI) GO TO 586
       IF(T.LT.0.01) GO TO 586
C      IF(IX .EQ. 2)GO TO 586
```

```
       IF(ID.EQ.1) GO TO 568
       IF(ID.EQ.2) GO TO 5544
       WRITE(6,160) T
      WRITE(6,562)
  562 FORMAT(///,10X,'MAP OF HEAD BUILDUP'//)
      CALL DRAW(S,IP,DB)
      WRITE(6,564)
  564 FORMAT(///,10X,'MAP OF FRESHWATER LENS'//)
      IF(Z(IXP,IYP).GE.5.0) CALL DRAW(Z,IP,DB)
      IF(Z(IXP,IYP).LT.5.0.AND.Z(IXP,IYP).GT.0.05) CALL DRAW1(Z,IP,DB)
      IF(Z(IXP,IYP).LT.0.05) WRITE(6,561)
      WRITE(6,565)
      IP=2
  565 FORMAT(///10X,'MAP OF TRANSITION ZONE'///)
      IF(DB.GE.5.) CALL DRAW(DL,IP,DB)
      IF(DB.LT.5.0.AND.DB.GT.0.05) CALL DRAW1(DL,IP,DB)
      IF(DB.LT.0.05) WRITE(6,561)
      IP=1
  567 GOTO 586
  568 WRITE(6,570)
  570 FORMAT(/2X,'NODE',5X,'S',11X,'Z',8X,'NODE',5X,'S',11X,'Z',8X,
     *  'NODE',5X,'S',11X,'Z',8X,'NODE',5X,'S',11X,'Z'/)
      DO 584 I=1,N
      DO 582 K=1,10
      J=(K-1)*4+1
      J1=J+1
      J2=J+2
      J3=J+3
      WRITE(6,580) I,J,S(I,J),Z(I,J),I,J1,S(I,J1),Z(I,J1)
     * ,I,J2,S(I,J2),Z(I,J2),I,J3,S(I,J3),Z(I,J3)
  580 FORMAT(4(I3,I3,2E12.4))
  582 CONTINUE
  584 CONTINUE
      GO TO 586
 5544 WRITE(6,160) T
      WRITE(6,562)
      DO 5555 J=1,M
       WRITE(6,9876) (S(I,J), I=1,N)
 5555 CONTINUE
      WRITE(6,564)
      DO 6555 J=1,M
       WRITE(6,9876) (Z(I,J), I=1,N)
 6555 CONTINUE
      WRITE(6,565)
      DO 7555 J=1,M
       WRITE(6,9876) (DL(I,J), I=1,N)
 7555 CONTINUE
 9876 FORMAT(1X,21F6.2//)
  586 CONTINUE
      GOTO 350
C     ----------------------------------------------------------------
C     IMPLICIT SCHEME IN THE Y DIRECTION
C     ----------------------------------------------------------------
  590 SBIG=0.
```

```
      DO 650 I=2,N1
      DO 600 J1=2,M2
      J=J1+1
      A(J1)=.5*XKT*(BI(I,J-1)+BI(I,J)+(DLE(I,J-1)+DLE(I,J))*ALF)
  600 CONTINUE
      DO 610 J1=1,M2
      J=J1+1
      B(J1)=ST+XKT*0.5*(BI(I,J+1)+2.*BI(I,J)+BI(I,J-1)+
     *  (DLE(I,J+1)+2.*DLE(I,J)+DLE(I,J-1))*ALF)
      D(J1)=ST*S(I,J)-PN*DT*DZ(I,J)+XN(I,J)*DT+XKT*0.5*((BI(I+1,J)+
     *  BI(I,J)+(DLE(I+1,J)+DLE(I,J))*ALF)*(S(I+1,J)-S(I,J))+
     *  (BI(I,J)+BI(I-1,J)+(DLE(I,J)+DLE(I-1,J))*ALF)*
     *  (S(I-1,J)-S(I,J)))
  610 CONTINUE
      DO 620 J1=1,M3
      J=J1+1
      C(J1)=0.5*XKT*(BI(I,J)+BI(I,J+1)+(DLE(I,J+1)+DLE(I,J))*ALF)
  620 CONTINUE
      CALL THOMAS(A,B,C,D,X,M2)
      DO 630 J=2,M1
      J1=J-1
      SN1=X(J1)
      SB=ABS(SN1-SN(I,J))
      IF(SB.GT.SBIG) SBIG=SB
      SN(I,J)=0.5*(SN1+SN(I,J))
  630 CONTINUE
      DO 640 J=2,M1
      SE(I,J)=0.5*(S(I,J)+SN(I,J))
  640 CONTINUE
  650 CONTINUE
      DO 655 I=2,N1
      DO 654 J=2,M1
      IF(Z(I,J).LT.0.0001) GOTO 654
      SCK=(SE(I,J)-SE(I,J-1))/DX
      SCK2=(SE(I,J)-SE(I-1,J))/DX
      II=I
      JJ=J
      IF(J.LT.IYS) GO TO 651
      IF(SCK.LT.0) JJ=J+1
 651  IF(I.LT.IXS) GO TO 653
      IF(SCK2.LT.0) II=I+1
 653  CONTINUE
C   TEMPORARY FIX (SAME AS X )
      IF(J.GT.IYS)JJ=J+1
      IF(I.GT.IXS)II=I+1
C   END OF TEMPORARY FIX
C***  BALANCED TRANS. Y
      DEN=PNL-XKT*AB*(SE(I,J+1)+SE(I,J-1)-2.0*SE(I,J)+XSGN*0.5*
     *  SE(I,JJ)-XSGN*0.5*SE(I,JJ-1))
      DN2(I,J)=(D2(I,J)*PNL+XKT*AB*
     *  (-XSGN*0.5*DN2(I,JJJ-1)*(SE(I,JJ)-SE(I,JJ-1))+D2(I,J)*
     *  (SE(I+1,J)+SE(I-1,J)-2.*SE(I,J))+.5*(SE(II,J)-SE(II-1,J))*
     *  (D2(II,J)-D2(II-1,J)))-DX*AL1*XKT*SQRT((-SE(II,J)+
     *  SE(II-1,J))**2+(-SE(I,JJ)+SE(I,JJ-1))**2))/DEN
```

```
C*** END BALANCED TRANS. Y
      IF(DN2(I,J).LT.0.) DN2(I,J)=0.
  654 CONTINUE
  655 CONTINUE
      GOTO 285
  660 CONTINUE
      STOP
      END
C     ------------------------------------------------------------------
C     SUBROUTINE THOMAS SOLVES A SYSTEM OF LINEAR EQUATIONS
C        REPRESENTED BY A TRIDIAGONAL MATTRIX
C     ------------------------------------------------------------------
      SUBROUTINE THOMAS(A,B,C,D,X,N)
      DIMENSION A(N),B(N),C(N),D(N),X(N),ALFA(70),SI(70)
      ALFA(1)=B(1)
      SI(1)=D(1)
      DO 20 I=2,N
      E=A(I)/ALFA(I-1)
      ALFA(I)=B(I)-E*C(I-1)
      SI(I)=D(I)+E*SI(I-1)
   20 CONTINUE
      X(N)=SI(N)/ALFA(N)
      N1=N-1
      DO 30 I=1,N1
      J=N-I
      X(J)=(SI(J)+C(J)*X(J+1))/ALFA(J)
   30 CONTINUE
      RETURN
      END
C     ------------------------------------------------------------------
C     SUBROUTINE DRAW MAPS VARIABLES BY APPLYING THE TYPEWRITER
C     ------------------------------------------------------------------
      SUBROUTINE DRAW(W,IP,DB)
      COMMON/INIT/N1,M1,IXP,IYP
      CHARACTER *3 AA,BB,CC
      DIMENSION W(50,50),BB(50),AA(50),CC(50)
      DATA CC/'   ','+1+',' 2 ','+3+',' 4 ','+5+',' 6 ','+7+',' 8 ',
     * '+9+',' 10','+11',' 12','+13',' 14','+15',' 16','+17',' 18',
     * '+19',' 20','+21',' 22','+23',' 24','+25',' 26','+27',' 28',
     * '+29',' 30','+31',' 32','+33',' 34','+35',' 36','+37',' 38',
     * '+39',' 40','+41',' 42','+43',' 44','+45',' 46','+47',' 48',
     * ' 50'/
      BB(1)=' ++'
      M=M1+1
      N=N1+1
      BB(N)='++ '
      DO 10 I=2,N1
      BB(I)='+++'
   10 CONTINUE
      WRITE(6,20) (BB(I),I=1,N)
   20 FORMAT(40A3)
      BB(1)=' + '
      BB(N)=' + '
      DO 60 J=2,M1
```

```
      DO 40 I=2,N1
      DO 30 K=1,50
      AK=K
      X1=AK-1.5
      X2=X1+1
      IF(W(I,J).LT.X2.AND.W(I,J).GE.X1) BB(I)=CC(K)
   30 CONTINUE
   40 CONTINUE
      WRITE(6,20) (BB(I),I=1,N)
   25  FORMAT('     ')
       WRITE(6,25)
   60 CONTINUE
      BB(1)=' ++'
      BB(N)='++ '
      DO 70 I=2,N1
      BB(I)='+++'
   70 CONTINUE
      WRITE(6,20) (BB(I),I=1,N)
      IF(IP.EQ.2) GOTO 75
      WRITE(6,80) W(IXP,IYP)
      RETURN
   75 WRITE(6,80) DB
   80 FORMAT(//5X,'MAXIMAL ORDINATE=',F8.3,' METER'//)
      RETURN
      END
C     ----------------------------------------------------------------
C     SUBROUTINE DRAW1 MAPS PUMPAGE BY APPLYING THE TYPEWRITER
C     ----------------------------------------------------------------
      SUBROUTINE DRAW1(W,IP,DB)
      COMMON/INIT/N1,M1,IXP,IYP
      CHARACTER *3 AA,BB
      DIMENSION W(50,50),BB(50),AA(50)
      DATA AA/'   ',' .1',' .2',' .3',' .4',' .5',' .6',' .7',' .8',
     *  ' .9','1. ','1.1','1.2','1.3','1.4','1.5','1.6','1.7','1.8',
     *  '1.9','2. ','2.1','2.2','2.3','2.4','2.5','2.6','2.7','2.8',
     *  '2.9','3. ','3.1','3.2','3.3','3.4','3.5','3.6','3.7','3.8',
     *  '3.9','4. ','4.1','4.2','4.3','4.4','4.5','4.6','4.7','4.8',
     *  '4.9'/
      BB(1)=' ++'
      N=N1+1
      M=M1+1
      BB(N)='++ '
      DO 10 I=2,N1
      BB(I)='+++'
   10 CONTINUE
      WRITE(6,20) (BB(I),I=1,N)
   20 FORMAT(40A3)
      BB(1)=' + '
      BB(N)=' + '
      DO 60 J=2,M1
      DO 40 I=2,N1
      DO 30 K=1,50
      AK=K
      X=.1*AK-0.05
```

```
      X1=X-0.10
      IF(W(I,J).LT.X.AND.W(I,J).GE.X1) BB(I)=AA(K)
30    CONTINUE
40    CONTINUE
      WRITE(6,20) (BB(I),I=1,N)
 25   FORMAT('   ')
      WRITE(6,25)
60    CONTINUE
      BB(1)=' ++'
      BB(N)='++ '
      DO 70 I=2,N1
      BB(I)='+++'
70    CONTINUE
      WRITE(6,20) (BB(I),I=1,N)
      IF(IP.EQ.2) GOTO 75
      WRITE(6,80) W(IXP,IYP)
      RETURN
75    WRITE(6,80) DB
80    FORMAT(//5X,'MAXIMAL ORDINATE=',F8.3,' METER'//)
      RETURN
      END
```

APPENDIX B

MODIFIED MODEL PROGRAM LISTING

```
C     A MODIFIED NUMERICAL-ANALYTICAL MODEL FOR THE SIMULATION
C     OF AN INJECTION INTO A CONFINED DENSITY-STRATIFIED AQUIFER.
C
C                           LIST OF ARRAYS
C
C           SN,SE,S= PRESENT,MEAN,PAST VALUES OF HEAD-BUILDUP
C           ZN,ZE,Z= PRESENT,MEAN,PAST VALUES OF FRESHWATER LENS
C           DZ= RATE OF CHANGE OF THICKNESS OF FRESHWATER LENS
C           DN2,D2=PRESENT,PAST SQUARED THICKNESS OF THE TRANSITION ZONE
C           DLN,DLE,DL= PRESENT,MEAN,PAST THICKNESS OF THE
C                       TRANSITION ZONE
      DIMENSION SE(50,50),S(50,50),ZN(50,50),ZE(50,50),Z(50,50)
      DIMENSION DZ(50,50),DN2(50,50),DLN(50,50),DLE(50,50),DL(50,50)
      DIMENSION D2(50,50)
      COMMON /NM/ N,M
      COMMON /DEL/ DX,DY,TIME
      COMMON /PARAM/ T,STO
      COMMON /DD/ SN(50,50)
      COMMON /NEW/ B1,B,XK
      COMMON /GOOD/ III(10),JJJ(10),QWELL(10),JI
      COMMON /MOI/ SXM(50,50),SXP(50,50),SYM(50,50),SYP(50,50)
      COMMON /HEY/ XD,YD
C     ****************************************************
C                 INPUT GRID DATA
C
C        N= NUMBER OF X-DIRECTION NODES    M= NUMBER OF Y-DIRECTION NODES
C        DX= DISTANCE BETWEEN X-DIR NODES  DY= DISTANCE BETWEEN Y-DIR NODES
C        DT= TIME INCREMENT
C        TIMAX= MAXIMUM TIME MODELED
C        XD= X-DISTANCE USED FOR FINITE-DIFFERENCE APPROXIMATION
C        YD= Y-DISTANCE USED FOR FINITE-DIFFERENCE APPROXIMATION
C     ****************************************************
      READ(5,200) N,M
      WRITE(6,400) N,M
      READ(5,205) DX,DY,DT,TIMAX
      WRITE(6,410) DX,DY,DT,TIMAX
      READ(5,207) XD,YD
      WRITE(6,412) XD,YD
C     *****************************************************
C               INPUT AQUIFER DATA
C
C        T= TRANSMISSIVITY OF AQUIFER
C        STO= STORATIVITY OF AQUIFER
C        B1= THICKNESS OF AQUIFER
C        B= THICKNESS OF SEMI-CONFINING FORMATION
C        XK= VERTICAL CONDUCTIVITY OF SEMI-CONFINING FORMATION
C        PN= POROSITY OF AQUIFER
C        BET= INTEGRAL OF L(ETA)*D(ETA)
C        AL= L'(0)
C        A1= DISPERSIVITY
C        XKSI= DENSITY RATIO
C        AB= INTEGRAL OF F(ETA)*L(ETA)*D(ETA)
C     *****************************************************
      READ(5,210) T,STO
```

```
      WRITE(6,420) T,STO
      READ(5,220) B1,B,XK
      WRITE(6,430) B1,B,XK
      READ(5,250) PN,BET,AL,A1,XKSI,AB
      WRITE(6,440) PN,BET,AL,A1,XKSI,AB
C     ****************************************************
C                INPUT WELL DATA
C
C        JI= NUMBER OF WELLS TO BE INPUT
C        III(IRD)= X-COORDINATE OF WELL IRD
C        JJJ(IRD)= Y-COORDINATE OF WELL IRD
C        QWELL(IRD)= INJECTION RATE OF WELL IRD
C     ******************************************************
      READ(5,230) JI
      WRITE(6,450) JI
      DO 2 IRD=1,JI
        READ(5,240) III(IRD),JJJ(IRD),QWELL(IRD)
        WRITE(6,460) III(IRD),JJJ(IRD),QWELL(IRD)
 2    CONTINUE
      PNL=PN*BET*0.5
      AL1=AL*A1
      XKK=T/(B1*PN*(1.0+XKSI))
      M1=M-1
      N1=N-1
C        INITIALIZE VECTORS AND ARRAYS
      DO 4 J=1,M
        DO 3 I=1,N
           SN(I,J)=0.0
           SE(I,J)=0.0
           S(I,J)=0.0
           DN2(I,J)=0.0
           D2(I,J)=0.0
           DLN(I,J)=0.0
           DLE(I,J)=0.0
           DL(I,J)=0.0
           DZ(I,J)=0.0
           ZN(I,J)=0.0
           ZE(I,J)=0.0
           Z(I,J)=0.0
 3      CONTINUE
 4    CONTINUE
      ICNT=0
      ISKIP=0
      TIME=0.0
C        INCREMENT TIME
 5    TIME=TIME+DT
      XKT=T*DT/(B1*DX**2)
      AK=T*DT*AB/B1
      ICNT=ICNT+1
      SBIG=0.0
      IF(ICNT.GE.3) ICNT=1
      IF(ISKIP.EQ.1) GO TO 25
C        CALCULATE HEAD-BUILDUP ANALYTICALY FOR PRESENT TIME-STEP
      CALL HANT
```

```
      DO 20 J=1,M
       DO 10 I=1,N
        SB=ABS(SN(I,J)-S(I,J))
        IF(SB .GT. SBIG) SBIG=SB
        SE(I,J)=(SN(I,J) + S(I,J))/2.0
        S(I,J)=SN(I,J)
 10   CONTINUE
 20   CONTINUE
      IF(SBIG.LT.0.01) ISKIP=1
C        IF HEAD-BUILDUP REACHES STEADY-STATE, DO NOT RECALCULATE
C        HEAD-BUILDUP
      IF(ISKIP .EQ. 1)WRITE(6,22)
 22   FORMAT(1X,' *******************'/'  STEADY STATE REACHED'/
     $'  *******************')
 25   DO 40 J=2,M1
       DO 30 I=2,N1
       JJ=J
       II=I
      SCK=(SN(I,J)-SN(I-1,J))/DX
      SCK2=(SN(I,J)-SN(I,J-1))/DY
C        CALCULATE VELOCITIES (HEAD-GRADIENTS) USING VARIABLE-
C        SPACING FINITE DIFFERENCE APPROXIMATION
      DSDX=(SN(I,J)-SXM(I,J))/XD
      DSDY=(SN(I,J)-SYM(I,J))/YD
      D2DX=(SXP(I,J)-2.0*SN(I,J)+SXM(I,J))/XD**2
      D2DY=(SYP(I,J)-2.0*SN(I,J)+SYM(I,J))/YD**2
C        CHECK SLOPE OF HEAD-GRADIENT FOR SYMMETRY CONTROL
      IF(SCK.LT.0) DSDX=(SXP(I,J)-SN(I,J))/XD
      IF(SCK.LT.0) II=I+1
      IF(SCK2.LT.0) DSDY=(SYP(I,J)-SN(I,J))/YD
      IF(SCK2.LT.0) JJ=J+1
C        CALCULATE THE SQUARED THICKNESS OF THE TRANSITION ZONE
      DN2(I,J)=(D2(I,J)*PNL+AK*(D2(I,J)*(D2DX+D2DY)
     $ +0.5*DSDX*(D2(II,J)-D2(II-1,J))/DX
     $ +0.5*DSDY*(D2(I,JJ)-D2(I,JJ-1))/DY)
     $ -AL1*AK/AB*SQRT(DSDX**2+DSDY**2))/PNL
      IF(TIME.LT.7.1.OR.TIME.GT.20.) GO TO 30
      IF(J.LT.9.OR.J.GT.11) GO TO 30
      IF(I.LT.9.OR.I.GT.11) GO TO 30
      WRITE(6,4321) I,J,II,JJ,D2(I,J),D2(II,J),D2(II-1,J),
     $ D2(I,JJ),D2(I,JJ-1),DSDX,DSDY,D2DX,D2DY,DN2(I,J)
 4321 FORMAT(1X,' I=',I3,' J=',I3,' II=',I3,' JJ=',I3,' D2(I,J)=',
     $ F8.3,' D2(II,J)=',F8.3,' D2(II-1,J)=',F8.3,' D2(I,JJ)=',
     $ F8.3,' D2(I,JJ-1)=',F8.3/' DSDX=',F10.5,' DSDY=',F10.5,
     $ ' D2DX=',F10.5,' D2DY=',F10.5,' DN2(I,J)=',F8.3)
 30    CONTINUE
 40   CONTINUE
      DO 100 J=2,M1
       DO 90 I=2,N1
        IF(DN2(I,J).LT.0) DN2(I,J)=0.0
        DLN(I,J)=SQRT(DN2(I,J))
        IF(DLN(I,J).GE.Z(I,J)) DLN(I,J)=Z(I,J)
        DLE(I,J)=(DLN(I,J) + DL(I,J))/2.0
        DL(I,J)=DLN(I,J)
```

```
        D2(I,J)=DN2(I,J)
        ZBZ=ZN(I,J)
C         ITERATIVELY CALCULATE THE THICKNESS OF THE FRESHWATER LENS
        DO 85 JIT=1,20
         DZ(I,J)=XKK/(B1-ZE(I,J))*(SN(I,J)+XKSI*(-ZE(I,J)
     $     +BET*XKSI*DLE(I,J)))
         ZN(I,J)=Z(I,J)+DZ(I,J)*DT
         ZB=ABS(ZN(I,J) - ZBZ)
         ZE(I,J)=(ZN(I,J) + Z(I,J))/2.0
C     WRITE(6,555) DZ(I,J),ZN(I,J),Z(I,J),ZBZ,ZB,ZE(I,J),I,J,JIT
C    $ ,DLE(I,J),DLN(I,J),DL(I,J),BET,XKSI,XKK,XKT
C555  FORMAT(1X,' DZ=',F7.2,' ZN=',F7.2,' Z=',F7.2,' ZBZ=',F7.2,
C    $ ' ZB=',F7.2,' ZE=',F7.2,' I=',I2,' J=',I2,' JIT=',I2
C    $ /' DLE=',F10.2,' DLN=',F10.2,' DL=',F10.2,' BET=',F6.4,
C    $ ' XKSI=',F6.4,' XKK=',F10.1,' XKT=',F12.2)
         IF(ZB .LT. 0.01) GO TO 87
         ZBZ=ZN(I,J)
 85     CONTINUE
        WRITE(6,86) I,J
 86   FORMAT(1X,' DZ DID NOT CONVERGE (20 IT) AT I=',I3,' J=',I3)
 87     Z(I,J)=ZN(I,J)
 90    CONTINUE
 100  CONTINUE
C     IF(TIME.GE.1.0) DT=1.0
C     IF(TIME.LT.0.184) GO TO 5
C     IF(ICNT.EQ.1) GO TO 5
C        PRINT CYCLE
      WRITE(6,299) TIME
      DO 106 J=1,M
        WRITE(6,300) (S(I,J), I=1,N)
 106  CONTINUE
      WRITE(6,310)
      DO 107 J=1,M
        WRITE(6,320) (DL(I,J), I=1,N)
 107  CONTINUE
      WRITE(6,330)
      DO 108 J=1,M
        WRITE(6,340) (Z(I,J), I=1,N)
 108  CONTINUE
      IF(TIME.LT.TIMAX) GO TO 5
      STOP
 200  FORMAT(2I2)
 205  FORMAT(2F6.1,F7.3,F6.1)
 207  FORMAT(2F7.3)
 210  FORMAT(F10.2,F7.5)
 220  FORMAT(2F6.1,F8.4)
 230  FORMAT(I3)
 240  FORMAT(2I2,F10.1)
 250  FORMAT(F4.2,F6.4,2F6.3,F5.3,F8.4)
 299  FORMAT(1X//' HEAD BUILDUP AT TIME=',F10.3//)
 300  FORMAT(1X,50F6.3)
 310  FORMAT(1X//' THICKNESS OF TRANSITION ZONE'//)
 320  FORMAT(1X,50F6.3)
 330  FORMAT(1X//' PENETRATION OF FRESHWATER LENS'//)
```

```
 340   FORMAT(1X,50F6.3)
 400   FORMAT(1X,' N=',I2,' M=',I2)
 410   FORMAT(1X,' DX=',F6.1,' DY=',F6.1,' DT=',F6.2,' TIMAX=',F6.2)
 412   FORMAT(1X,' XD=',F8.4,' YD=',F8.4)
 420   FORMAT(1X,' T=',F10.1,' S=',F10.6)
 430   FORMAT(1X,' B1=',F10.1,' B=',F10.1,' XK=',F10.4)
 440   FORMAT(1X,' PN=',F6.4,' BET=',F6.4,' AL=',F6.3,' A1=',F7.4/
      $    ' XKSI=',F6.3,' AB=',F8.4)
 450   FORMAT(1X,' JI=',I4)
 460   FORMAT(1X,' III=',I4,' JJJ=',I4,' QWELL=',F10.1)
       END
       SUBROUTINE HANT
C         SUBROUTINE CALCULATES HEAD-BUILDUP IN AQUIFER USING
C         ANALYTICAL RELATIONSHIPS
       COMMON /DD/ DOWN(50,50)
       COMMON /NM/ N,M
       COMMON /DEL/ DELX,DELY,TIME
       COMMON /PARAM/ T,STO
C      WRITE(6,200) STO
C200   FORMAT(1X,' STO=',F10.5)
       CALL BEGIN
       CALL CONST
       CALL BDAY
C      WRITE(6,100) T,STO
C      WRITE(6,110) DELX,DELY
       RETURN
C100   FORMAT(1X,' TRANSMISSIVITY=',F10.1/'  STORATIVITY=',F10.4)
C110   FORMAT(1X,' DELX=',F10.2/'  DELY=',F10.2)
       END
       SUBROUTINE BEGIN
C         SUBROUTINE SETS UP REQUIRED SPATIAL VECTORS
       COMMON /NM/ N,M
       COMMON /DEL/ DELX,DELY,TIME
       COMMON /XY/ X(50),Y(50)
       COMMON /PARAM/ T,STO
       DO 5 I=1,N
           X(I)=(I-1)*DELX
 5     CONTINUE
       DO 7 J=1,M
           Y(J)=(J-1)*DELY
 7     CONTINUE
       RETURN
       END
         SUBROUTINE CONST
C        COMPUTE CONSTANTS
C
         IMPLICIT COMPLEX (C)
C
         COMMON  /MATH/          PI, EPS
         COMMON  /OMEGA/        COMREF, CC
C
         C=(0.,1.)
         CC=(0.,0.)
         PI=4.0*ATAN(1.0)
```

```
          EPS=1.0
 1        EPS=EPS/2.0
          EPSO=EPS+1.0
          IF (EPSO.GT.1.0) GOTO 1
          RETURN
          END
      SUBROUTINE BDAY
      COMMON /PUSH/ RB
      COMMON /NEW/ B1,B,XK
      COMMON /GOOD/ III(10),JJJ(10),QWELL(10),JI
      COMMON /NM/ N,M
      COMMON /DEL/ DELX,DELY,TIME
      COMMON /XY/  X(50), Y(50)
      COMMON /PARAM/  T,STO
      COMMON /MATH/ PI,EPS
      COMMON /DD/  DOWN(50,50)
      COMMON /MOI/ SXM(50,50),SXP(50,50),SYM(50,50),SYP(50,50)
      COMMON /HEY/ XD,YD
      HALF=35.0
      DO 5 J=1,M
           DO 3 I=1,N
              DOWN(I,J)=0.00
              SXP(I,J)=0.00
              SXM(I,J)=0.00
              SYP(I,J)=0.00
              SYM(I,J)=0.00
 3         CONTINUE
 5    CONTINUE
      XK1=T/B1
      K=0
C        INCREMENT INJECTION WELL
 10   K=K+1
      II=III(K)
      JJ=JJJ(K)
      QW=QWELL(K)
      XW=X(II)
      YW=Y(JJ)
C        CALCULATE VALUES FOR EACH POINT ON SPATIAL GRID
      DO 30 J=1,M
           DO 20 I=1,N
C             CALCULATE RADIUS AT AND AROUND DESIRED GRID-POINT
             R=SQRT((X(I)-XW)**2+(Y(J)-YW)**2)
             IF(R.LT.HALF) R=HALF
             RXP=SQRT((X(I)+XD-XW)**2+(Y(J)-YW)**2)
             IF(RXP.LT.HALF) RXP=HALF
             RXM=SQRT((X(I)-XD-XW)**2+(Y(J)-YW)**2)
             IF(RXM.LT.HALF) RXM=HALF
             RYP=SQRT((X(I)-XW)**2+(Y(J)+YD-YW)**2)
             IF(RYP.LT.HALF) RYP=HALF
             RYM=SQRT((X(I)-XW)**2+(Y(J)-YD-YW)**2)
             IF(RYM.LT.HALF) RYM=HALF
             AMULT=SQRT(XK/(XK1*B1*B))
C             CALCULATE LEAKANCE PARAMATER AT AND AROUND GRID-POINT
C             (FIRST WELL FUNCTION PARAMETER)
```

```
                RB=R*AMULT
                RBXP=RXP*AMULT
                RBXM=RXM*AMULT
                RBYP=RYP*AMULT
                RBYM=RYM*AMULT
                BMULT=STO/(4.0*T*TIME)
C                CALCULATE SECOND WELL FUNCTION PARAMETER
                U=R**2*BMULT
                UXP=RXP**2*BMULT
                UXM=RXM**2*BMULT
                UYP=RYP**2*BMULT
                UYM=RYM**2*BMULT
C                CALCULATE WELL FUNCTION AT AND AROUND A GRID POINT
                IF(RB.GT.3.0)CE=XCOEF(U)
                IF(RB.LE.3.0)CE=XCOEF2(U)
                RB=RBXP
                IF(RB.GT.3.0)CXP=XCOEF(UXP)
                IF(RB.LE.3.0)CXP=XCOEF2(UXP)
                RB=RBXM
                IF(RB.GT.3.0)CXM=XCOEF(UXM)
                IF(RB.LE.3.0)CXM=XCOEF2(UXM)
                RB=RBYP
                IF(RB.GT.3.0)CYP=XCOEF(UYP)
                IF(RB.LE.3.0)CYP=XCOEF2(UYP)
                RB=RBYM
                IF(RB.GT.3.0)CYM=XCOEF(UYM)
                IF(RB.LE.3.0)CYM=XCOEF2(UYM)
                CMULT=QW/(4.0*PI*T)
C                CALCULATE HEAD-BUILDUP AT AND AROUND GRID-POINT
                DOWN(I,J)=CE*CMULT+DOWN(I,J)
                SXP(I,J)=CXP*CMULT+SXP(I,J)
                SXM(I,J)=CXM*CMULT+SXM(I,J)
                SYP(I,J)=CYP*CMULT+SYP(I,J)
                SYM(I,J)=CYM*CMULT+SYM(I,J)
C        WRITE(6,5432) I,J,R,RB,U,CE,DOWN(I,J)
C5432  FORMAT(1X,' I=',I3,' J=',I3,' R=',F10.3,' RB=',E10.3,' U=',
C     $  E10.3,' CE=',E10.3,' DOWN=',F10.3)
 20           CONTINUE
 30           CONTINUE
C      WRITE(6,150) TIME
C      DO 70 J=1,M
C           WRITE(6,140) (DOWN(I,J), I=1,N)
C70    CONTINUE
       IF(K.LT.JI) GO TO 10
       RETURN
C150   FORMAT(1X,'DRAWDOWN AT TIME=',F10.2)
C140   FORMAT(1X,50F6.2)
       END
        DOUBLE PRECISION FUNCTION XCOEF(U)
C          SUBROUTINE CALCULATES THE WELL FUNCTION FOR A LEAKY AQUIFER
C          GIVEN INPUT PARAMETERS OF U AND RB
C
C          THIS SUBROUTINE IS ACCURATE IN THE FOLLOWING RANGE:
C
```

```
C         FOR RB > 1.0       ACCURACY WITHIN 10%
C         FOR RB > 10.0      ACCURACY WITHIN 1%
      REAL*8 U,RB,XCOEF
      COMMON /MATH/ PI,EPS
      COMMON /PUSH/ RB
C
      XCOEF=DSQRT(PI/(2*RB))*DEXP(-RB)
     $ *DERFC(-(RB-2*U)/(2*DSQRT(U)))
      RETURN
      END
      DOUBLE PRECISION FUNCTION XCOEF2(U)
C         SUBROUTINE CALCULATES WELL FUNCTION FOR INPUT PARAMETERS
C
C             WELL FUNCTION FOR A LEAKY AQUIFER--USING NUMERICAL
C             INTEGRATION OF THE WELL FUNCTION
C
C                              INPUT GUIDE
C
C                INPUT IS PASSED TO SUBROUTINE IN THE CALL STATEMENT
C                AND IN A COMMON STATEMENT
C
C                RB= PARAMETER # 2.... PASSED THROUGH COMMON
C
C         WILL CALCULATE THE WELL FUNCTION FOR SPECIFIC PARAMETERS
C
C
C         THIS SUBROUTINE CAN BE SUBSTITUTED BY ANY SUBROUTINE THAT
C         CALCULATES THE WELL FUNCTION GIVEN THE NECESSARY INPUT
C         PARAMETERS.
       REAL*8 U,RB,XCOEF2,ANS
      EXTERNAL FFX
      COMMON /PUSH/ RB
      AA=20.0
      EPSS=0.05
      MAXIT=25
C         CALL SCHEME TO NUMERICALLY INTEGRATE THE WELL FUNCTION
      CALL QA04AD(ANS,U,AA,EPSS,MAXIT,FFX)
      XCOEF2=ANS
      RETURN
      END
      DOUBLE PRECISION FUNCTION FFX(X)
C         SUBROUTINE SUPPLYS THE WELL FUNCTION TO SUBROUTINE QA04AD
      REAL*8 RB,X,A,FFX
      COMMON /PUSH/ RB
      A=RB**2/(4.0*X)
      A=X+A
      FFX=DEXP(-A)/X
      RETURN
      END
C   QA04AD - A SUBROUTINE TO APPROXIMATE
1
C
2
C                                            AA
```

```
C                                              I   F(X)DX,
C                                               BB
C
C  USING AN ADAPTIVE 3-POINT GAUSSIAN INTEGRATION SCHEME.
C
      SUBROUTINE QA04AD(ANS,AA,BB,EPSS,MAXIT,F)
      IMPLICIT REAL*8 (A-H,O-Z)
      REAL*8 R(30),B(30),B1(30),A1(30),EPS(30),EST2(30),EST3(30),FW(30),
     1FV(30),F3(30),F4(30),F5(30),F6(30)
      REAL*8 F
      DIMENSION J(30)
      COMMON/QA04BD/DIVD,LPD,NFD,ERREST
      COMMON /QA04B/DIVS,LPS,NFS,ESTS
      REAL*4 DIVS,ESTS,SANS,SAA,SBB,SEPS
C
C  THE ARGUEMENT LIST IS AS FOLLOWS:-
C  ANS   ON ENTRY:UNDEFINED.ON RETURN:SET BY THE SUBROUTINE TO THE
C        APPROXIMATION OF THE INTEGRAL I.
C  AA    ON ENTRY:SET BY THE USER TO THE UPPER LIMIT OF THE INTEGRAL.
C        ON RETURN:NO CHANGE.
C  BB    ON ENTRY:SET BY THE USER TO THE LOWER LIMIT OF THE INTEGRAL I.
C        ON RETURN:NO CHANGE.
C  EPSS  ON ENTRY:SET BY THE USER TO THE RELATIVE ACCURACY REQUIRED.
C        ON RETURN:NO CHANGE.
C
C  MAXIT ON ENTRY:IS THE MAXIMUM NO. OF ITERATIONS TO BE ALLOWED.
C        (LE.30) ON RETURN:CONTAINS THE MAXIMUM NO. OF ITERATIONS
```

```
C        ACHIEVED.
C  F       IS THE FUNCTION F(X) TO BE INTEGRATED.MUST BE SET BY THE
C        USER.
C
C        P AND Q ARE ONE HALF OF THE THREE POINT GAUSS-LEGENDRE WEIGHTS.
      DATA P,Q /4.444444444444444D-01,2.777777777777778D-01/
C
C        R(K)=R**K,WHERE R=1-SQRT(15)/5 USED FOR GENERATION OF POINTS OF
C        SUBDIVISION.
      DATA R(1)/2.254033307585167D-01/,R(2)/5.080666151703326D-02/,
     1R(3)/1.145199073065985D-02/,R(4)/2.581316854506389D-03/,
     2R(5)/5.818374167488376D-04/,R(6)/1.311480916951191D-04/,
     3R(7)/2.956121669070321D-05/,R(8)/6.663196703358761D-06/,
     4R(9)/1.501906730436233D-06/,R(10)/3.385347795289606D-07/,
     5R(11)/7.630686688342781D-08/,R(12)/1.719982195527138D-08/,
     6R(13)/3.876897157171633D-09/,R(14)/8.738655322347104D-10/,
     7R(15)/1.969722016007677D-10/,R(16)/4.439819030765107D-11/,
     8R(17)/1.000749997499504D-11/,R(18)/2.255723826929655D-12/,
     9R(19)/5.084476638612921D-13/,R(20)/1.146057969507219D-13/,
     1R(21)/2.583252835692698D-14/,R(22)/5.822737933565171D-15/,
     2R(23)/1.312464524359553D-15/,R(24)/2.958338752930355D-16/,
     3R(25)/6.668194084224985D-17/,R(26)/1.503033156728549D-17/,
     4R(27)/3.387886797671025D-18/,R(28)/7.636409684278539D-19/,
     5R(29)/1.721272177872976D-19/,R(30)/3.879804820345346D-20/
C
C        S=(1-R)/R.USED FOR GENERATION OF POINTS OF SUBDIVISION.
      DATA S/3.436491673103706D00/
```

```
C
C       DIV IS ADAPTIVE DIVISOR OF EPS(I)
      DIV=DIVD
      LP=LPD
   90 IERRC=0
      ERREST=0.D0
      IF(MAXIT.GT.30)MAXIT=30
      II=1
      ANS=0D0
      J(1)=4
      A=AA
      B(1)=BB
      BT=BB
      R1=BB-AA
      R2=0.1127016653792583D0*R1
C       R2=(1-SQRT(3/5))/2*R1
      FU=P*F(AA+R2)
      FV(1)=P*F(5D-1*(AA+BB))
      FW(1)=P*F(BB-R2)
      NF=3
      EST=R1*(625D-3*(FU+FW(1))+FV(1))
      ABSA=DABS(EST)
      EPS(1)=EPSS
      IMAX=1
      K=1
   10 I=II
```

```
      IF(I.GT.IMAX)IMAX=I
C        FORM GAUSSIAN SUMS AND TEST.
      R1=R(K)*(BT-A)
      A1(I)=A+R1
      B1(I)=A+S*R1
      R2=2D-1*(B(I)-A)
      W1=A+R2
      U3=B(I)-R2
      F1=F(A1(I)-R2)
      F2=F(W1)
      F3(I)=F(2D0*W1-5D-1*(A+A1(I)))
      F4(I)=F(2D0*U3-5D-1*(B(I)+B1(I)))
      F5(I)=F(U3)
      F6(I)=F(B1(I)+R2)
      NF=NF+6
      EST1=R1*(Q*(F1+F2)+FU)
      EST2(I)=(B1(I)-A1(I))*(Q*(F3(I)+F4(I))+FV(I))
      EST3(I)=R1*(Q*(F5(I)+F6(I))+FW(I))
      SUM=EST1+EST2(I)+EST3(I)
      ABSA=ABSA+DABS(EST1)+DABS(EST2(I))+DABS(EST3(I))-DABS(EST)
      IF(DABS(SUM-EST).LE.EPS(I)*ABSA)GO TO 20
C         IF NO. OF ITERATIONS ACHIEVED IS GREATER THAN NO. REQUESTED,
C        PRINT DIAGNOSTIC AND RETURN.
      IF(I.GE.MAXIT)GO TO 70
C        DEFINE LEFTMOST SUBINTERVAL.
      K=K+1
      II=I+1
```

```
      B(II)=A1(I)
      FW(II)=P*F2
      FV(II)=FU
      FU=P*F1
      EST=EST1
      EPS(II)=EPS(I)/DIV
      J(II)=1
      GO TO 10
C        WHEN ACCURACY IS REACHED AT ONE LEVEL,PROCEED TO NEXT
C        APPROPRIATE LEVEL.
   20 JJ=J(I)
      ERREST=ERREST+DABS(SUM-EST)
      I=I-1
      GO TO (30,40,50,60),JJ
C        DEFINE MIDDLE SUBINTERVAL.
   30 ANS=ANS+SUM
      K=1
      II=I+1
      A=A1(I)
      B(II)=B1(I)
      BT=B(II)
      FU=P*F3(I)
        FV(II)=FV(I)
      FW(II)=P*F4(I)
      EST=EST2(I)
      EPS(II)=EPS(I)/DIV
      J(II)=2
```

```
      GO TO 10
C        DEFINE RIGHTMOST SUBINTERVAL.
   40 ANS=ANS+SUM
      II=I+1
      A=B1(I)
      B(II)=B(I)
      BT=B(II)
      FU=P*F5(I)
      FV(II)=FW(I)
      FW(II)=P*F6(I)
      EST=EST3(I)
      EPS(II)=EPS(I)/DIV
      J(II)=3
      GO TO 10
   50 ANS=ANS+SUM
      SUM=0D0
      EST=0D0
      GO TO 20
   60 MAXIT=IMAX
      IF(NF.EQ.9)ANS=SUM
      IF(IERRC.LE.0)GO TO 100
      WRITE(LP,81)IERRC
   81 FORMAT(' QA04A/AD ACCURACY SUSPECT AT',I6,' POINTS',
     1' IN RANGE.     BEST ESTIMATE RETURNED.')
      MAXIT=-MAXIT
  100 SANS=ANS
      NFS=NF
```

```
      NFD=NF
      ERREST=ERREST*.01536D0
      ESTS=ERREST
      RETURN
C          REQUIRED ACCURACY NOT REACHED IN MAXIT ITERATIONS.
   70 IERRC=IERRC+1
      GO TO 20
      ENTRY QA04A(SANS,SAA,SBB,SEPS,MAXIT,F)
      DIV=DIVS
      LP=LPS
      AA=SAA
      BB=SBB
      EPSS=SEPS
      GO TO 90
      END
      BLOCK DATA
      REAL*8 DIVD,ERREST
      COMMON/QA04BD/DIVD,LPD,NFD,ERREST
      COMMON /QA04B/DIVS,LPS,NFS,ESTS
      REAL*4 DIVS,ESTS
      DATA DIVD/1.4D0/,LPD/6/,DIVS/1.4/,LPS/6/
      END
```

REFERENCES

Bachmat, Y., and J. Bear, The General Equations of Hydrodynamic Dispersion in Homogeneous Isotropic Porous Mediums, J. Geophys. Res., 69, 2561-2567, 1964.

Bear, J., Hydraulics of Groundwater, McGraw-Hill Inc., New York, 1979.

Bear, J., and G. Dagan, Moving Interface in Coastal Aquifers, J. Hydraul. Div., Amer. Soc. Civil Eng., 90 (HY4), 193-216, 1964.

Benedict, B. A., J. L. Anderson, and E. L. Yandell, Analytical Modeling of Thermal Discharges: A Review of the State of the Art, Argonne National Laboratory, Report No. ANL/ES-18, April, 1974, 321 p.

Benedict, B. A., H. Rubin, and S.A. Means, Movement of Salt and Hazardous Contaminants in Groundwater Systems, Florida Water Resources Research Center, University of Florida, Research Project Technical Completion Report, Publication No. 71, 1983

Blasius, H., Grenzschichten in Flüssigkeiten mit kleiner Reibung. Z. Math. Phys. 56, 1-37, 1908. English translation in NACA TM 1256.

Calderon, M. R., Saltwater Intrusion Potential in Southwest Florida, M.E. Thesis, Dept. of Civil Engineering, University of Florida, Gainesville, Fla., 1981.

Christensen, B. A., Mathematical Methods in Analysis of Fresh Water Lenses in the Coastal Zones of the Floridan Aquifer, Florida Water Resources Research Center, Research Project Technical Completion Report, University of Florida, Publication No. 44, 1978.

CH_2M Hill Publication, Injection Wells in the State of Florida, From Brochure by CH_2M Hill, Gainesville, Florida, 1983.

Dagan, G., Pertubation Solutions of the Dispersion Equation in Porous Medium, Water Resources Res., 7 (1), 135-142, 1971.

Dagan, G., and J. Bear, Solving the Problem of Interface Upconing in a Coastal Aquifer by the Method of Small Pertubation, J. Hydraul. Res., 6(1), 15-44, 1968.

Eldor, M., and G. Dagan, Solutions of Hydrodynamic Dispersion in Porous Media, Water Resources Res., 8(5), 1316-1331, 1972.

Gelhar, L. W., and M. A. Collins, General Analysis of Longitudinal Dispersion in Nonuniform Flow, Water Resources Res., 7 (6), 1511-1521, 1971.

Ghyben, B. W., and J. Drabbe, Nota in Verband met de voorgenomen Putboring nabij Amsterdam, Tijdscrift von het koninklujk Institut von Ingenieurs, The Hague, Netherlands, 8-22, 1888.

Hantush, M. S., Unsteady Movement of Freshwater in Thick Unconfined Saline Aquifers, Bulletin of the I.A.S.H., 13 (2), 40-48, 1968.

Hantush, M. S., and C. E. Jacob, Non-steady Radial Flow in an Infinite Leaky Aquifer, Trans. Am. Geophys. Union, 36 (1), 95-100, 1955.

Helpling, C. L., Deep Well Injection In Florida, Proceedings of a Southeast Regional Conference on Ground Water Management, January 30-31, 1980, 152-163.

Herzberg, B., Die Wasserversorgung einiger Nordseebader, Jour. Gasbeleuchtung und Wasserversorgung, 44, 815-819, 842-844, 1901.

Hickey, J. J., Hydrology and Results of Injection Tests at Waste Injection Test Sites in Pinellas County, Florida, U.S. Geological Survey, Water Supply Paper 2183, 1982.

Hickey, J. J., Personal communication, 1986.

Hubbert, M. K., The Theory of Ground-Water Motion, The Journal of Geology, Volume 48, No. 8, 785-944, 1940.

Hunt, B., Dispersive Sources in Uniform Groundwater Flow, Journal of the Hydraulics Division, ASCE, Vol. 104, No. 1, Proc. Paper 13467, 75-85, January, 1978.

Hunt, B., Dispersion Calculation in Nonuniform Seepage, J. of Hydrology, 36, 261-277, 1978.

INTERCOMP Resource Development and Engineering, Inc., A Model for Calculating Effects of Liquid Waste Fisposal in Deep Saline Aquifer, U.S. Geological Survey Water Resources Investigation 76-61, 1976.

Koh, R. C. Y., Stratified Flow Towards a Sink in a Porous Medium, W.M. Keck Lab. of Hydro. Water Res., Tech. Mem. 64-2, California Inst. of Tech, 1964.

Kohout, F. A., Cyclic Flow of Salt Water in the Biscayne Aquifer of Southeastern Florida, J. Geophys. Res., 65(7), 2133-2141, 1960.

List, E. J., The Stability and Mixing of a Density Stratified Horizontal Flow in a Saturated Porous Medium, W.M. Keck Lab. of Hydr. Water Res., Report No. KH-R-11, California Inst. of Tech., 1965.

List, E. J., A Two-dimensional Sink in a Density Stratified Porous Medium, J. Fluid Mech., 33 (3), 529-543, 1968.

Means, S. A., Numerical Simulation of Aquifer Mineralization in Northeastern Florida, M.E. Thesis, Dept. of Civil Engineering, University of Florida, Gainesville, Florida, 1982.

Merritt, M. L., Subsurface Storage of Freshwater in South Florida: A Digital Model Analysis of Recoverability, U.S.G.S. Water Supply Paper No. 2261, 1983.

Morton, B. R., On a Momentum-Mass Flux Diagram for Turbulent Jets, Plumes, and Wakes, Journal of Fluid Mechanics, 10, (1), 101-112, 1961.

Muskat, N., and R. D. Wychoff, An Approximate Theory of Water-Coning in Oil Production, Trans. Am. Inst. Mining Met. Engrs., 114, 144-163, 1937.

Peaceman, D. W., and H. H. Rachford, The Numerical Solution of Parabolic and Elliptic Differential Equations, J. Soc. Indust. App. Math.,3, 28-41, 1955.

Pinder, G. F., and H. H. Cooper, A Numerical Technique for Calculating the Transient Position of the Saltwater Front, Water Resour. Res., 6 (3), 875-882, 1970.

Prandtl, L., Über Flüssigkeitsbewegung bei sehr kleiner Reibung. Verhandlungen IIIrd International Math. Kongress Heidelberg 1904, 484-491 (1904), Teubner, Leipzig, 1905. English translation: NACA Memo No. 452 (1928). Reprinted in Vier Abhandlungen zur Hydro- und Aerodynamik, Göttingen, 1927; Coll. Works, Vol. II, 575-584.

Puri, H. S., and R. O. Vernon, Summary of the Geology of Florida and a Guideline to the Clastic Exposures: Florida Geological Survey Special Publication 5, 1964, 312 p.

Rubin, H., On the Application of the Boundary Layer Approximation for the Simulation of Density Stratified Flows in Aquifers, to be published in Advances in Water Resources.

Rubin, H., Modelling Fresh Water Injection Into a Partially Saline Partially Fresh (PASPAF) Aquifer, to be published in the Journal of Hydrology.

Rubin, H., and B. A. Christensen, Simulation of Stratified Flow in the Floridan Aquifer, ASCE Irrigation and Drainage Division Specialty Conference, Orlando, FL, July 21-23, 1982.

Rubin, H., and G. F. Pinder, Approximate Analysis of Upconing, Advances in Water Resources, 1, 97-101, 1977.

Segol, G., G. F. Pinder, and W. G. Gray, A Galerkin Finite Element Technique for Calculating the Transient Position of the Saltwater Front, Water Resources Res., 11 (2), 343-347, 1975.

Strack, O. D. L., A Single-Potential Solution for Regional Interface Problems in Coastal Aquifers, Wat. Resour. Res., 12(6), 1165-1174, 1976.

Theis, C. V., The Relationship Between the Lowering of the Piezometric Surface and the Rate and Duration of Discharge of a Well Using Groundwater Storage, Trans. Amer. Geophys. Union, 2, 519-524, 1935.

Wheatcraft, S. W., and F. L. Peterson, Numerical Modeling of Liquid Waste Injectim into a Two-Phase Fluid System: Water Resources Research Center, University of Hawaii at Manoa, Technical Report No. 125, 1979.

Wilson, J. L., and P. J. Miller, Two-Dimensional Plume in Uniform Groundwater Flow, Journal of the Hydraulics Division, American Society of Civil Engineers, 108, No. HY4, 503-514, April, 1982.

Wooding, R. A., Convection in a Saturated Porous Medium at Large Rayleigh Number or PéClet Number, J. Fluid Mech., 15, 527-544, 1963.

Wooding, R. A., Mixing Layer Flows in a Saturated Porous Medium, J. Fluid Mech., 19, 103-112, 1964.

BIOGRAPHICAL SKETCH

Steven Laux was born May 2, 1960, at Dover Air Force Base in Dover, Delaware. He completed high school in 1978 at Winter Haven High School in Winter Haven, Florida.

He enrolled at the University of Florida in the fall of 1978 where in the spring of 1983 he received his Bachelor of Science in Civil Engineering degree. He entered the master's program in civil engineering hydraulics in the fall of 1983.

In the summer of 1984, he began full time employment with the consulting firm of Jones, Edmunds and Associates in Gainesville, Florida. After graduation, Steven Laux plans to continue his career in civil engineering hydraulics with Jones, Edmunds and Associates.